

**Identification and Functional Analysis of a
Novel Renal Cell Carcinoma (RCC)
Susceptibility Gene from an RCC associated
Constitutional Chromosomal Translocation.**

By

Naomi Catherine Wake

A thesis submitted to
the University of Birmingham
for the degree of
DOCTOR OF PHILOSOPHY

Medical and Molecular Genetics
College of Medicine & Dentistry
The University of Birmingham

Date Submitted: September 2012

Date Resubmitted: January 2013

UNIVERSITY OF
BIRMINGHAM

University of Birmingham Research Archive

e-theses repository

This unpublished thesis/dissertation is copyright of the author and/or third parties. The intellectual property rights of the author or third parties in respect of this work are as defined by The Copyright Designs and Patents Act 1988 or as modified by any successor legislation.

Any use made of information contained in this thesis/dissertation must be in accordance with that legislation and must be properly acknowledged. Further distribution or reproduction in any format is prohibited without the permission of the copyright holder.

Abstract

Familial renal cell carcinoma (RCC) only accounts for 3% of all RCC, yet the study of these inherited forms has provided important insights into the more common sporadic RCC. Somatic *VHL* inactivation is found in 70% of sporadic clear cell RCC (ccRCC) though is rarely found in other forms of RCC including papillary and chromophobe types. *VHL*-independent RCC tumourigenesis is poorly understood and current research involves identifying novel RCC candidate genes to further understand the mechanisms involved. In this study a constitutional balanced translocation, t(5;19)(p15.3;q12), associated with familial RCC was characterised using an oligonucleotide CGH array followed by genomic sequencing and the previously uncharacterised gene, *UBE2QL1*, was found to be disrupted by the 5p15.3 breakpoint. *UBE2QL1* expression was down-regulated in 78.6% of sporadic RCC and *UBE2QL1* promoter region hypermethylation and gene deletions were detected in 20.3% and 17.3% of sporadic RCC, respectively. Re-expression of *UBE2QL1* in deficient RCC cell lines suppressed anchorage independent growth and colony formation. *UBE2QL1* shows homology to the E2 class of ubiquitin conjugating enzymes and was shown to possess an active-site cysteine (C88) that is monoubiquitinated *in vivo*. In addition, *UBE2QL1* co-immunoprecipitation and co-localisation studies demonstrated a protein interaction with FBXW7 (an F box protein for the SCF E3 ubiquitin ligase) and was shown to facilitate the degradation of the known FBXW7 substrates, cyclin E1 and mTOR. These findings demonstrate that *UBE2QL1* functions as a novel renal tumour suppressor gene and ubiquitin conjugating enzyme.

Acknowledgements

I would like to thank everyone in the Medical and Molecular Genetics lab for all their help and support over the years, with a special thanks to Chris Ricketts and Mark Morris for their continued help and advice throughout my project. I would also like to say a big thank you to my supervisor Emma Woodward who has helped make this experience enjoyable and who continued to give me support and guidance throughout my project, congratulating me when things went well and giving me the encouragement I needed when things weren't quite going to plan. Thank you also to my second supervisor Eamonn Maher for his help and guidance. I would like to thank Andy Turnell who kindly took the time to introduce me to the world of ubiquitin, allowing me to work and learn techniques alongside him at Cancer Studies and to Anne-Bine Skytte for supplying the immunohistochemistry data. I would also like to say a big thank you and congratulations to all my fellow PhD students in our department who took this journey along side of me and whom I have shared some awesome and memorable experiences with. I would also like to say a huge thank to my family and friends for their continued support, and a massive thank you to my mum who has encouraged and supported me throughout my life, pushing me to achieve my full potential (and only nagging occasionally) and without whom, none of this would have been possible. Finally to my wonderful partner Janet Hoffman, who has stuck with me over these last four years with continued support and encouragement, through the late nights in the lab and thesis writing on the weekends and without whom, things would have been much more difficult, thank you.

Contents

Abstract	1
Acknowledgements	2
List of Figures	9
List of Tables	11
Abbreviations	12
Gene and Protein Names	16
Chapter One: Introduction	20
1.1 CANCER IS A GENETIC DISEASE	21
1.1.1 Oncogenes and mechanisms of activation	23
1.1.2 Tumor suppressor genes and the ‘two-hit’ model	24
1.1.3 Tumour suppressor gene haploinsufficiency	26
1.1.4 Epigenetic tumour suppressor gene inactivation	27
1.1.5 DNA repair genes in cancer development	32
1.2 CHROMOSOMAL REARRANGEMENTS	34
1.2.1 Chromosomal translocations	35
1.2.2 Somatic chromosomal translocations in cancer	39
1.2.3 Chromosomal translocations used to identify candidate cancer genes	40
1.2.4 FISH based cytogenetic techniques to detect chromosomal abnormalities	43
1.2.5 Array based cytogenetic techniques to detect chromosomal abnormalities	44
1.3 RENAL CELL CARCINOMA	47
1.3.1 Familial RCC	49
1.3.2 Familial constitutional translocations used to identify candidate RCC genes	52
1.3.3 Sporadic RCC	54
1.3.4 Epigenetics in RCC	57
1.3.5 <i>VHL</i> substrates and RCC treatment	58
1.4 THE UBIQUITIN PATHWAY	62
1.4.1 Ubiquitinating conjugating enzymes (E2s) – not just ubiquitin carriers	67
1.5 THE UBIQUITIN PATHWAY IN CANCER	69
1.5.1 Ubiquitin ligase enzymes (E3s) and their involvement in cancers	69
1.5.2 The ubiquitin pathway in kidney cancer	72
Chapter Two: Methods	76

2.1 MATERIALS.....	77
2.1.1 Companies purchased from.....	77
2.1.2 General chemicals and equipment.....	78
2.2 SEQUENCING.....	78
2.2.1 PCR.....	78
2.2.2 Agarose gel electrophoresis.....	80
2.2.3 EXOSAP reaction.....	81
2.2.4 Sanger sequencing reaction.....	82
2.2.5 Sequencing Precipitation.....	84
2.2.6 Sequencing analysis.....	84
2.3 CLONING.....	85
2.3.1 Plasmid constructs.....	85
2.3.2 Designing cloning primers.....	85
2.3.3 PCR (pfu taq).....	86
2.3.4 Site directed mutagenesis.....	88
2.3.5 Gel extractions.....	90
2.3.6 Restriction enzyme digest.....	91
2.3.7 Ligation reaction.....	91
2.3.8 pGEM-T easy vector ligation.....	93
2.3.9 Transformation.....	94
2.3.10 Minipreps.....	95
2.3.11 Maxipreps.....	96
2.3.12 Glycerol stocks.....	97
2.3.13 DNA quantification.....	97
2.4 DNA METHYLATION ANALYSIS.....	97
2.4.1 Bisulphite DNA modification.....	97
2.4.2 Designing non bias primers for methylated and unmethylated DNA.....	100
2.4.3 COmbined Bisulphite Restriction Analysis (COBRA).....	100
2.5 DNA DELETION ANALYSIS.....	103
2.5.1 Multiplex Ligation-dependent Probe Amplification (MLPA).....	103
2.5.2 Loss of heterozygosity (LOH).....	108
2.6 RNA ANALYSIS.....	111
2.6.1 RNA quantification.....	111
2.6.2 Reverse transcription cDNA synthesis.....	112
2.6.3 Reverse transcription PCR (RT-PCR).....	113
2.6.4 Quantitative Real time-PCR.....	115
2.7 TISSUE CULTURE.....	117
2.7.1 Cell lines and clinical samples.....	117

2.7.2 Culture conditions.....	118
2.7.3 Transfections.....	118
2.7.4 Colony formation assays and stable clones	119
2.7.5 Soft agar colony assays.....	120
2.8 PROTEIN ANALYSIS.....	122
2.8.1 Antibodies.....	122
2.8.2 Protein extraction from cells.....	122
2.8.3 Determining Protein concentration.....	123
2.8.4 Western Blot analysis	124
2.8.5 Protein synthesis using a Coupled reticulocyte lysate system.....	127
2.9 PULLDOWNS AND IMMUNOPRECIPIATIONS	128
2.9.1 Hisx6 ubiquitin pulldown	128
2.9.2 Antibody binding	129
2.9.3 Co-immunoprecipitation.....	130
2.10 IMMUNOFLOURESENCE	131
2.10.1 Cell fixing	131
2.10.2 Cell staining.....	131
2.11 PROTEIN DEGRADATION ASSAY	132
Chapter Three: Characterisation of the t(5;19)(p15.3;q12) breakpoints.....	134
3.1 INTRODUCTION: A NOVEL FAMILIAL CONSTITUTIONAL TRANSLOCATION, T(5;19)(P15.3;Q12), ASSOCIATED WITH RCC.....	135
3.1.1 Aims.....	135
3.2 RESULTS	138
3.2.1 Mapping of the t(5;19)(p15.3;q12) breakpoint region.....	138
3.2.2 Sequence of t(5;19)(p15.3;q12) derivative breakpoints	139
3.2.3 Map of genes within breakpoint vicinity	142
3.2.4 Existing knowledge on <i>UBE2QL1</i>	142
3.2.5 Loss of <i>UBE2QL1</i> second allele.....	144
3.2.6 Expression analysis of HIF-1/2 targets in t(5;19)(p15.3;q12) renal tumours.....	149
3.3 CONCLUSION.....	151
Chapter Four: Genetic and epigenetic analysis of UBE2QL1 in RCC...152	

4.1 INTRODUCTION: IS UBE2QL1 INACTIVATED IN OTHER FAMILIAL AND SPORADIC RCCS?	153
4.1.1 Aims	153
4.2 RESULTS	154
4.2.1 <i>UBE2QL1</i> mutation analysis in RCCs	154
4.2.2 <i>UBE2QL1</i> CpG island	155
4.2.3 <i>UBE2QL1</i> expression and methylation analysis in RCC cell lines	157
4.2.4 Expression and methylation analysis of <i>UBE2QL1</i> in sporadic RCCs	160
4.2.5 LOH (Loss of heterozygosity) of 5p15.3 in sporadic RCCs	166
4.2.6 Multiplex Ligation-dependent Probe Amplification (MLPA) of <i>UBE2QL1</i> in sporadic and familial RCCs	169
4.3 CONCLUSION	171
Chapter Five: UBE2QL1 suppresses RCC cell line proliferation and colony formation	172
5.1 INTRODUCTION: DOES UBE2QL1 FUNCTIONS AS A TUMOUR SUPPRESSOR?	173
5.1.1 Aims	174
5.2 RESULTS	175
5.2.1 <i>UBE2QL1</i> colony formation assays	175
5.2.2 Stable <i>UBE2QL1</i> expressing SKRC47 clones	177
5.2.3 <i>UBE2QL1</i> soft agar assays	177
5.3 CONCLUSION	179
Chapter Six: UBE2QL1 ubiquitin conjugation, E3 binding partners and protein substrates	180
6.1 INTRODUCTION: UBE2QL1 IS PART OF THE UBIQUITIN CASCADE	181
6.1.1 Aims	186
6.2 RESULTS:	187
6.2.1 <i>UBE2QL1</i> ubiquitin binding	187
6.2.2 <i>UBE2QL1</i> and FBXW7 protein interaction	190
6.2.3 Does FBXW7 target <i>UBE2QL1</i> for proteasome degradation?	201
6.2.4 FBXW7 substrate degradation assays	205
6.3 CONCLUSION	211

Chapter Seven: Discussion	214
7.1 UBE2QL1 IS A NOVEL RCC TSG GENE AND E2 CONJUGATING ENZYME	215
7.2 UBE2QL1 REGULATES ONCOGENES MTOR AND CYCLIN E1	216
7.3 E2 UBIQUITIN CONJUGATING ENZYMES IN CANCER.....	217
7.4 FUTURE EXPERIMENTS	220
7.4.1 Investigations of UBE2QL1 function within the cell	220
7.4.2 UBE2QL1 tumour suppressor activity	221
7.5 CONCLUSION.....	223
Chapter Eight: Appendices	224
8.1 PRIMER SEQUENCES	225
8.1.1 PCR and sequencing primers.....	225
8.1.2 t(5;19)(p15.3;q12) primers.....	226
8.1.3 Vector sequencing primers	226
8.1.4 Cloning primers	227
8.1.5 Site directed mutagenesis primers	227
8.1.6 COBRA primers	227
8.1.7 Custom designed MLPA probes	228
8.1.8 LOH microsatellite marker primers.....	229
8.1.9 RT-PCR primers	230
8.2 PLASMID MAPS	231
8.2.1 PGEM-T.....	231
8.2.2 PCDNA 3.1-.....	232
8.2.3 pFLAG-CMV-4	233
8.2.4 p3xFLAG-MYC-CMV-24.....	234
8.2.5 pCMV-MYC	235
8.3 UBE2QL1 NUCLEOTIDE AND AMINO ACID SEQUENCE.....	236
8.4 UBE2QL1 ORTHOLOGUE SEQUENCE VARIATION.....	237
8.5 UBE2QL1 KNOWN SINGLE NUCLEOTIDE POLYMORPHISMS (SNPS).....	239

Chapter Nine: References	240
Chapter Ten: Peer Reviewed Publications.....	258

List of Figures

Figure 1.1 Clonal evolution of tumourigenesis.....	22
Figure 1.2 Gene silencing by methylation	30
Figure 1.3 Robertsonian and reciprocal chromosomal translocations.....	38
Figure 1.4 Identifying cancer genes from disease associated translocations.....	42
Figure 1.5 Array painting used to map chromosomal translocations.	46
Figure 1.6 The ubiquitin pathway.....	64
Figure 1.7 Ubiquitin chains and substrate outcomes	66
Figure 1.8 The structure and substrates of the SCF, EVC and APC/C ubiquitin ligase complexes	70
Figure 1.9 Ubiquitin pathways involved in RCC tumourigenesis	74
Figure 2.1 schematic diagram of Multiplex Ligation-dependent Probe Amplification (MLPA) Probes.....	105
Figure 3.1 Pedigree of family with a constitutional t(5;19)(p15.3;q13.1) and predisposition to renal cell carcinoma (RCC).....	137
Figure 3.2 Custom designed oligonucleotide array painting of der(5) and der(19).....	140
Figure 3.3 Characterisation of the t(5;19) breakpoints.	141
Figure 3.4 Derivative chromosome breakpoint maps.....	146
Figure 3.5 t(5;19)(p15.3;q12) derivative breakpoints.....	147
Figure 3.6 MLPA deletion analysis of UBE2QL1 exon 1 in t(5;19) patient III:II.....	148
Figure 3.7 HIF-1/2 target gene immunohistochemistry on t(5;19)(p15.3;q13.1) tumours carried out by Anne-Bine Skytte.....	150
Figure 4.1 UBE2QL1 CpG island.....	156
Figure 4.2 UBE2QL1 expression, pre and post 5-aza and methylation results in RCC cell lines	159

Figure 4.3 Expression analysis of UBE2QL1 in sporadic RCCs.....	161
Figure 4.4 BstU1 digest of bisulphite modified UBE2QL1 CpG island in sporadic RCCs.....	164
Figure 4.5 Schematic diagram representing UBE2QL1 CpG island clones for 4 sporadic RCCs.....	165
Figure 4.6 Microsatellite marker analysis for 5p13.3 in sporadic RCC tumours	168
Figure 4.7 UBE2QL1 deletion analysis via MLPA in sporadic RCCs.....	170
Figure 5.1 Colony formation assays to assess UBE2QL1 growth suppression function in RCC cell lines.....	176
Figure 5.2 Soft agar growth assays to assess UBE2QL1 inhibition of anchorage independent growth.....	178
Figure 6.1 UBE2QL1 amino acid alignment with the ubiquitinating conjugating (UBC) domain.....	184
Figure 6.2 Schematic illustration of UBE2QL1 protein domains.....	185
Figure 6.3 UBE2QL1 binds ubiquitin via an active cysteine, C88.....	189
Figure 6.4 FLAG and MYC tag UBE2QL1 immunofluorescence in HeLa cells.....	195
Figure 6.5 FBXW7 α , β and γ isoform localisation staining within HeLa cells.....	196
Figure 6.6 UBE2QL1 and FBXW7 α/γ co-localisation in HeLa cells.....	198
Figure 6.7 UBE2QL1 and FBXW7 α/γ co-immunoprecipitations	200
Figure 6.8 FBXW7 does not facilitate the degradation of UBE2QL1 under normal cellular conditions and UBE2QL1 interacts with endogenous RBX-1.....	203
Figure 6.9 Schematic illustration of Cdc34 protein domains	204
Figure 6.10 UBE2QL1 stable clones demonstrate decreased cyclin E1 and mTOR expression compared to controls.....	207
Figure 6.11 UBE2QL1 enhances mTOR and cyclin E1 degradation.....	208
Figure 6.12 Immunohistochemistry with cyclin E1 (cyclin E1) in t(5;19)(p15.3;q13.1) associated renal tumours carried out by Anne-Bine Skytte ..	210

List of Tables

Table 1.1 Known clinico-pathological and genetic features of sporadic RCC tumours...	49
Table 1.2 Inherited syndromes and known genes that predispose to familial RCC.	51
Table 6.1 Linear motifs identified in the UBE2QL1 protein sequence by ELM.....	191

Abbreviations

5-Aza-	5-Aza-2'-deoxycytidine
A-	Alanine
APC/C -	Anaphase-Promoting Complex/Cyclosome
APS-	Ammonium Persulfate
ATP-	Adenosine Triphosphate
BHD-	Birt-Hogg-Dube
BSA-	Bovine Serum Albumin
C-	Cysteine
ccRCC-	clear cell Renal cell carcinoma
CGH-	Comparative Genome Hybridisation
CHX-	Cycloheximide
CML-	Chronic Myeloid leukaemia
CN-	Corresponding Normal
COBRA-	COmbined Bisulphite Restriction Analysis
Cy5/3-	Cyanine 5/3
DAPI-	4'-6-Diamidino-2-phenylindole
DMEM-	Dulbecco's Modified Eagle Medium
dNTPS-	Deoxynucleotide Triphosphates
DTT-	Dithiothreitol

E1-	Ubiquitin-activating enzyme
E2-	Ubiquiting conjugating enzymes
E3-	Ubiquitin ligase
EBV-	Epstein-Barr Virus
ECL-	Enhanced Chemiluminescence
ECV -	Elongin B/C-cullin 2-VHL
EDTA-	Ethylenediaminetetraacetic Acid
ELM-	Eukaryotic Linear Motif
EV-	Empty Vector
Ex-	Exon
EXOSAP-	EXOnuclease I and Alkaline Phosphatase treatment
Exp-	Expected
FBS-	Fetal Bovine Serum
FDA-	Food and Drug Administration
FISH-	Fluorescence In Situ Hybridization
G418-	Geneticin
HCL-	Hydrochloride
HECT-	Homologous to the E6-AP Carboxyl Terminus
His-	Histidine
HRP-	Horse Radish Peroxide
IP-	Immunoprecipitation
K-	Lysine

LCR-	Low Copy Repeats
LOH-	Loss Of Heterozygosity
MeOH-	Methanol
MG-132-	Carbobenzoxy-Leu-Leu-leucinal
MI-	Methylation Index
MLPA-	Multiplex Ligation-dependent Probe Amplification
NaAc-	Sodium Acetate
NI-	Non-Informative
NN-	Normal renal tissue
Obs-	Observed
OD-	Optical Density
ONC-	Oncogene
ORF-	Open Reading Frame
PBS-	Phosphate Buffered Saline
PH-	Peak Height
pRCC-	Papillary Renal cell Carcinoma
PVDF-	Polyvinylidene Difluoride
qRT-PCR-	Quantitative Real-Time Polymerase Chain Reaction
RCC-	Renal cell carcinoma
RING-	Really Interesting New Gene
RT-PCR -	Reverse Transcription Polymerase Chain Reaction
S-	Serine

SCF-	SKP1–CUL1–F-box
SDS-	
PAGE-	Sodium Dodecyl Sulphate Polyacrylamide Gel
SEM-	Standard Error of the Mean
SKY-	Spectral Karyotyping
SWI/SNF -	SWItch/Sucrose NonFermentable complex
T-	Tumour
TBS-T -	Tris-Buffered Saline and Tween 20
TEMED -	Tetramethylethylenediamie
TRIS-	Tris(hydroxymethyl)aminomethane
TSG-	Tumour Suppressor Gene
Ub-	Ubiquitin
UBC-	Ubiquitin-conjugating domain
UIM-	Ubiquitin-Interacting Motifs
UMPP-	Ubiquitin-Mediated Proteolysis Pathway
UV-	Ultra Violet
WHO-	World Health Organization
Wt-	Wild-type

Gene and Protein Names

AKT-	v-Akt murine thymoma viral oncogene homolog 1
AML1-	Acute myeloid leukemia 1
ARID1A-	AT rich interactive domain 1A (SWI-like)
BAP1-	BRCA1 associated protein-1
BCR-	Breakpoint Cluster Region
BRCA1-	Breast Cancer 1
CA9-	Carbonic Anhydrase IX
CCND1-	Cyclin D1
cyclin E1-	Cyclin E1
CDC20-	Cell Division Cycle 20 homolog
CDC34-	Cell Division Cycle 34 homolog
CDH1-	Cadherin 1
CDKN2A-	Cyclin-Dependent kinase inhibitor 2A (melanoma, p16, inhibits CDK4)
DIRC3-	Disrupted in Renal Carcinoma 3
DKK-	Dickkopf
E2-EPF -	Ubiquitin-conjugating enzyme E2-EPF (UBE2S)
EMI1/2-	Early Mitotic Inhibitor 1/2
ETS-	Erythroblastosis virus E26 oncogene homolog 1
EWS-	EWing Sarcoma

EZH2-	Enhancer of Zeste Homolog 2
FBXW7-	F-box and WD repeat domain containing 7
FH-	Fumarate Hydratase
FHIT-	Fragile Histidine Triad protein
FLCN-	Folliculin
GAPDH-	Glyceraldehyde-3-Phosphate Dehydrogenase
HIF-	Hypoxia Inducible Factor 1
HSPBAP1-	(heat shock 27kDa) associated protein 1
IRS-1 -	Insulin Receptor Substrate 1
JARID1C-	Jumonji, AT rich Interactive Domain 1C (RBP2-like)
JUN-	V-jun avian sarcoma virus 17 oncogene homolog
KCNIP4-	Kv channel interacting protein 4
LSAMP-	Limbic System-Associated Membrane Protein
MAPK-	Mitogen-Activated Protein Kinase 1
MET-	Met proto-oncogene (hepatocyte growth factor receptor)
MLH1-	mutL homolog 1
MLL2-	Mixed-Lineage Leukemia 2
mTOR-	mechanistic Target Of Rapamycin (serine/threonine kinase)
NF1-	Neurofibromin 1
NFκB-	F-box and WD-40 domain protein 7
NORE1-	Novel Ras Effector 1
PAX5-	Paired Box protein 5

PBRM1 -	Polybromo 1
PDGF-	Platelet-Derived Growth Factor
PDGFR-	Platelet-Derived Growth Factor Receptor
PHD-	Prolyl Hydroxylase
PML-	Promyelocytic Leukemia
PTEN -	Phosphatase and TENsin homolog
RAR-	Retinoic Acid Receptor
RASSF1-	Ras Association (RalGDS/AF-6) domain Family member 1
RB1-	Retinoblastoma 1
RBX-1 -	Ring-Box 1
SCL-	Stem Cell Leukaemia
SDH-	Succinate Dehydrogenase
SETD2-	SET Domain containing 2
SFRP-	Secreted Frizzled-Related Protein 2
SKP2-	S-Phase Kinase-associated Protein 2
TEL	Transcription factor ETV7
TRC8-	Translocation in Renal Cancer from Chromosome 8
TSC-	Tuberous Sclerosis
UbcH10-	Ubiquitin conjugating enzyme H5 (UBE3D)
UbcH5-	Ubiquitin conjugating enzyme H5 (UBE2D1)
UBE2QL1-	Ubiquitin-Conjugating Enzyme E2Q family-Like 1
VEGF-	Vascular Endothelial Growth Factor

VHL- Von Hippel-Lindau
 β -TRCP - β -Transducin Repeat-Containing Protein

Chapter One: Introduction

1.1 Cancer is a genetic disease

In 1960 the abnormal Philadelphia (ph) chromosome found in chronic myelogenous cells was the first evidence of a genetic abnormality causing cancer (Randolph 2005). Following this it was soon realised that mutations and alterations in normal cellular genes are able to initiate the onset of cancer leading to the now accepted notion that cancer is a genetic disease (Cairns 1975). Since then the central aim of cancer research has been to identify these cancer genes in the hope of further understanding the changes in the molecular biology of the cancer cell.

Tumour karyotypes often show multiple abnormalities that arise due to the genetic instability of the cancer genome (Liang et al. 2010). This instability is due to the accumulation of mutations and aberrations of cancer genes along with multiple cycles of clonal selection leading to the disruption of cell signaling pathways involved in proliferation, migration, transcription, growth, DNA repair, differentiation and cell death (Feinberg et al. 2006). Cancer genes often play a major role in these cell signalling pathways and can be altered in cancers in a number of ways including single nucleotide mutations, small deletions, promoter methylation, whole gene deletions, alterations in structural components of chromosomes and whole chromosomes deletions or duplications (Balmain et al. 2003). Cancer genes are loosely characterised into two types; tumour suppressor genes and oncogenes (Cornelisse & Devilee 1997) (*Figure 1.1*).

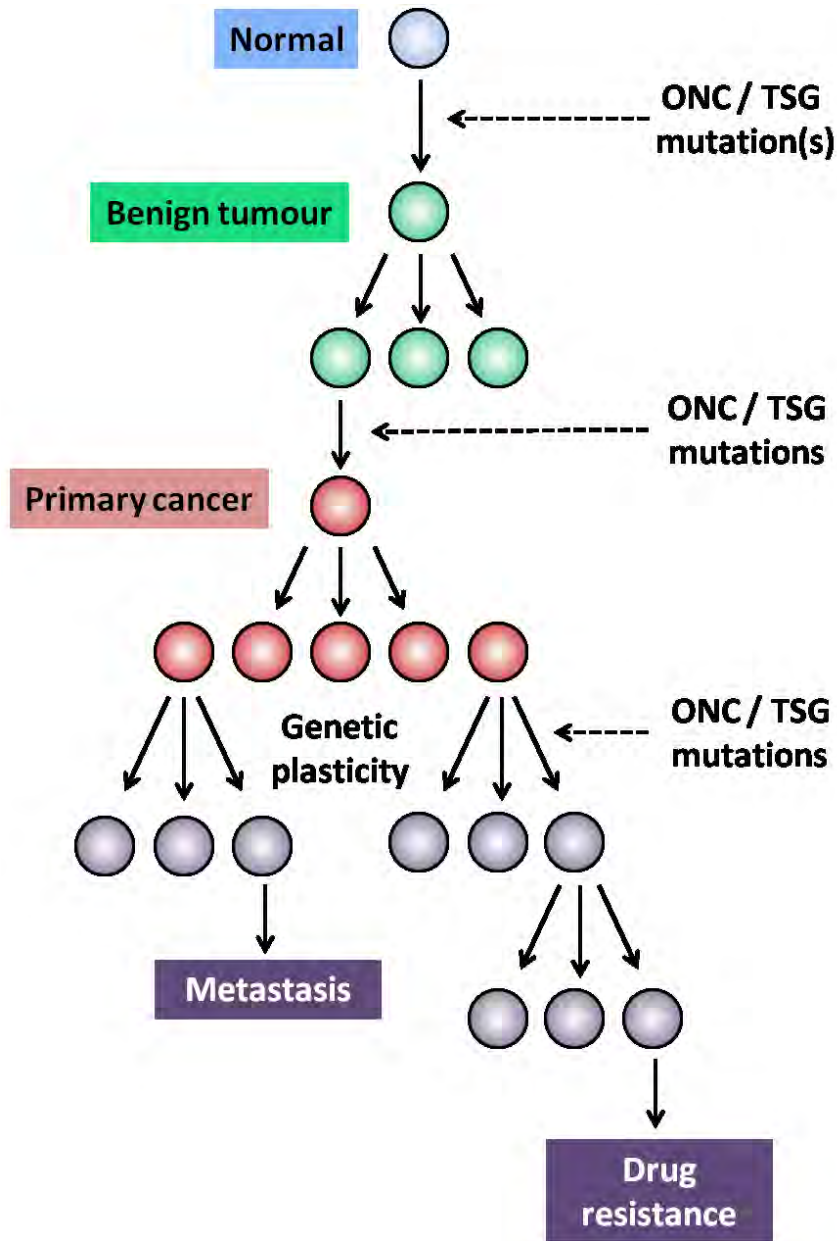


Figure 1.1 Clonal evolution of tumourigenesis

The theory of cancer arising from multiple rounds of clonal selection involves the initial mutation(s) of important disease causing oncogenes (ONC) and/or tumours suppressor genes (TSG). Each ONC and/or TSG mutation is thought to give the cell a competitive advantage leading to the selective expansion of a clonal population. Further ONC and TSG mutations lead to successive waves of clonal expansion thus increasing genetic plasticity which ultimately leads to the progression of tumour characteristics such as metastasis and drug resistance (Feinberg et al. 2006).

1.1.1 Oncogenes and mechanisms of activation

Cancer causing viruses provided the first evidence of cancer genes that appeared to drive oncogenesis in a dominant fashion and thus were subsequently termed oncogenes. When mouse fibroblasts were transfected with DNA from human cancer cells they began to show similar properties to the malignant cells. This transforming ability of the human DNA was found to be due to the mutated human homologue of the retroviral *RAS* oncogene (Capon et al. 1983). Since then many oncogenes have been identified and have often been shown to code for proteins that play an important role in cell proliferation, growth, differentiation and apoptosis, for example the RAS proteins were later found to deliver signals from cell surface receptors which fed into a number of these pathways (Hofer et al. 1994).

The non-mutated form of an oncogene is termed a proto-oncogene: these are genes that have the potential to become oncogenes when mutated. There are many different mechanisms that can lead to the structural alteration of a proto-oncogene causing the activation of its oncogenic affects, these include mutations, translocations leading to gene fusion or juxtaposition of enhancer elements and gene amplification (Croce 2008). Chromosomal rearrangements can cause the transcriptional deregulation of an proto-oncogene, for example in Burkitt's lymphoma the t(8;14) translocation causes the c-MYC proto-oncogene to be translocated next to the immunoglobulin enhancer thus leading to its increased expression (Joos et al. 1992). Fusion genes that are created by

chromosomal translocations can act in an oncogenic fashion, the most well-documented example of this is the ph chromosome associated with chronic myeloid leukaemia, created by a reciprocal translocation involving chromosomes 9 and 22 creating a BCR/ABL fusion protein with increased tyrosine kinase activity, thus exhibiting oncogenic effects (Randolph 2005). Mutations that cause the activation of an proto-oncogene often change the structure of the encoded protein allowing the enhancement of its oncogenic activity, for example mutations found in the *RAS* oncogenes (*KRAS*, *HRAS* and *NRAS*) encode for RAS proteins that remain constitutively active thus continuously transduce signals (Bos 1988).

1.1.2 Tumor suppressor genes and the ‘two-hit’ model

Tumour suppressor gene (TSG) protein products often function in cell cycle control, growth, proliferation, apoptosis initiation, senescence and DNA damage repair pathways. They are inactivated through a number of mechanisms including genetic alterations such as nucleotide mutations, gene deletions and chromosome translocations or by epigenetic alterations such as DNA methylation and chromatin alterations (Berger et al. 2011). In 1969 a number of somatic cell fusion experiments demonstrated the existence of TSGs by fusing normal cells with malignant cells which caused the suppression of the tumorigenicity in the malignant cells (Harris et al. 1969). These experiments suggested TSGs were recessive and that both alleles of the TSG must be completely inactive for the tumorigenicity to occur which led to the hypothesis of the ‘two-hit’ model of tumour suppressor gene inactivation (Knudson 1971). Knudsons two-

hit model came from his work on the genetic mechanisms of retinoblastoma, a childhood cancer of the retina. Researchers at the time originally thought that retinoblastoma could be caused by either somatic or germline mutations of the causative gene, now known as *RBI* (Schappert-Kimmijser et al. 1966). Yet Knudson's studies observed that in some cases offspring from an affected parent did not develop retinoblastoma, though their offspring did, thus suggesting a germline mutation could be inherited without developing the disease. Knudson also noted that the majority of non-inherited retinoblastoma cases were unilateral whereas inherited cases were more commonly bilateral, more importantly he examined the age at which inherited bilateral cases occurred and bilateral non-inherited cases occurred. Not surprisingly he established that diagnosis of bilateral inherited retinoblastoma occurred at a much younger age to that of bilateral non-inherited cases, suggesting only one mutation needed to occur in inherited cases. Knudson produced mathematical calculations from his clinical data to conclude retinoblastoma was most likely caused by two mutations, one in each allele of the *RBI* gene, thus leading to the two-hit hypothesis (Knudson 1971). It was later discovered that many families with familial retinoblastoma showed germline *RBI* mutations or deletions (this was the first hit) and RB tumours were nearly always shown to contain a mutation or deletion in the second *RBI* allele (the second hit) (Benedict et al. 1983). Biallelic disruption of *RBI* was soon after shown to occur in non-hereditary retinoblastomas (Dryja et al. 1984). The 'two-hit' model allowed an explanation for the susceptibility of hereditary cancer and instigated the study of chromosome deletions and genetic linkage in hereditary cancers along with analysis of the second alleles. These investigations ultimately led to the

identification of a number of important and well known tumor suppressor genes including *TP53*, *BRCA1* and *BRCA2* (Malkin et al. 1990; Smith et al. 1992; Gudmundsson et al. 1995). It was initially thought that the two hits would be sufficient to cause tumorigenesis in some cancers where in others more mutations would be needed. It is now thought that in hereditary cancer syndromes complete inactivation of the cancer causing gene could be the rate-limiting step for the initiation of tumorigenesis yet other events most likely occur to promote tumour progression. Sporadic cancers are thought to require at least four distinct mutation events resulting in the deregulation of important signalling pathways (Fearon & Vogelstein 1990; Berger et al. 2011).

1.1.3 Tumour suppressor gene haploinsufficiency

Although the ‘two-hit’ model has been proven for TSGs in many cancer syndromes and sporadic cancers there are still cases where second hits are not found. For example in sporadic cancers the re-occurrence of chromosomal deletions in specific regions has been observed suggesting an importance of these regions in tumorigenesis, though second hits in the genes within these regions are not often found (Paige 2003). One theory to explain this is the existence of haploinsufficient tumor suppressor genes. Haploinsufficiency indicates that in certain circumstances one working allele is insufficient for the gene product to accomplish normal activity (Fisher & Scambler 1994). There have been a number of tumour suppressor genes that have shown evidence of haploinsufficiency for example one study showed *p53* +/- mice showed a higher number of chromosomal aberrations compared to *p53* ++ and a lower number compared

to *p53*^{-/-} (Venkatachalam et al. 1998). In the cancer susceptibility syndrome Li-Fraumeni syndrome, caused by germline *p53* mutations, loss of the wildtype *p53* allele in the tumour is not always shown (Varley et al. 1997). Another example is the TSG *PAX5* found to be disrupted in about 30% of acute lymphoblastic leukaemia patients, although, in most cases, this only occurs in one allele and is thought to function as a hypomorph, that is the mutations only cause partial loss of the gene function (Mullighan et al. 2007). The hypothesis of haploinsufficient TSG involvement in cancer has been met with scepticism. This mainly derives from the inability to determine which single mutations are involved in tumorigenesis due to haploinsufficiency and which are simply passenger mutations caused by the genetic instability of the cancer cell (Santarosa & Ashworth 2004). TSGs involved in tumorigenesis can be identified by the disruption of the second allele when applying the ‘two-hit’ model though this method cannot be applied to determining haploinsufficient TSGs. In fact the only method to date to determine if a haploinsufficient TSG is involved in tumorigenesis is by performing lengthy *in vitro* or *ex vivo* functional studies (Berger & Pandolfi 2011).

1.1.4 Epigenetic tumour suppressor gene inactivation

The field of cancer epigenetics is rapidly growing as it was revealed that many cancers show global changes in their epigenetic landscape compared to normal cells (Cheung et al. 2009). Cancer is no longer seen as a solely genetic disease but as a genetic and epigenetic disease. The term epigenetic refers to changes in gene expression that occur independent of changes in the primary DNA sequence. Cancer epigenetics has

shown disruptions in a number of epigenetic machinery including DNA methylation, non-coding RNAs and histone modification (Clark & Melki 2002).

TSG DNA methylation has become one of the more extensively studied regions of cancer epigenetics. DNA methylation occurs by covalently modifying cytosine residues in CpG dinucleotides found at CpG islands. These CpG rich islands are located at the 5' promoter regions of ~60% of human genes (Wang & Leung 2004). The CpG dinucleotide occurs at a much lower frequency than what would be expected within the human genome; the GC content is 42% in the human genome therefore the expected frequency of CpGs occurring due to chance should be ~4.41% (0.21×0.21), though CpGs actually occur at a frequency of ~1% within the genome. This lower frequency of CpG dinucleotides is thought to be due to spontaneous deamination of methylated cytosines (methylcytosines) to thymine as CpGs within the genome are normally methylated (Bird 1980). This is not the case for CpGs within CpG islands found at gene promoters as these are normally unmethylated and are extremely GC-rich, thus the human genome is made up of regions of extremely high GC content at gene promoter regions and low GC content elsewhere (Antequera & Bird 1999). The majority of CpG islands often remain unmethylated in differentiated tissue and during development. Gene silencing through promoter methylation normally occurs to regulate expression of tissue specific genes and where long term transcriptional silencing must occur for example X-chromosome inactivation and imprinted genes (Suzuki & Bird 2008). The methylated CpG islands initiate gene silencing by either promoting or preventing the recruitment of

regulatory proteins to the gene promoter, for example promoter methylation can block transcription factors from binding thus inhibiting gene transcription (Prendergast & Ziff 1991). Methylated CpGs can also bind methyl-binding domain proteins which can interact with histone deacetylases instigating chromatin compaction and gene silencing (Szyf 2006) (*Figure 1.2*).

Many cancer genomes are globally hypo-methylated with only site specific hyper-methylation occurring often at the promoters of TSGs (Jones & Baylin 2002). It has been suggested that some of these methylation events can occur early on in the development of cancer and could potentially contribute to the initiation of tumourigenesis (Feinberg et al. 2006). The first TSG promoter found to be hyper-methylated as a mechanism of gene inactivation was the *RB* gene in retinoblastoma (Greger et al. 1989). Since then, numerous TSGs have been found to undergo tumour-specific hyper-methylation, for example the *BRCA1* gene in breast cancer, the *VHL* gene in renal cell carcinoma and the *MLH1* mismatch repair gene in colorectal cancer (Jing et al. 2007; Gnarra et al. 1994; Vlaykova et al. 2011). TSG promoter methylation has therefore been shown to function as one of the two hits in sporadic cancers. There are also a number of cases where promoter methylation has constituted as a second hit in familial cancers for example *APC* and *BRCA1* in breast and colorectal inherited cancers (Esteller et al. 2001). Hyper-methylation of both alleles of known TSGs has also been noted in sporadic tumours in the absence of any genetic disruptions (Herman & Baylin 2003).

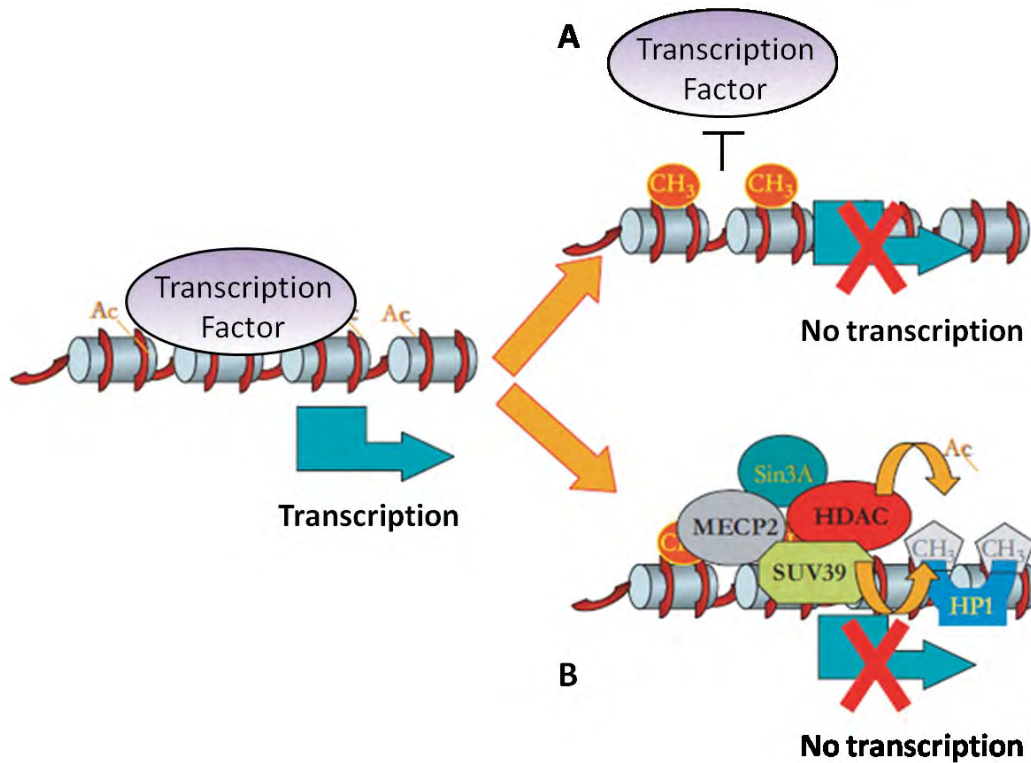


Figure 1.2 Gene silencing by methylation

Histones linked to unmethylated genes become hyperacetylated and allow the access of transcription factors to the promoter region, activating gene transcription. **A**, Promoter methylation can prevent the binding of important transcription factors, inhibiting gene transcription. **B**, Methylated CpGs can recruit methyl-binding domain proteins such as MeCP2 which interact with histone deacetylases (HDAC) and histone methyltransferases such as SUVh3, which in turn methylate H3-histones further inactivating the chromatin by recruiting HP1 an important component of heterochromatin packaging, thus preventing gene transcription (Adapted from Szyf, 2006).

How TSGs are specifically targeted for this aberrant methylation in cancers is still unclear. One idea is that random silencing of certain genes by hyper-methylation offers the cell a growth advantage which ultimately leads to their clonal selection and continued proliferation (Huang et al. 1999). Another theory involves the initial activation of oncogenic transcription factors which can signal to DNA methyltransferases to target specific genes for methylation, for example the PML-RAR fusion protein found in acute promyelocytic leukemia initiates the hyper-methylation and silencing of a number of specific genes through this mechanism (Croce et al. 2002). It has also been observed that direct alterations and dysregulation of histone methyltransferases that normally mark specific regions of the genome for methylation can lead to altered distribution of these marks and aberrant TSG methylation, for example the histone methyltransferase EZH2 has often been shown to be overexpressed in prostate and breast cancers leading to hyper-methylation of a number of TSGs in these cancers (Simon & Lange 2008). Large sections of DNA are commonly found to be methylated in many cancers thus resulting in the hyper-methylation of important TSGs due to their location within these regions (Frigola et al. 2006).

As epigenetic changes are often reversible a number of epigenetic drugs have been discovered that could potentially reverse the epigenetic aberrations that occur in cancers. DNA methylation inhibitors 5-azacytidine (azacitidine) and 5-aza-2'-deoxycytidine (decitabine) are nucleoside analogs which can become incorporated into

the DNA of tumour cells due to their rapid growth and can lead to the inhibition of DNA methylation as they trap DNA methyltransferases onto the DNA, inhibiting their activity. As the TSGs are no longer methylated in the cancer cells treated with these two drugs their expression causes growth inhibition (Yoo & Jones 2006). Azacitidine and decitabine are both FDA approved in the treatment of myelodysplastic syndromes and haematological malignancies (Plimack et al. 2007; Santini 2009).

1.1.5 DNA repair genes in cancer development

Another set of genes that are often deregulated in cancers are the DNA repair pathway genes. The normal functioning of DNA repair pathways are essential for cell viability and genome integrity. DNA damage and double stranded breaks (DSB) can be caused by a number of factors, including environmental factors such as ionising radiation, UV light and some chemicals, and normal biological factors such as during DNA replication, V(D)J recombination and oxidative deamination (Hoeijmakers 2009). There are a number of DNA repair mechanisms in place to ensure the integrity of the cells genome including excision repair processes to repair single bases and single DNA strands, for example base excision repair (BER), nucleotide excision repair (NER) and mismatch repair (MMR) (Marti et al. 2002). When both strands of DNA are disrupted these are known as double stranded breaks (DSB) and can be extremely damaging to cells as they can cause genome rearrangements. In Eukaryotic cells there are two primary pathways that are involved in DSB repair; nonhomologous end joining (NHEJ) and homologous recombination (HR) (Chapman et al. 2012). Homologous recombination

(HR) involves repair of DSBs through the use of a complementary template strand of DNA; either a sister chromatid or homologous chromosome. HR often occurs during late S to G2 phase of the cell cycle when sister chromatids are present. NHEJ involves the joining of DNA strands without the need for a homologous template. DSB often have short single stranded overhangs at the ends of the strands, these are known as microhomologies and are often utilised in NHEJ to guide repair. When these microhomologies are not complementary imprecise repairing can occur leading to loss of nucleotides during the re-joining of strands. Inappropriate NHEJ can lead to telomere fusions and chromosomal translocations (Lieber et al. 2010). Failure or disruption of DNA repair pathways can cause permanent cell cycle arrest, cell death by apoptosis or can lead to unregulated cell division which can contribute to tumourigenesis.

Accumulation of DNA damage significantly contributes to the development of cancer due to the disruption of genes involved in the regulation of critical cell pathways such as proliferation. It is suggested that most cancer cells are genetically unstable due to selective pressures to lose their DNA repair pathway components. Therefore it is not surprising that a number of the components involved in DNA repair pathways have been found to be associated with both inherited and sporadic cancers (Jin & Robertson 2013). Hereditary nonpolyposis colorectal cancer (HNPCC) and lynch syndrome have both been associated with mutations in DNA mismatch repair (MMR) genes such as *MLH1*. Disruptions in MMR genes often lead to microsatellite instability which is a hallmark of HNPCC (Bellizzi & Frankel 2009; Andersen et al. 2012). *BRCA1* and *BRCA2* are well

known to be associated with both hereditary and sporadic breast cancer, both of these genes are important components of the HR DNA repair pathway and *BRCA2* along with other known HR genes: *PALB2*, *RAD51C* and *BRIP1*, have also been associated with Fanconi anaemia (FA), a recessive disorder that is characterised by genomic instability and cancer susceptibility (Evers et al. 2010). Dysregulation of NHEJ can result in chromosomal rearrangements including deletions, insertions and translocations and thus can ultimately contribute to tumourigenesis in a number of ways, for example chromosomal translocations formed by inappropriate NHEJ can lead the formation of oncogenic fusion genes found in a number of human cancers (Kasperek & Humphrey 2011) (see section 1.2).

1.2 Chromosomal rearrangements

Chromosomal rearrangements play an important role in human birth defects, infertility and cancer. In the general population the frequency of constitutional chromosomal rearrangements has been shown to vary in populations from 1/625 to 1/5000 (Bandyopadhyay et al. 2002). These chromosomal aberrations can either be constitutional; those that are inherited from carrier parents or occur in the gametes and are therefore present in every cell of the body, and acquired; those that occur during the development or life of an organism (Page et al. 1996). They can be further divided into intra-chromosomal and inter-chromosomal rearrangements. Intra-chromosomal rearrangements are aberrations that occur in a single chromosome, either a single homologue or a pair of homologous chromosomes. The type of intra-chromosomal

aberrations that can occur include interstitial deletions and duplications (occur within the interior of a chromosome), terminal deletions and duplications (occur at the ends of a chromosome), inversions (a segment of a chromosome is flipped around and re-inserted) and isochromosomes (one arm is deleted and replaced with an exact copy of the other arm). Inter-chromosomal rearrangements involve two different chromosomes and occur in the form of chromosomal translocations which can be divided into Robertsonian and reciprocal translocations (Shaffer & Lupski 2000).

1.2.1 Chromosomal translocations.

Chromosome translocations are labelled using a standard system devised by the International System for Human Cytogenetic Nomenclature (ISCN), which designates that $t(A;B)(p1;q2)$ should be used where 't' stands for translocation and A and B are the two chromosomes involved. The second parenthesis gives the exact location of the translocation where p refers to the short arm of the chromosome and q refers to the long arm. The numbers after p and q indicate the cytogenetic bands seen on the chromosome after staining (G-banding) which are numbered successively from the centromere outwards. Robertsonian translocations are denoted as $rob(AqBq)$ where rob stands for Robertsonian and Aq and Bq refer to the long arms of each of the chromosomes involved (Gonzalez Garcia & Meza-Espinoza 2006).

Robertsonian translocations occur in approximately 1/1000 individuals and involve whole arm exchanges between acrocentric chromosomes; chromosomes with

their centromere close to one end producing one very short arm and one long arm (Hamerton et al. 1975). There are five acrocentric chromosomes present in humans; chromosomes 13, 14, 15, 21 and 22. All possible combinations of acrocentric chromosomes in robertsonian translocations have been identified though their frequency is not random as rob(13q14q) and rob(14q21q) constitute for about 85% of all robertsonian translocations (Page et al. 1996) (*Figure 1.3*).

Reciprocal translocations are the most common type of translocation and occur in approximately 1/625 individuals in the general population (Shaffer & Lupski 2000). They involve the transfer of material between two nonhomologous chromosomes and often results from a single break in each of the two chromosomes. All chromosomes have been shown to participate in reciprocal translocations. When there is no loss or gain of chromosomal material (on normal cytogenetic preps) the translocation can be described as balanced, conversely if there is a loss or gain of genetic material the translocation is said to be unbalanced (Strefford et al. 2009) (*Figure 1.3*). The majority of reciprocal translocations are often random private events that are specifically found in related family members. However the recurrent t(11;22)(q23;q11.2) has been revealed to be relatively common in the general population and has been shown to be associated with increased risk of breast cancer (Youings et al. 2004; Lindblom et al. 1994).

Reciprocal translocations often occur at region specific low-copy repeats (LCRs); these repetitive regions of DNA are thought to predispose the region to nonhomologous recombination events that result in chromosomal rearrangements. The major recombination pathway thought to facilitate the occurrence of translocations is the repair of DNA double-strand breaks (DSB) by non-homologous end joining (NHEJ) (Pierce et al. 2001) (section 1.1.5). Other repetitive genomic regions that are often involved in chromosomal translocations include variable number tandem repeats (VNTRs) and AT-rich regions (Stankiewicz & Lupski 2002). For example the common t(11;22) breakpoint has been mapped within a LCR on chromosome 22q and a 190bp AT-rich region on chromosome 11q (Edelmann et al. 1999).

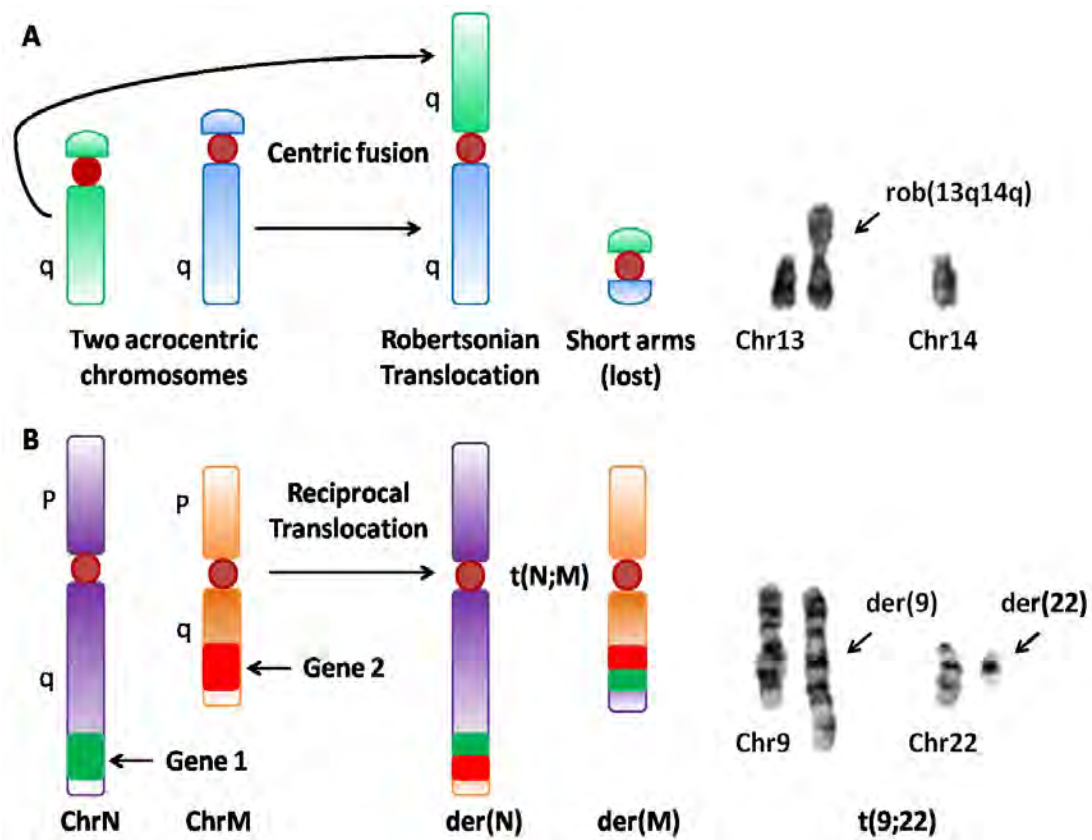


Figure 1.3 Robertsonian and reciprocal chromosomal translocations.

*A, To the right a schematic diagram of a Robertsonian translocation where q stands for the q arm of the acrocentric chromosomes. The short arm fusions are often lost. To the left G-banding of chromosomes 13 and 14 showing rob(13q14q).
 B, To the right an illustration of a reciprocal translocation involving the ends of the q arms from each chromosome, disrupting two genes (shown as green or red bands) potentially creating a fusion gene(s). To the left G banding of chromosomes 9 and 22 showing t(9;22), der(22) shows the infamous Philadelphia chromosome associated with CML.(G-band images taken from Shamsi et al. 2011; Czuchlewski et al. 2011).*

1.2.2 Somatic chromosomal translocations in cancer

Chromosomal translocations are frequently detected in human cancers and are divided into primary aberrations where by the translocation acts as an initiation event towards the development of cancer, or secondary aberrations that have been acquired due to clonal selection and often play a role in cancer progression (Mitelman et al. 2007). Reciprocal balanced translocations often produce fusion genes which can be found in a number of cancers for example the *BCR/ABL* fusion gene caused by the t(9;22) found in CML described in section 1.1.1 (*Figure 1.3*) and the fusion of ETS and EWS gene families caused by a number of different translocations often involved in Ewing's sarcoma (Nambiar et al. 2008). In fact more than 350 fusion genes involving over 330 different genes have been detected in a variety of cancers, though their prevalence varies considerably between tumour types with the majority occurring in malignant haematological disorders. (Mitelman et al. 2007). Translocations that do not lead to the formation of fusion genes have also been detected in cancers including unbalanced translocations that lead to gene dysregulation due to the loss or gain of genetic material for example in acute lymphoblastic leukaemia a number of t(1;14) with interstitial deletions have been shown to disrupt the *SCL* (Stem cell leukaemia) gene locus causing dysregulation of *SCL* gene expression (Bernard et al. 1990). Translocations can also directly disrupt genes due to their position being at or close to the breakpoint for example t(1;17) reciprocal translocations have been characterised in neuroblastomas that lead to the dysregulation of a number of tumour suppressor genes found at the breakpoints

including the *NFI* gene on chromosome 17 (Laureys et al. 1995). In some instances translocations relocate genes close to or away from transcription enhancers leading to gene dysregulation for example the t(8;14) that causes the c-MYC oncogene to be overexpressed due to the neighbouring immunoglobulin enhancer previously described in section 1.1.1 (Joos et al. 1992).

1.2.3 Chromosomal translocations used to identify candidate cancer genes

Although many translocations have been detected in cancers it is important to determine which are primary and therefore disease causing aberrations and which are secondary aberrations. Translocations involved in disease initiation can be used to identify candidate disease genes which could become potential therapeutic targets. One method is to identify recurrent genomic aberrations found in particular cancers. Key genes within these regions can then be identified through breakpoint characterisation using techniques such as FISH and array-based profiling (see sections 1.2.4 and 1.2.5). Once a specific gene or a number of genes have been ascertained further investigation on copy number changes, mutation analysis, epigenetic changes and expression alterations can be undertaken in a larger sample cohort to determine if the genes are potentially disease causing, this method is outlined in *Figure 1.4* (Albertson et al. 2003; Strefford et al. 2009). Common translocations in cancer syndromes have been used to identify candidate cancer causing genes for example the acquired t(5;12) is a rare translocation found in some cases of chronic myelomonocytic leukaemia (CMML) a myelodysplastic syndrome that often progresses to acute myeloid leukaemia. The t(5;12) was shown to

produce a fusion protein involving the *PDGFR* and *TEL* genes (Golub et al. 1994). This identification of *PDGFR-TEL* helped discover that *TEL* was also an important candidate gene in childhood acute lymphoblastic leukaemia where it often forms a fusion protein with *AML1* (Golub et al. 1995).

Familial constitutional translocations that correlate with a specific cancer can be used to determine candidate genes that may also play a role in the sporadic forms of that particular cancer, for example constitutional chromosomal aberrations involving 13q including translocations and deletions were shown to occur in a number of familial cases of retinoblastoma (Bunin et al. 1989). The 13q region was later revealed to contain the *RBI* gene, shown to be disrupted in all sporadic and familial retinoblastoma cases (Horsthemke 1992).

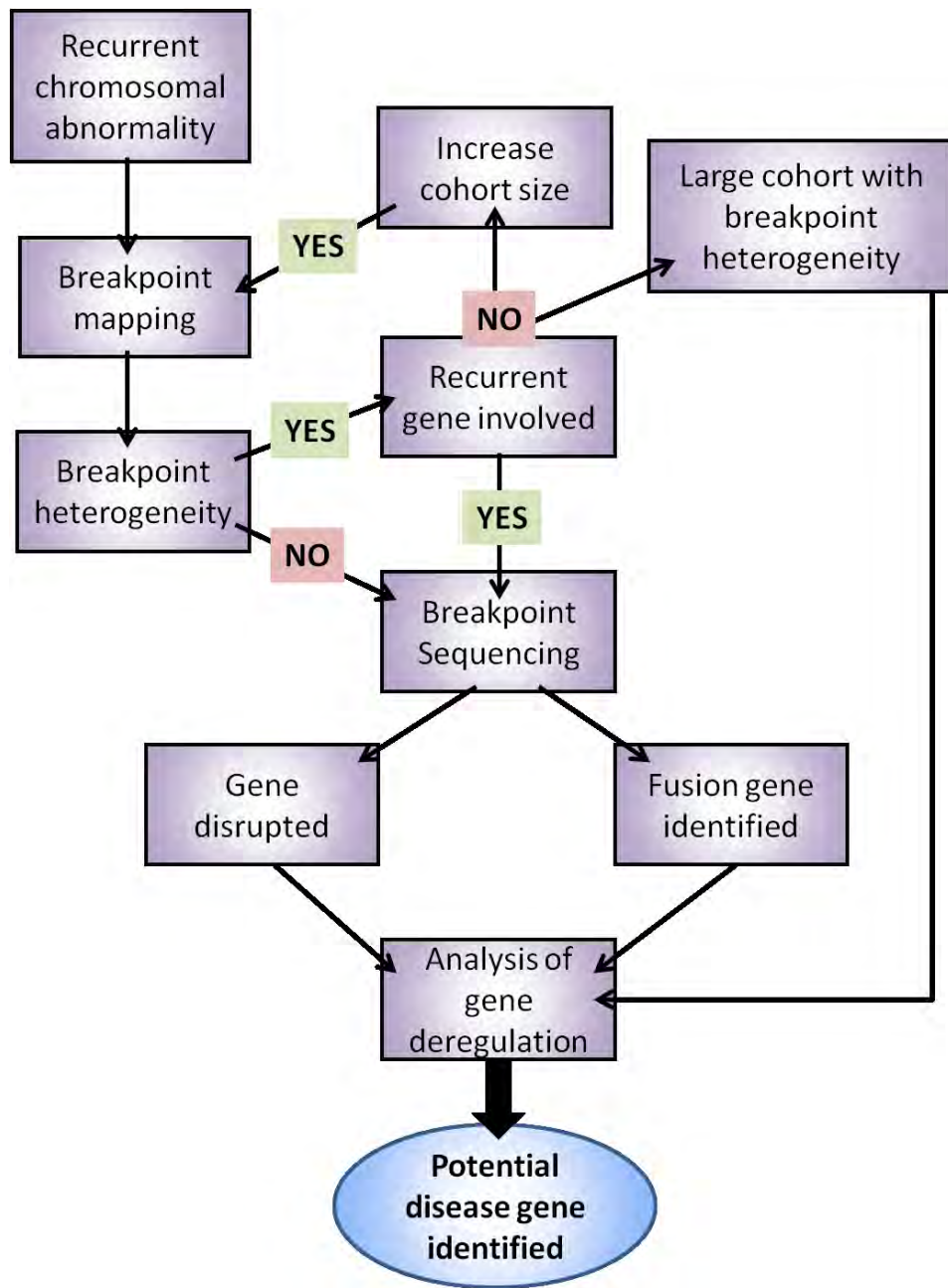


Figure 1.4 Identifying cancer genes from disease associated translocations.
 A schematic diagram outlining one method to identify cancer causing genes from cancer associated translocation (Strefford et al. 2009).

1.2.4 FISH based cytogenetic techniques to detect chromosomal abnormalities

There has been significant progress in cytogenetic analysis over the last decade which has allowed fast and accurate detection of structural aberrations using high resolution techniques. Although conventional techniques such as karyotyping and chromosome banding are still used today their detection is limited to the identification of microscopic structural abnormalities along with numerical abnormalities including aneuploidy and polyploidy (Sandberg 1985). New high resolution methods have now been developed which allow detection of submicroscopic cytogenetic aberrations. These new techniques were initiated from the development of FISH (fluorescence *in situ* hybridisation) in the 1980s which involves designing specific fluorescently labelled DNA probes that are used to bind complementary target sequences often on metaphase spreads (Bauman et al. 1980). To label whole chromosomes for the detection of aberrations such as translocations, chromosome painting was introduced which utilises whole chromosome specific DNA probes as opposed to region specific probes (Cremer et al. 1988). Since then a number of techniques have been developed that apply similar methods to the FISH technique while using different probes and/or target sequences, for example oligonucleotide probes have been used to increase resolution in oligonucleotide-based high resolution FISH and chromatin fibres have been used instead of condensed chromosomes as target sequences in fibre-FISH methods (Yamada et al. 2011; Heng & Tsui 1998). Other FISH modified techniques allow detection of abnormalities on a whole genome scale for example comparative genome hybridisation (CGH) can be used to detect copy number differences between two genomes as well as multipoint-FISH and

SKY (spectral karyotyping) which allow detection of more complex rearrangements by labelling all chromosomes thus allowing identification of cytogenetic aberrations with no prior knowledge (Darai-Ramqvist et al. 2006; Schröck et al. 1996). Although useful in determining chromosomal aberrations at a higher resolution than chromosome staining these FISH based techniques are still restricted due to the use of chromosomes as target sequences (Scouarnec & Gribble 2012).

1.2.5 Array based cytogenetic techniques to detect chromosomal abnormalities

Array-based technologies involve the immobilisation of nucleic acid probes such as oligonucleotide probes which function as the arrays. RNA or DNA targets are then directed to the array surface where they hybridise to the complementary probes thus allowing for increased sensitivity and resolution as the targets can represent thousands of regions within the genome. Array-CGH is one of the more widely used array techniques and though originally the arrays consisted of large BAC (bacterial artificial chromosomes) clones they have recently been modified to consist of small oligonucleotide probes increasing resolution to up to a few kilobases (Fiegler et al. 2003; Barrett et al. 2004). Array-CGH enables the detection of deletions and amplifications allowing identification of unbalanced translocations though they cannot detect balanced aberrations such as inversions and reciprocal balanced translocations (Scouarnec & Gribble 2012). Array painting is a relatively new technique that combines the methods of chromosome painting and CGH-arrays to allow fine mapping of chromosomal breakpoints. The technique initially involves the separation and isolation of the derivative

chromosomes involved in the translocation by flow sorting. The flow-sorted derivative chromosomes are then amplified using techniques such as whole genome amplification and are labelled with fluorescent dyes then co-hybridised onto a high-resolution oligonucleotide array (Gribble et al. 2009). These high-resolution techniques allow more precise breakpoint characterisation and have enabled sequencing of exact breakpoint positions (Gribble et al. 2007) (*Figure 1.5*).

The development of next-generation sequencing allows the sequencing of the whole human genome which can now be completed in a few days at a much lower cost (Coffey et al. 2011). This technique could now be utilised to determine chromosome aberrations by sequencing isolated chromosomes or derivative chromosomes which when aligned to the reference genome could be used to detect all types of chromosome aberrations including deletions, duplications, insertions, balanced/unbalanced translocations and inversions, thus providing a more rapid and accurate method to determine cytogenetic abnormalities (Scouarnec & Gribble 2012).

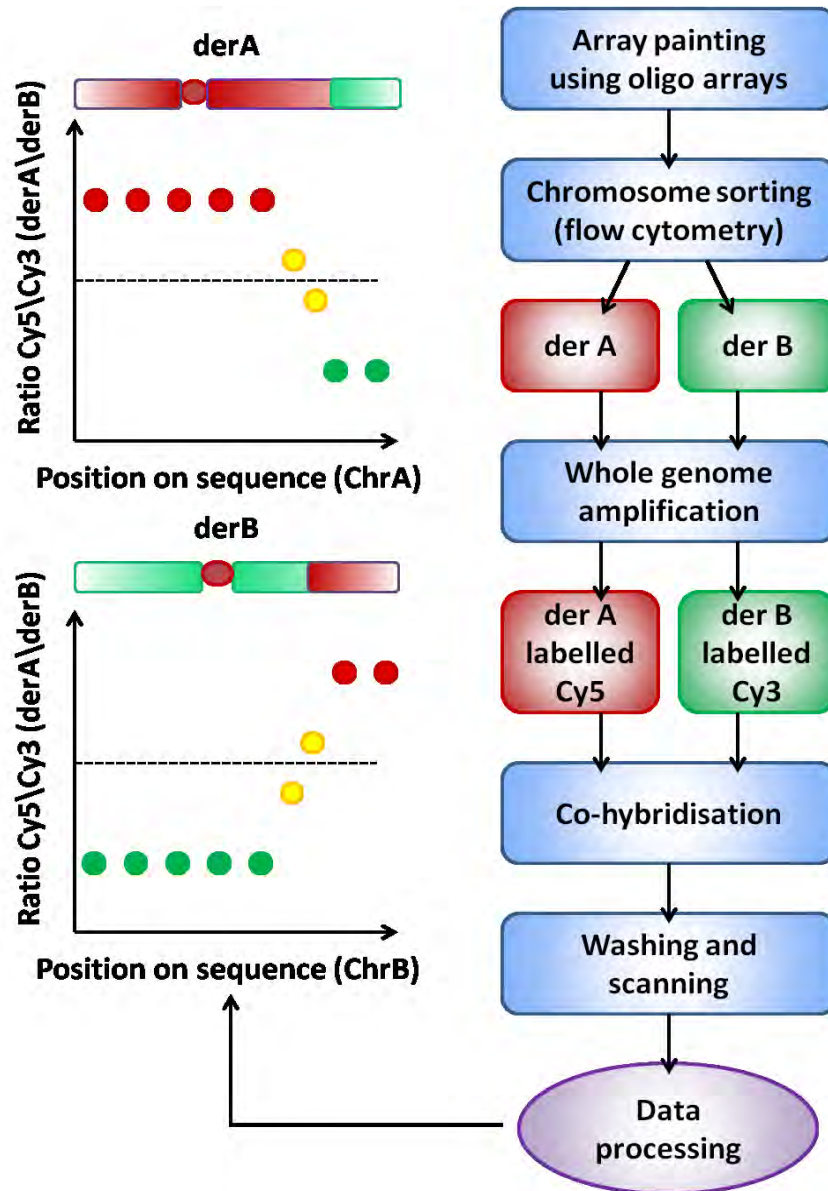


Figure 1.5 Array painting used to map chromosomal translocations.

Diagram of the main steps involved in oligonucleotide array painting involving separation and amplification of the derivative chromosomes which are then fluorescently labelled with cyanine 5 (cy5) or cy3 and co-hybridised to the oligonucleotide array (to the right) and a schematic illustration of the processed array data showing the change in cy5 (red)/ cy3 (green) ratio at the breakpoint position (yellow) (to the left) (Gribble et al. 2009).

1.3 Renal cell carcinoma

Renal cell carcinoma (RCC) attributes for approximately 85% of all renal cancers and 3% of total adult malignancies (Bodmer et al. 2002). It is a heterogeneous disease with varying histopathology based on the cell type and location in the nephron. Clear cell RCC (ccRCC) is the most common form of RCC and accounts for 60-80% of all sporadic renal carcinomas. Other histopathologies include papillary types I and II (10-15%), oncocytomas (~5%) and chromophobe tumours (~5%). ccRCC and papillary RCC originate from the epithelial cells of the proximal part of the renal tube and chromophobes and oncocytomas originate from the collecting tubule of the nephron (Oosterwijk et al. 2011). A number of newly identified RCCs were recently recognised which contribute to <1% of RCCs including translocation-linked carcinoma that arises from the proximal tubule and results in the *MiTF/TFE* fusion genes, mucinous tubular and spindle cell carcinoma both originating from the loop of Henle and tubulocystic carcinomas that develop from the collecting tubule (Argani & Ladanyi 2005; Yang et al. 2010; Deshmukh et al. 2011). RCCs can be further classified due to marked (cyto)genetic differences associated with each histopathology, this was originally demonstrated by the Mainz classification in 1986 and the Heidelberg classification of renal tumours in 1997 (Thoenes et al. 1990; Kovacs et al. 1997). More recently a renal cell tumour classification was proposed by the World Health Organization (WHO) in 2004, and updated in 2009, which is summarised in *Table 1.1* (Lopez-Beltran et al. 2006; Lopez-Beltran et al. 2009).

RCC subtype	Clear cell	Papillary	Chromophobe	Collecting ducts of Bellini	Medullary	Multilocular cystic	Xp11 translocation	After neuroblastoma	Mucinous tubular and spindle cell	Unclassified
Incidence	75%	10%	5%	1%	Rare	Rare	Rare	Rare	Rare	4-6%
Development	Solitary, rare multicentric or bilateral	Multicentric, bilateral or solitary	Solitary	Solitary	Solitary	Solitary, rare bilateral	Solitary	Solitary	Solitary	Solitary
Cell/tissue characteristics	clear cytoplasm; cells with eosinophilic cytoplasm occasionally	Type 1 (basophilic) or type 2 (eosinophilic)	Pale or eosinophilic granular cytoplasm	Eosinophilic cytoplasm	Eosinophilic cytoplasm	clear cytoplasm, small dark nuclei	Clear and eosinophilic cells	Eosinophilic cells with oncocytoid features	Tubules, extracellular mucin and spindle cells	Variable, sarcomatoid
Growth pattern	Solid, tubular, cystic, rare papillae	Tubulo-papillary, solid	Solid	Irregular channels	Reticular pattern	Cystic, no solid component	Tubulo-papillary	Solid	Solid	Solid
Prognosis	Aggressiveness according to grade, stage and sarcomatoid change	Aggressiveness according to grade, stage and sarcomatoid change	10% mortality	Aggressive, 2/3 of patients die within two years	Mean survival of 15 weeks after diagnosis	No progression or metastases	Indolent	Related to grade and stage	Rare metastases,	High mortality
Somatic genetic changes	-3p, +5q22, -6q, -8p, -9p, -14q, VHL gene mutation	+3q, +7, +8, +12, +16, +17, +20, -Y	-1, -2, -6, -10, -17, -21, hypodiploidy	-1q, -6p, -8p, -13q,	Unknown	VHL gene mutation	t (X; 1) (p11.2; q21), t (X; 17) (p11.2; q25), Other	Allelic imbalance at 20q13	-1, -4, -6, -8, -13, -14, +7, +11, +16, +17	Unknown

Table 1.1 Known clinico-pathological and genetic features of sporadic RCC tumours.

Table adapted from Lopez-Beltran et al. 2009.

1.3.1 Familial RCC

Although familial RCC accounts for only ~2% of all RCCs it is the study of these inherited forms which has provided important clues into the pathogenesis of the more common sporadic forms of the disease. Familial RCCs often present at an earlier age than sporadic RCCs and are frequently caused by inherited syndromes that predispose to RCC. VHL (Von Hippel-Lindau) disease is the most common cause of familial RCC and is characterised by a predisposition to the development of ccRCC (>70% lifetime risk), haemangioblastomas of the central nervous system, renal, pancreatic and epididymal cysts and pancreatic islet cell tumours (Maher et al. 1990). It was found to be caused by disruptions in the *VHL* tumour suppressor gene (Latif et al. 1993). Following its identification the *VHL* gene was subsequently shown to be mutated in up to 70% of sporadic clear cell RCCs (Crossey et al. 1994; Gnarra et al. 1994). Other inherited syndromes that predispose to RCC include Birt-Hogg-Dubé syndrome caused by disruptions in the folliculin (*FLCN*) gene, hereditary leiomyomatosis and renal cancer associated with mutations of the fumarate hydratase (*FH*) gene, hereditary pheochromocytoma-paranglioma syndromes are caused by mutations in the subunits of succinate dehydrogenase (*SDHB*, *SDHC* and *SDHD*) and Hereditary Papillary RCC syndrome correlating with mutations in the proto-oncogene *c-MET* (Maher 2011) (*Table 1.2*). In nonsyndromic cases of familial RCC the genetic basis of the disease is often unknown although in some cases germline mutations of *FLCN* and *SDHB* have been

detected with no clinical evidence of the RCC susceptibility syndromes (Silva et al. 2003; Woodward et al. 2008; Ricketts et al. 2008).

Constitutional chromosome 3 translocations have been shown to be associated with nonsyndromic familial RCCs in a small number of cases. The first was a constitutional $t(3;8)(p14;q24)$ translocation found in a large family, with ten family members developing RCC, while RCC did not develop in non-translocation carriers (A. J. Cohen et al. 1979). Since then 6 more constitutional translocations involving chromosome 3 have been associated with familial RCC these include $t(2;3)(q35;q21)$, $t(3;6)(q11.2;q13)$, $t(2;3)(q33;q21)$, $t(1;3)(q32;q13.3)$, $t(3;8)(p13;q24)$ and $t(3;8)(p14;q24.1)$ (Koolen et al. 1998; Kessel et al. 1999; Bonne et al. 2007; Podolski et al. 2001; Kanayama et al. 2001; Meléndez et al. 2003; Poland et al. 2007). A number of RCC cases that involve single individuals with chromosome 3 constitutional translocations have also been reported; $t(3;12)(q13.2;q24.1)$, $t(3;6)(p13;q25.1)$, $t(3;4)(p13;p15)$, $t(3;15)(p11;q21)$, $t(3;6)(q22;q16.2)$ and $t(3;4)(q21;q31)$ (Kovacs & Hoene 1988; Kovacs et al. 1989; Kessel et al. 1999; Bonne et al. 2007; Foster et al. 2007; Kuiper et al. 2009).

Syndrome	Gene	Tumour
Von Hippel-Lindau (VHL)	VHL (3p25)	Clear cell
Tuberous Sclerosis	TSC1, TSC2	Angiomyolipoma, clear cell, other
Constitutional chromosome 3 translocation	Responsible gene not found*	Clear cell
Familial renal carcinoma	Gene not identified (rare FLCN, SDHB)	Clear cell
Hereditary PRCC	MET	Papillary type 1
Birt-Hogg-Dube (BHD)	FLCN	Chromophobe**
Familial oncocytoma	Partial or complete loss of multiple chromosome	Oncocytoma
Hereditary leiomyoma-RCC	FH	Papillary type 2
Hereditary pheochromocytoma-paraganglioma syndromes	SDHB, SDHC, SDHD	Clear cell

Table 1.2 Inherited syndromes and known genes that predispose to familial RCC.
**VHL gene mutated in some families. **Renal oncocytomas, hybrid oncocytic and clear cell carcinomas may occur. RCC = Renal cell carcinoma; PRCC = Papillary RCC (Lopez-Beltran et al. 2009)*

1.3.2 Familial constitutional translocations used to identify candidate RCC genes

Loss of heterozygosity of 3p in sporadic ccRCC has been reported by numerous groups with not all demonstrating a loss or aberration of the *VHL* locus 3p25, thus suggesting other important tumour suppressor genes, apart from *VHL*, reside within the 3p region (D Bodmer et al. 1998; Martinez et al. 2000). Other common deleted 3p regions include 3p12, 3p14.2, 3p21.3 and studies involving chromosome transfer of 3p12-p21, 3p14-p21, and 3p21-p22 fragments into sporadic RCC cell lines demonstrated significant tumour suppression and rapid cell death (Killary et al. 1992; Sanchez et al. 1994). Non ccRCCs are rarely associated with 3p deletions or *VHL* aberrations and rare kindreds with familial non-*VHL* ccRCC have been detected, thus evidence suggests there are *VHL*-independent pathways involved in RCC tumourigenesis (Woodward et al. 2000; Woodward et al. 2008). The characterisation of translocation breakpoints associated with RCC has helped to identify a number of candidate tumour suppressor genes, many found within the 3p region, involved in sporadic RCC.

The t(3;8)(p14.2;q24.1) was found in a family with a number of cases of familial RCC (Cohen et al. 1979). The breakpoint was cloned and it was determined that the *FHIT* gene on chromosome 3p14.2 and the *TRC8* gene on chromosome 8q24.1 were disrupted producing a fusion gene (Poland et al. 2007). One sporadic RCC was found to carry a *TRC8* mutation and *TRC8* was shown to inhibit growth of cancer cell lines and directly interact with *VHL* (Gemmill et al. 1998; Gemmill et al. 2002; Gemmill et al.

2005). *FHIT* is a TSG found on the chromosome 3p arm that is often deleted in ccRCC and was shown to be methylated in >50% of ccRCC (Sükösd et al. 2003; Kvasha et al. 2008). A t(1;3)(q32.1;q13.3) breakpoint was identified in a family with four cases of ccRCC. The breakpoint was cloned which led to the identification of breakpoint spanning genes *NORE1* at 1q32.1 and *LSAMP* at 3q13.3. Both genes were found to be epigenetically inactivated in a number of sporadic ccRCCs and further research identified them to have tumour suppressing properties (Chen et al. 2003). Recently the characterisation of a t(3;4)(q21;q31) found in one individual with RCC allowed the identification of a disrupted gene, *FBXW7*, a known tumour suppressor gene found to be disrupted in other cancers (Welcker & Clurman 2008). *FBXW7* is part of an E3 ubiquitin ligase complex involved in the proteasomal degradation of several oncogenic proteins involved in growth and cell cycle progression including mTOR and cyclin E1 (Zhang & Koepp 2006; Akhoondi et al. 2007; Mao et al. 2008). *FBXW7* has subsequently found to be mutated in a small number of sporadic RCC (Kuiper et al. 2009; Guo et al. 2011). Other potential candidate genes found to be disrupted at translocation breakpoints associated with RCCs include *DIRC3* and *HSPBAP1* in a t(2;3)(q35;q21) translocation and *KCNIP4* in a t(3;4)(p13;p15) translocation (Bodmer et al. 2003; Bonne et al. 2007)

In some cases there are no candidate genes found within the vicinity of the breakpoints of associated familial RCC translocations and in these cases a ‘three hit’ model has been proposed; the initial translocation increases chromosome instability of the derivative chromosome involving chromosome 3, this increased instability ultimately

leads to the loss of the derivative containing part of the chromosome 3 arm which also includes one of the *VHL* alleles, the third hit involves the disruption of the second *VHL* allele leading to tumorigenesis (Clifford et al. 1998; Bodmer et al. 1998; Meléndez et al. 2003). A recent population study has shown that there is little increased risk of developing RCC in chromosome 3 translocation carriers with no family or personal history of RCC (Woodward et al. 2010). This suggests that where there is an association with RCC it is likely that the breakpoints have disrupted gene(s) critical in tumorigenesis of RCC thus the positioning of the chromosome 3 translocation breakpoints are important.

1.3.3 Sporadic RCC

The majority of RCCs (98%) are sporadic and although *VHL* was found to be mutated >70% of sporadic clear cell RCCs (ccRCC), other familial RCC associated genes were found to be rarely disrupted in the sporadic forms. Loss of genetic material leading to inactivation of TSGs is often detected in sporadic renal cancers (Wilhelm et al. 2002). In ccRCC after the deletion of 3p, the most common chromosomes to exhibit loss of heterozygosity (LOH) with deletions detected in 20-40% of ccRCC include 6, 8, 9 and 14. Less frequent chromosome deletions have also been detected in chromosomes 18q, 17p, 13q, 10q, 4 and 1 (Cairns 2010). A small number of known TSGs reside in these deleted regions including p53 on 17q, PTEN on 10q, Retinoblastoma (RB) on 13q and CDKN2A on 9p. Point mutations of p53 and RB are very rare in RCC and a small number of homozygous deletions of both CDKN2A and PTEN have been detected in sporadic

ccRCC, therefore these TSGs are only disrupted in a minority of sporadic ccRCC (Vignoli & Martorana 1997; Cairns et al. 1995; Brenner et al. 2002). Tumour suppressor genes have thus far not been identified that reside in the more commonly deleted regions 6q, 8p or 14q in ccRCC. In 2011 a whole exome sequencing project identified *PBRMI* gene complex truncating mutations in 92/227 (41%) of sporadic ccRCC and in 88/257 of non clear cell RCC thus suggesting *PBRMI* is a major sporadic RCC candidate gene (Varela et al. 2011). *PBRMI* is a component of the SWI/SNF chromatin-remodeling complex and the same study identified RCC mutations in other components of the complex including *ARID1A* and *ARID5B*, though at much smaller frequencies. An earlier exome sequencing study reported histone modification genes *MLL2*, *JARID1C*, *UTX* and *SETD2* to be mutated in 12-17% of ccRCC. Thus suggesting chromatin remodeling and histone modification pathways play an important role in ccRCC (Dalglish et al. 2010).

The MET proto-oncogene functions as a receptor tyrosine kinase that becomes activated when its ligand, the hepatocyte growth factor, binds. Germline activating point mutations within the tyrosine kinase domain of MET were found to cause hereditary papillary RCCs (Schmidt et al. 1997). *MET* was found to be mutated in a small number of sporadic papillary RCCs with one study showing activating mutations in 17/129 (13%), though germline *MET* mutations were later detected in 8 of the 17 cases even though no family history was present (Schmidt et al. 1999). The MET gene resides on chromosome 7 and most papillary RCCs demonstrate trisomy 7 without MET mutations, thus although this may not be as oncogenic as activating mutations, the increased expression of MET

may present a growth advantage (Zhuang et al. 1998). Other common events in papillary RCC include trisomy 17 and loss of chromosome Y in men. Chromosomes 6, 8 and 14 have also demonstrated LOH in papillary RCC, which interestingly are the same chromosomes to show LOH in ccRCC, other than 3p (Kovacs et al. 1991).

Chromophobe RCCs often (75-100%) exhibit monosomy of multiple chromosomes including 1, 2, 6, 10, 13, 17, and 21. Deletions of 9p, 8p and 3p have also been detected in 25% of Chromophobe RCCs (Speicher et al. 1994). Although folliculin (FLCN) mutations are found in the inherited Birt-Hogg-Dube (BHD) syndrome that predisposes to RCCs including chromophobe RCC (23%) and chromophobe RCC with oncocytoma (67%), FLCN mutations are rarely found in sporadic chromophobe RCCs (Toro et al. 2008; Nagy et al. 2004). However *p53* point mutations have been reported in 24-30% of sporadic chromophobe RCCs (Contractor et al. 1997; Gad et al. 2007).

Excluding *VHL*, most known familial RCC genes have not been shown to be associated with the sporadic forms of the disease. Although a number of candidate RCC genes have been found many of these genes are often only disrupted in the minority of cases, thus it is essential that new candidate genes are identified to allow deeper insight into the mechanisms of RCC tumourigenesis which could lead to improved therapeutic outcomes.

1.3.4 Epigenetics in RCC

VHL was among the first TSGs to be shown to be epigenetically silenced via promoter methylation in RCCs (Herman et al. 1994). Since then over 60 TSGs have been shown to be dysregulated in RCCs due to promoter methylation including the *RASSF1* TSG which maps to the 3p21 loci often deleted in RCCs as well as other cancers (Mark R Morris & Eamonn R Maher 2010). Mutations in *RASSF1* are rarely found in cancers thus epigenetic silencing was shown to be the major mechanism of *RASSF1* gene inactivation with promoter methylation occurring in approximately 51% of RCC cases and often as biallelic inactivation or as a second hit after 3p deletion (Morrissey et al. 2001; Lusher et al. 2002). *RASSF1* methylation is thought to be an early initiation event in RCC tumourigenesis as analysis of normal kidney tissue adjacent to the tumour showed aberrant *RASSF1* methylation which was not detected in kidney tissue further away from the tumour (Costa et al. 2007). Thus epigenetic inactivation of TSGs in RCC could be an important initiation event suggesting both genetic and epigenetic analysis are necessary in identifying important candidate cancer genes.

Activation of the Wnt pathway leads to cell proliferation and survival and thus contains a number of oncogenes often activated in cancers (Vincan 2004). Inhibitors of this pathway have been shown to be hyper-methylated in a number RCCs including the SFRP (Secreted Frizzled-Related Proteins) proteins (47-73%) which prevent Wnt signalling by binding to the Wnt protein and the DKK (Dickkopf) proteins (44-58%) which bind to the Wnt receptor (Morris & Maher 2010). A number of these Wnt pathway

inhibitors shown to be methylated RCCs have been investigated as potential RCC prognostic biomarkers for example *SFRP1* methylation showed a negative correlation with RCC patient survival in two independent studies and both *DKK1* and *DKK2* methylation were shown to positively correlate with pathological grade (with high graded tumours often correlating with poor prognosis) (Dahl et al. 2007; Awakura et al. 2008; Hirata et al. 2009; Hirata et al. 2011). Further identification of novel methylated TSGs in RCC could potentially help to identify novel pathways involved in RCC tumourigenesis and lead to new therapeutic targets.

1.3.5 VHL substrates and RCC treatment

30% of RCC cases present with metastatic RCC which is often highly resistant to conventional chemotherapy, and immunotherapy produces modest results. The 5 year survival rate is less than 10% of patients with advanced RCC (Cáceres & Cruz-Chacón 2011). Studies into the function of the VHL protein as well as other RCC candidate genes have helped identify new therapeutic targets leading to the development of RCC targeted therapy.

The VHL protein was shown to be part of an E3 ubiquitin ligase multiprotein complex (including elongins B and C, cullin-2, and the RBX-1 proteins) involved in the ubiquitination of specific target proteins (Conaway et al. 1998). VHL has two functional domains, the α domain which interacts with elongin C in the complex while the β domain acts as a substrate receptor recruiting target proteins into the complex including the HIF α

subunit (Ohh 2006). HIF is a transcription factor consisting of α and β subunits. The β subunit is constitutively expressed whereas the α -subunit is regulated depending on the oxygen level of the cell (Semenza 2001). When oxygen levels are adequate the HIF α subunit undergoes prolyl-hydroxylation via a prolyl hydroxylase (PHD) and is recruited to the VHL β domain in the ubiquitin complex and is degraded through ubiquitylation and proteasomal degradation (Ohh et al. 2000). In hypoxic conditions the HIF α subunit does not undergo prolyl-hydroxylation and therefore does not bind to VHL and instead heterodimerizes with the β subunit in the nucleus and binds to hypoxia response elements (HREs) promoting the transactivation of hypoxia-inducible genes (Semenza 2001). Inactivation of the *VHL* gene leads to a similar outcome as hypoxic conditions, thus the HIF α subunit can no longer bind to VHL and is therefore not degraded leading to the expression of HIF α target genes such as VEGF (Maxwell et al. 1999). Other substrates of the VHL ubiquitin complex that have been identified and include VHL-interacting deubiquitinating enzyme (VDU1), atypical protein kinase C (aPKC) and substrates of RNA polymerase II (POLR2G) (Li et al. 2002; Okuda et al. 1999; Na et al. 2003; Cockman et al. 2000). There are over 60 hypoxia-inducible genes transactivated by HIF including platelet-derived growth factor (PDGF) a known oncogene, vascular endothelial growth factor (VEGF) involved in angiogenesis promotion and the transforming growth factor α (TGF α) which activates the epidermal growth factor receptor (EGFR) (Dibb et al. 2004; Veikkola & Alitalo 1999; Ananth et al. 1999). The functions of these hypoxia-inducible genes have been shown to be involved in the development of cancer thus making the α -subunits of HIF (HIF1 α and HIF2 α) the most likely VHL-ubiquitin complex substrates to

play a vital role in the development of ccRCC (Maynard & Ohh 2007). It has also been demonstrated the majority (>50%) of ccRCCs show up-regulation of HIF target genes including VEGF.

Bevacizumab is a recombinant human monoclonal anti-VEGF antibody capable of neutralizing VEGF isoforms (Presta et al. 1997). Bevacizumab combined with IFN- α was used in a phase III trial with ccRCC patients, and showed increased progression free survival time compared to a placebo (Escudier et al. 2007). TGF- α is a ligand for the EGF receptor (EGFR) which activates a number of pathways including the MAPK pathway and AKT pathways that can lead to cell proliferation. Gefitinib, an EGFR inhibitor, has been tested in an RCC phase II trial with patients showing disease stability (Dawson et al. 2004). Multikinase inhibitors are a group of therapeutics that inhibit the downstream effects of growth factors. A number of multikinase inhibitors were found to show positive effects in the treatment of RCC, for example Sorafenib, originally found as a Raf inhibitor, was shown to also inhibit other kinases including VEGFR and PDGF- β (S. M. Wilhelm et al. 2004). Sorafenib has shown positive effects in a phase II trial with metastatic RCC patients showing tumour shrinkage and increased progression free survival time (Ratain et al. 2006). Other multikinase inhibitors which have been used in RCC treatment trials include Sunitinib, Pazopanib and Axitinib which have all shown increased progression free survival and/or disease stability in clinical trials (Motzer et al. 2007; Sonpavde et al. 2008; Rini et al. 2009). HIF protein translation (along with many other proteins) is regulated via the mTOR pathway. Temsirolimus an inhibitor of mTOR

activity was used in a large trial with untreated RCC patients and showed increased progression free survival and over-all survival time (Hudes et al. 2009).

These new biological agents have shown positive effects in the treatment of RCC such as increased progression free survival, improvements in quality of life and increased survival time. In fact it has been estimated that targeted RCC therapies have increased the overall survival of metastatic RCC from 10 months to 40 months with an average progression-free survival of 27 months (Sun et al. 2010). Yet there is still no curative treatment for metastatic RCC. The discovery of other important pathways involved in RCC tumourigenesis could lead to better understanding of the molecular events driving RCC initiation and progression which could eventually lead to the development of new biological agents that further improve the survival rate of RCC patients. Due to the clonal diversity within a tumour it is likely that a cocktail of therapeutic agents that target the key pathways involved in RCC would be the most effective method to eradicate the cancer, as the use of single targeted therapeutic agents inevitably leads to the outgrowth of resistant sub-populations within the tumour, due to selective pressure (Greaves & Maley 2012). Therefore it is important that further research is undergone to understand the key mechanisms that lead to the initiation and progression of RCC.

1.4 *The ubiquitin pathway*

Ubiquitin is a small, 8.5KDa protein that is ubiquitously expressed in eukaryotic organisms and is highly conserved between species. Ubiquitin is attached to protein substrates (termed substrate ubiquitylation) within the cell and labels them for a specific fate, for example to be degraded by the proteasome (Herrmann et al. 2007). These ubiquitin tags essentially direct proteins to different locations within the cell thereby controlling the fate of many proteins. There are many ubiquitin pathways in human cells that are involved in the ubiquitylation of specific protein substrates producing a highly effective mechanism for the regulation of almost all cellular biology. Ubiquitin is a member of a highly conserved family of proteins termed the ubiquitin-like proteins (UBLs) that include SUMO, ISG15, NEDD8, URM1, FAT10, ATG8, ATG12, FUB1, UFM1 and UBL5, these ubiquitin-like proteins function as tags that can be attached to substrate proteins and control the protein fate via a number of mechanisms depending the type of ubiquitin-like molecule attached (Welchman et al. 2005). The major steps in the ubiquitin pathways involve the activity of a ubiquitin-activating enzyme (E1), a ubiquitin-conjugating enzyme (E2) and a ubiquitin ligase (E3) (Herrmann et al. 2007). In the human genome two E1 enzymes have been identified which produce a thioester bond between their active cysteine (Cys) residue and the carboxy terminus of ubiquitin in an ATP dependent reaction. Ubiquitin is then transferred from the E1 to the active Cys residue in the ubiquitin-conjugating domain (UBC) of an E2 enzyme which would then engage an E3 enzyme to undergo substrate ubiquitylation (Schulman & Harper 2009). E3s bring the specific protein substrate and the ubiquitin charged E2 together which

initiates the ligation of the ubiquitin to a specific lysine (Lys) residue in the substrate (Yihong & Rape 2009) (*Figure 1.6*). E3s are categorized into three main groups: RING-finger-type, HECT-type and U-box-type. RING-finger-type E3s are subdivided into families including the cullin-based E3s which are one of the larger classes of E3s (Ardley & Robinson 2005). There are at least 38 active E2 enzymes and up to 1000 E3 enzymes in the human genome thus often a single E2 enzyme is able to interact with several E3s (Yihong & Rape 2009).

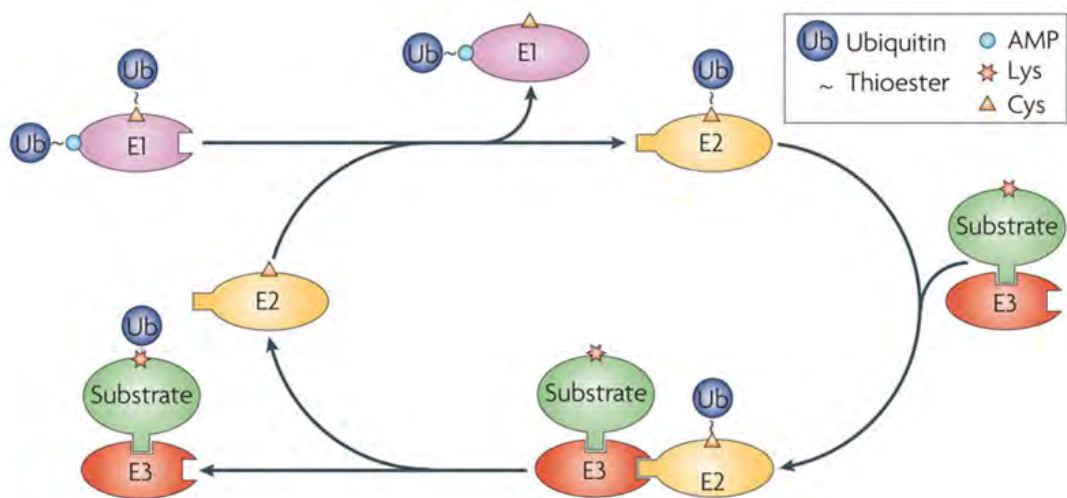


Figure 1.6 The ubiquitin pathway

Schematic illustration of the ubiquitin pathway involving the ubiquitylation of protein substrates via a hierarchical group of three enzymes: a ubiquitin-activating enzyme (E1), a ubiquitin-conjugating enzyme (E2) and a ubiquitin ligase (E3). E1s are loaded with ubiquitin (Ub) through an ATP dependent mechanism. Ub is transferred to an E2 enzyme bound by a thioester linkage on an active cys residue found in the E2 ubiquitin binding domain. E3 enzymes are often complexes containing a number of enzyme components that bind specific substrates as well as the loaded E2s. The Ub is transferred from the E2 to specific Lys residues found on the substrates. The E2 is then reloaded with Ub and the cycle starts again (image adapted from Ye & Rape 2009).

The number of ubiquitin molecules and type of linkages within a ubiquitin chain attached to a substrate has been shown to affect substrate outcome, for example substrate proteins can be attached with a single ubiquitin protein on one (monoubiquitylation) or many (multi-monoubiquitylation) Lys residues (Pickart & Fushman 2004). Polyubiquitylation involves the addition of a chain of ubiquitin molecules which are linked to each other via one of seven Lys (K) residues within ubiquitin (K48, K63, K11, K6, K27, K29 or K33) or the amino terminus (Li & Ye 2008). Branches of ubiquitin molecules extending from ubiquitin chains as well as multiple ubiquitin chains have been detected on substrates though the significance of these is unknown (Kim et al. 2007). Ubiquitylated substrates are then recognised by a number of proteins all containing types of ubiquitin-binding motifs, for example ubiquitin-associated domains (UBA) and ubiquitin-interacting motifs (UIM), often these ubiquitin binding proteins show a preference to specific ubiquitin conjugates such as ubiquitin chains linked together via a specific lys residue i.e. Lys48-ubiquitin chains attract proteins that chaperone the substrates for proteasomal degradation (Dikic et al. 2009; Richly et al. 2005). Ubiquitin binding proteins often bind downstream components of signalling pathways thus combining ubiquitylation with a specific biological effect for example NEMO (NF- κ B essential modulator) a protein that binds lys63-ubiquitin chains has been shown to facilitate NF κ B (nuclear factor κ B) activation (Hadian et al. 2011) (*Figure 1.7*).

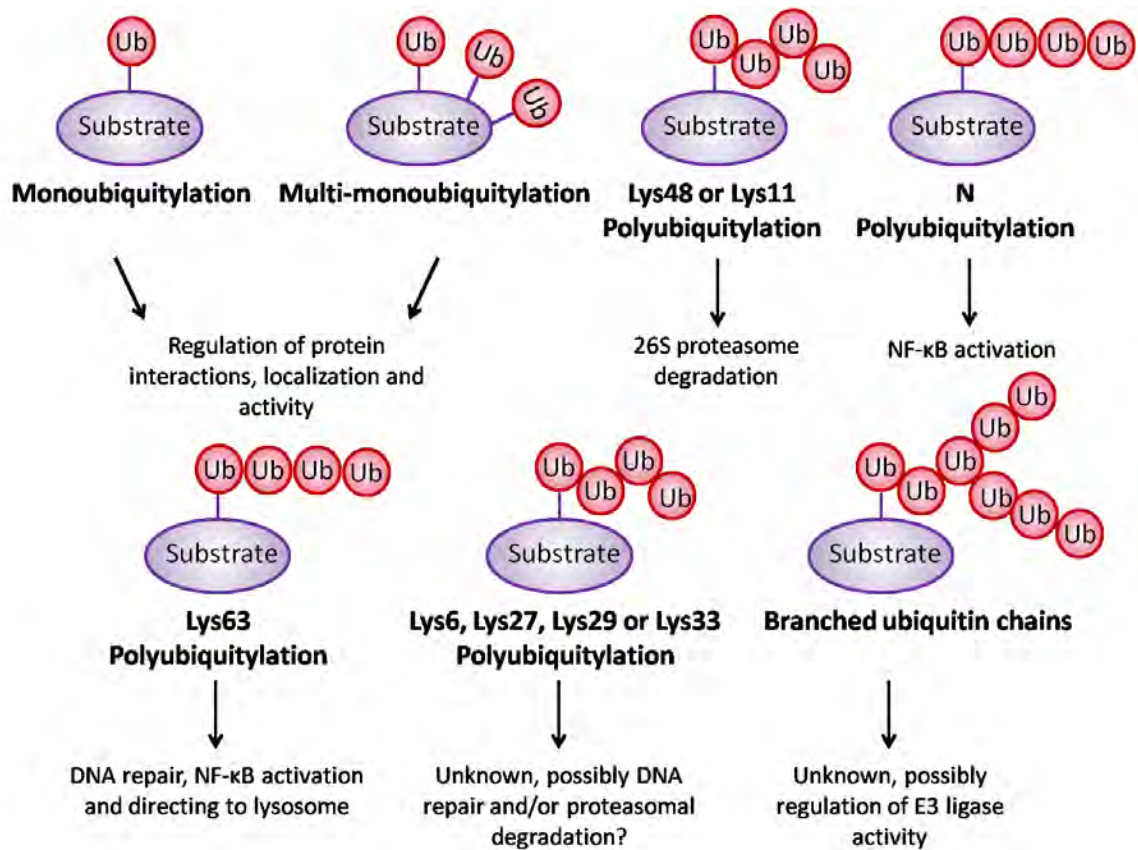


Figure 1.7 Ubiquitin chains and substrate outcomes

Schematic representation of the known Ubiquitin (Ub) modifications along with their known and predicted functional outcomes. A single Ub can be attached to a substrate (monoubiquitylation) or as a chain of multiple ub (polyubiquitylation) attached via 5 different lysine (lys) residues (Lys48, lys11, lys63, lys6, lys27, lys29 or lys33). In some cases ub molecules can also be attached via their amino terminus (N). (Yihong & Rape 2009).

1.4.1 Ubiquitinating conjugating enzymes (E2s) – not just ubiquitin carriers

E2 enzymes are distinguished by a conserved 150-200 amino-acid ubiquitin-conjugating domain (UBC) which contains the catalytic active cysteine that binds ubiquitin via a thioester bond (Wijk & Timmers 2010). E2 enzymes can bind a number of E3s thus affecting substrate ubiquitylation however the rules defining how an E2 chooses which E3 it binds to and when is a question for future research, though it is known that E3 binding motifs within the E2 proteins contain slight variations leading to specific E3 binding (Zheng et al. 2000). E2-E3 interactions are usually very weak this is thought to be due to the fact that the E2 regions used to bind E3s overlap with the regions used to interact with E1s. This suggests an E2 cannot be charged with a ubiquitin by an E1 while still bound to an E3, thus instead must undergo numerous cycles of E3 binding and dissociation to recharge during ubiquitin chain formation (Yihong & Rape 2009). As E3 enzymes bind specific substrates they were originally seen as the sole enzymes that brought substrate specificity to the ubiquitin cascade with E1 and E2 enzymes described simply as ubiquitin carriers. Recent research has indicated that E2s play an important role in the biological outcome of a substrate as the length and type of ubiquitin chains assembled by the E2 can affect the fate of the substrate (Li & Ye 2008).

It has been demonstrated that the choice of whether or not a lys residue in the substrate and/or ubiquitin will receive the next ubiquitin is made by the E2s as recent research has shown specific E2s are involved in ubiquitin chain initiation while others are

involved in chain elongation (Windheim et al. 2008). Ubiquitin chain assembly is often initiated by the binding of a single ubiquitin to the lys residue on a substrate protein. This first mono-ubiquitin initiation step is often carried out by a specific E2 which is then replaced by a different E2 that carries out ubiquitin chain elongation, for example the APC/C E3 complex uses the Ubc4 E2 to initiate ubiquitin chain formation while the E2 Ubc1 is then used to extend Lys-48 ubiquitin chains (Rodrigo-Brenni & Morgan 2007; Jin et al. 2008). Ubiquitin chain elongation E2s most often lack the ability to initiate chain formation themselves for example the UBE2N and UBE2V1 lys-63 specific E2s and the UBE2S lys11 specific E2 are unable to initiate ubiquitin chain formation and are therefore chain elongation specific E2s (Windheim et al. 2008). Substrates can attach ubiquitin on a number of lys residues, some initiation E2s can bind ubiquitin non-specifically to any lys residue allowing them to initiate ubiquitylation on many substrate types using numerous E3s (Kirkpatrick et al. 2006). Other E2s appear to be selective and only transfer ubiquitin to particular lys residues on substrates by recognising certain residues in close proximity to the lys residue thus providing specificity, for example UBE2T only mono-ubiquitylates specific lys residues on the substrate FANCD2 and is unable to catalyse ubiquitin chain extension (Alpi et al. 2008). E2 enzymes have therefore been shown to provide another level of substrate specificity, alongside the substrate receptor E3s, within the ubiquitin pathway cascade.

1.5 The ubiquitin pathway in cancer

Ubiquitylation of substrate proteins via the ubiquitin pathway can affect the substrates in a number of ways including protein stability, interactions and localisation. This in turn can lead to global cell signalling variations in pathways involved in proliferation, apoptosis, DNA repair and the cell cycle (Kirkin & Dikic 2007). Dysregulation of these cell signalling pathways can provide an advantage to cancerous cells leading to tumourigenesis, thus it is not surprising that defects in the ubiquitin machinery have been detected in a number of cancers (Kirkin & Dikic 2011).

1.5.1 Ubiquitin ligase enzymes (E3s) and their involvement in cancers

Many types of E3 ligases are involved in the regulation of oncogene and/or tumour suppressor gene expression levels within human cells including the SCF (SKP1–CUL1–F-box), ECV (Elongin B/C–cullin 2–VHL) and APC/C (anaphase-promoting complex/cyclosome) E3 complexes, see Figure 1.8 (Kitagawa et al. 2009). These three E3 complexes are structurally very similar, consisting of four specific subunits including a RING-finger protein, scaffold protein, adaptor protein and a substrate specific subunit (Nakayama & Nakayama 2006). VHL is the only identified substrate specific subunit for the ECV complex whereas the SCF and APC/C complexes have a number of substrate specific subunits including more than 70 F-box proteins that bind the SCF complex and CDC20 and CDH1 that bind the APC/C complex (Jin et al. 2004; Kraft et al. 2005). Various substrates have been identified for all three E3 complexes as shown in *Figure 1.8*.

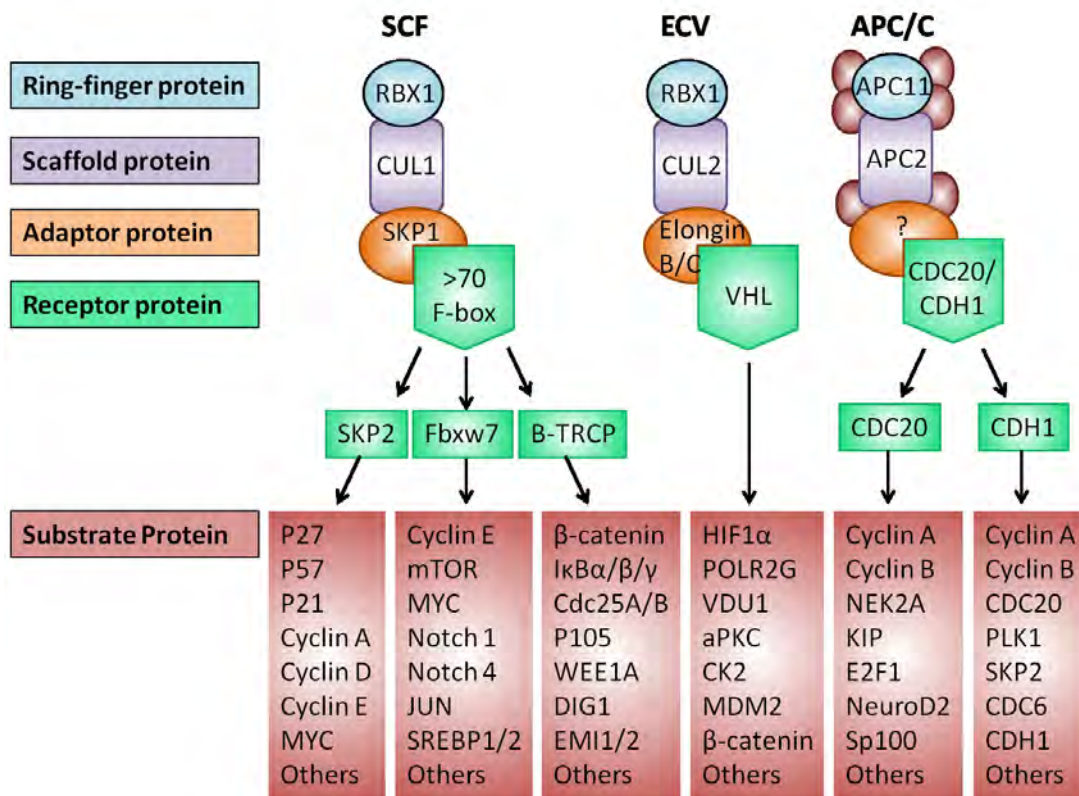


Figure 1.8 The structure and substrates of the SCF, EVC and APC/C ubiquitin ligase complexes

SCF, ECV and APC/C E3 ligases are comprised of similar components including a RING-finger protein: RBX1 or APC11 (an RBX1-related protein), a scaffold protein: cullin-1/2 or APC2 (a CUL1-related protein), an adapter protein SKP1 and elongin (the adapter protein is unknown for the APC/C complex) and finally a receptor protein responsible for substrate specificity: >70 F-box proteins act as receptor proteins for the SCF complex including SKP2, FBXW7 and β-TRCP whereas the ECV complex only recruits one receptor protein, VHL, and the APC/C complex recruits two, CDC20 or CDH1. A number of known substrates are shown for each complex (Nakayama & Nakayama 2006).

There are three major substrate recognition F-box proteins that become part of the SCF complex to regulate a number of cell cycle control proteins; FBXW7 (F-box and WD-40 domain protein 7), SKP2 (S-phase kinase-associated protein 2) and β -TRCP (β -transducin repeat-containing protein) (Nakayama & Nakayama 2006). FBXW7 has been shown to initiate the degradation of a number of oncogenes including Notch-1, Notch-4, JUN, c-MYC, Cyclin E and mTOR and has therefore been described as a tumour suppressor (Welcker & Clurman 2008; Tan et al. 2008). Mutations in *FBXW7* have been identified in numerous cancers including hereditary colorectal cancer, ovarian cancer and lymphoma (Miyaki et al. 2009; Kwak et al. 2005; Song et al. 2008). *FBXW7* gene deletions have also been detected in cancers including gastric cancer and colorectal cancer (Milne et al. 2010; Iwatsuki et al. 2010). Conversely it has been demonstrated that SKP2 has oncogenic potential with many of its targets functioning as tumour suppressors including p27, p21 and p57 (Kitagawa et al. 2009; Lin et al. 2010; Bretones et al. 2011). SKP2 expression has been shown to negatively correlate with p27 levels and poor prognosis in several cancers (Wang et al. 2012). β -TRCP has numerous substrates which can regulate various pathways leading to complex outcomes, for example β -TRCP targets cell cycle regulators EMI1/2, CDC25A/B and WEE1A for degradation as well as β -catenin, an essential component of the Wnt pathway and I κ B an inhibitor of the NF κ B pathway (Winston et al. 1999; Margottin-Goguet et al. 2003; Watanabe et al. 2004; Uchida et al. 2011). Thus β -TRCP appears to inhibit proliferation via degradation of cell cycle regulators and inactivation of the Wnt pathway yet activates the NF κ B pathway inhibiting apoptosis and promoting cell proliferation. Therefore it is not surprising that β -

TRCP is deregulated in what appear to be opposing methods depending on the type of cancer, for example it has been shown to be mutated in cancers such as gastric cancers, yet in others such as colorectal cancer it is shown to be overexpressed (Kim et al. 2007; Ougolkov et al. 2004). Although E2 enzymes have been shown to provide a degree of specificity to the ubiquitination of E3 substrates (see section 1.4.1) there has only been a few reports relating E2 enzyme overexpression to cancer development (Okamoto et al. 2003; Roos et al. 2011).

1.5.2 The ubiquitin pathway in kidney cancer

As already stated in section 1.3.3 VHL is mutated in up to 70% of sporadic ccRCCs and is part of the ECV ubiquitin ligase complex consisting of elongins B and C, Cullin-2 and RBX-1. A number of other components of the ubiquitin pathways have been shown to be mutated in a small number of sporadic kidney cancers including the tumour suppressor gene BAP1 which functions as a de-ubiquitin enzyme involved in cell proliferation regulation, CUL7 part of a novel SCF-like E3 ligase that potentially regulates cell growth through binding IRS-1 (insulin receptor substrate-1) and p53, β -TRCP and FBXW7 which are both substrate recognition components of the SCF-complex that regulate a number of known oncogenes (see section 1.5.1 for detail) and TRC8 which was revealed to be an E3 ubiquitin ligase (Guo et al. 2011; Yu et al. 2010; Sarikas et al. 2008; Kuiper et al. 2009; Gemmill et al. 2005). E2-EPF a ubiquitin conjugating enzyme involved in targeting VHL for proteasomal degradation has also been shown to be upregulated in papillary type RCCs (Roos et al. 2011).

Known familial RCC genes (VHL, FLCN, FH, SDH, MET) have all been shown to play a role in the mTOR, HIF or Wnt pathways shown to be involved in RCC tumorigenesis (Baldewijns et al. 2010) . Many of the disrupted ubiquitin pathway components found in sporadic RCCs, including VHL, are regulators of the mTOR and/or HIF pathway; for example FBXW7 found to be disrupted in a familial RCC case and mutated in a single sporadic RCC case, targets mTOR for proteasomal degradation and disruptions in the SCF/FBXW7 E3 ligase cause increased activation of the mTOR pathway (Mao et al. 2008), CUL7 found to be mutated in 3% of sporadic RCCs targets IRS-1 for proteasomal degradation; IRS-1 is activated by the insulin receptor and instigates the activation of the mTOR pathway thus mutations in CUL7 prevent degradation of IRS-1 and lead to increased activation of the mTOR pathway (Guo et al. 2011; Xu et al. 2008). Wnt/ β -catenin pathway activation has been detected in a number of RCC cases and is thought to be involved in RCC tumorigenesis (Saini et al. 2011). VHL has also been shown to target the β -catenin oncogene for proteasomal degradation thus linking both the HIF and Wnt/ β -catenin pathways in RCC (Peruzzi & Bottaro 2006). β -TRCP, shown to be mutated in ~2% of sporadic RCCs, acts as a substrate receptor for the SCF E3 ligase and has been shown to target β -catenin for ubiquitylation and proteasomal degradation (Guo et al. 2011; Liu et al. 2004) (*Figure 1.9*).

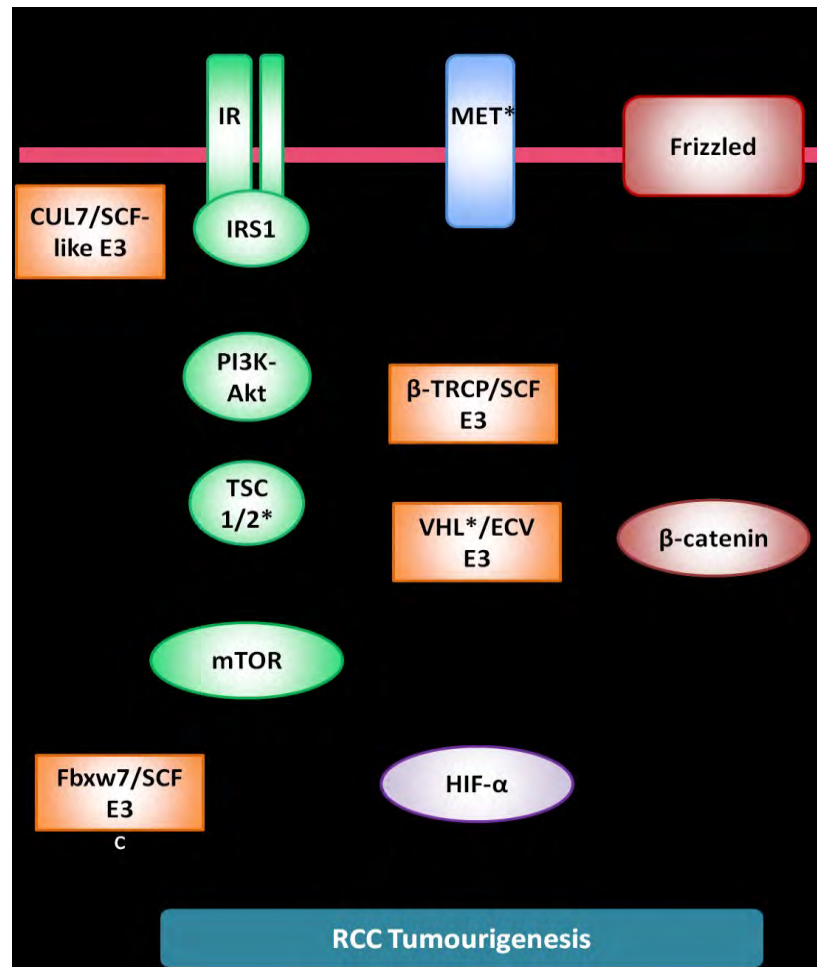


Figure 1.9 Ubiquitin pathways involved in RCC tumourigenesis

Overview of the signalling pathways involved in RCC including the HIF and mTOR (green/purple circles) and Wnt/ β -catenin pathways (red circles) showing the components that are often disrupted in RCC within these pathways (* known RCC causative genes). A number of ubiquitin systems regulate the HIF, mTOR and Wnt/ β -catenin pathways by binding specific components and targeting them for proteasomal degradation, within these ubiquitin pathways the substrate receptor subunit of the E3 ligases (orange boxes) have been shown to be deregulated in sporadic and/or familial RCC. VHL is part of the ECV E3 complex that has been shown to target both the HIF α subunit and β -catenin regulating both the HIF and Wnt pathways. The SCF complex has been shown to be involved in RCC tumourigenesis via deregulation of two different substrate receptor subunits; FBXW7 shown to target mTOR and β -TRCP shown to target β -catenin for proteasomal degradation. CUL7 is a substrate receptor subunit of an SCF-like E3 ligase known to target IRS1 for degradation, deregulating the mTOR pathway. Thus the ubiquitin system plays an important role in RCC tumourigenesis (Baldewijns et al, 2010; Linehan et al, 2010; Guo et al, 2011; Mao et al. 2008). IGF = insulin growth factor; IR = insulin Receptor; PI3K = Phosphatidylinositol 3-kinases; Akt = serine/threonine kinase; FLCN = folliculin; TSC = Tuberous sclerosis protein; mTOR = mammalian target of rapamycin; HGF = hepatocyte growth factor; MET = hepatocyte growth factor receptor (proto-oncogene); FH = fumarate hydratase; SDH = succinate dehydrogenase; PHD = prolyl hydroxylase.

The ubiquitin system consists of numerous ubiquitin pathways that regulate many signalling cascades. A small number of these ubiquitin pathways, including the SCF and ECV cascades, appear to play an important role in the development of both familial and/or sporadic RCCs and are often involved in the regulation of the mTOR, HIF and wnt/ β -catenin signalling cascades. Although a number of components of the SCF/ECV pathways, other than VHL, have been shown to be disrupted in sporadic RCCs, these only account for a small percent of sporadic RCCs (1-3%). It is likely that there are other, not yet detected, candidate sporadic RCC genes that are involved in the mTOR, HIF and wnt/ β -catenin signalling pathways. One of the most prominent ways to regulate these two pathways is through the ubiquitin system as a number of the pathway components are regulated through ubiquitylation, thus there maybe novel RCC genes within the ubiquitin system yet to be found. Further elucidation of these ubiquitin cascades and the signalling pathways they regulate could help to identify novel RCC components, thus increasing current knowledge of RCC tumourigenesis and allowing the development of new therapeutic targets.

Chapter Two: Methods

2.1 Materials

2.1.1 Companies purchased from

Company names and local branch locations are shown in the table below:

Company name	Address
Abcam	Cambridge, UK
Appleton Woods	Birmingham, UK
Applied Biosystems	Warrington, UK
Bioline	London, UK
Biorad	Hemel Hempstead, UK
Cell signaling	Hitchin, UK
Clontech	Saint-Germain-en-Laye, France
Corning	High Wycombe, UK
New England Biolabs	Hitchin, UK
European Cell and Culture Collection	Porton Down, UK
Fermentas (Thermo Scientific)	St. Leon-Rot, Germany
Fisher	Loughborough, UK
GE Healthcare	Amersham, UK
Integrated DNA Technologies	Glasgow, UK
Invitrogen	Paisley, UK
MRC-Holland	Amsterdam, Netherlands

PAA Laboratories	Yeovil, UK
Promega	Southampton, UK
Qiagen	Crawley, UK
Roche	Welwyn Garden City, UK
Sigma-Aldrich	Poole, UK
Stratagene	Cambridge, UK

2.1.2 General chemicals and equipment

Isopropanol, ethanol and methanol were purchased from Fisher. Phosphate Buffered Saline (PBS) tablets from Thermo scientific. Agarose was purchased from Biorline and DNA ladders from Fermentas. The Polyvinylidene difluoride (PVDF) membrane was purchased from GE Healthcare. Tissue culture flasks and dishes were purchased from Corning and pipettes from Appleton Woods. All other general chemicals were purchased from Sigma-Aldrich unless specified.

2.2 Sequencing

2.2.1 PCR

Polymerase chain reaction was used to amplify specific DNA fragments for sequencing or cloning. A list of the primers used in the PCR reactions are shown in appendix 8.1.1, 8.1.2 and 8.1.3. The reaction components are shown on the next page.

Reaction components*	1 x Volume
10x PCR reaction buffer with 20mM Mgcl ₂	2.5μl
2mM dNTP mix (1:1:1:1)	2.5μl
GC-RICH Solution, 5x conc.	5.0μl
Forward primer 20μM	1μl
Reverse primer 20μM	1μl
Fast start taq DNA polymerase 5U/μl	0.2μl
dH ₂ O	Up to 25μl
DNA**	/
* 10x reaction buffer, 5x GC-rich solution and fast start taq polymerase were purchased from Roche. dNTPs were purchased from Fermentas.	
**10-200ng genomic DNA or 1-10ng bacterial DNA or 0.1-1ng plasmid DNA	

PCR reactions were carried out in a thermal cycler with a heated lid at the conditions shown on the next page.

Step	Temperature	Duration	Cycles
Hot start: For heat activated enzymes.	95°C	5 minutes	/
Denaturation step: Separation of DNA strands to produce single stranded DNA	95°C	30-45s	Cycle 25 – 35x depending on the amount of starting DNA and amount of product needed
Annealing step: Anneal primers to single stranded DNA	Primer annealing temperature (50-65°C)	30-45s	
Extension step: Synthesis of new DNA strands complementary to DNA template	72°C	Depends on length of DNA template (~1 minute per kb)	
Final extension step:	72°C	10 minutes	/

2.2.2 Agarose gel electrophoresis

Agarose gels were used to analyse PCR products used for sequencing and cloning.

The percentage of the agarose gels ranged from 1% to 2.5% depending on the DNA fragment size. For example a 1% agarose gel was made by mixing 1% w/v agarose powder with 1X TBE buffer (90mM Tris-base, 90mM boric acid and 2mM EDTA, pH8.0) and dissolved by heating in a microwave. Once the agarose had cooled ethidium bromide was added to make a final concentration of 0.25µg/ml. The gel was poured into the casting tray with a comb and left to solidify at room temperature. Once solid, the comb was removed and the gel was placed in an electrophoresis chamber containing 1XTBE buffer. DNA samples were added along with 2x loading dye (50% glycerol, 2mM EDTA and 0.1% orange G). DNA ladders were added as size standards and the gels were run at 180 Volts for as long as needed.

2.2.3 EXOSAP reaction

The PCR products were cleaned using exonuclease I and alkaline phosphatase treatment. Single stranded DNA is digested by the exonuclease I enzyme into free dNTPs. The dNTPs are then inactivated by the antartic phosphates by removing the dNTP phosphate groups. The EXOSAP reaction conditions are shown on the next page.

Reaction components*	1x Volume
FastAP thermosensitive alkaline phosphatase	
1u/ μ l	1 μ l
10X FastAP buffer	1 μ l
Exonuclease I 20u/ μ l	1 μ l
PCR product	5 μ l
dH ₂ O	Up tp 10 μ l
* FastAP alkaline phosphatase, fastAP buffer and exo I were purchased from Fermentas.	

The reaction components were mixed well then incubated at 37°C for 30 minutes then at 85°C for 20 minutes to inactivate the reaction.

2.2.4 Sanger sequencing reaction

EXOSAP treated PCR products were used as the template for the terminator cycle sequencing reaction (Sanger sequencing). Terminator cycle sequencing involves the incorporation of fluorescent labelled dideoxynucleotides also known as dye terminators. Four different dyes are used to represent each of the four bases A, T, G and C. Each sample was sequenced bi-directionally therefore the forward and reverse primers are

added to separate PCR reactions for each sample. The terminator cycle sequencing reaction components and conditions are shown below.

Reaction components*	1X volume
BigDye Terminator v1.1/3.1 Sequencing Buffer 5x	2.0 μ l
BigDye Terminator v3.1**	0.75 μ l
Primer forward or reverse 20 μ M	1.0 μ l
Purified DNA	5 μ l
dH ₂ O	Up to 10 μ l
* Big dye terminator and big dye terminator buffer were purchased from applied biosystems. ** The BigDye terminator Cycle Sequencing Kit includes dye terminators, deoxynucleoside triphosphates, AmpliTaq DNA Polymerase, FS, rTth pyrophosphatase, magnesium chloride, and buffer.	

Step	Temperature	Duration
Denaturation	95°C	25s
Annealing	50°C	25s
Extension	60°C	4 minutes

The reaction was carried out in a thermocycler with a heated lid for 28 cycles.

2.2.5 Sequencing Precipitation

The sequencing products were cleaned from impurities such as excess fluorescent ddNTPs and enzymes from the sequencing reaction. Precipitation buffer was prepared using 0.5M EDTA and 3M NaAc in a 1:1 ratio. The samples to be precipitated were prepared in a 96 well plate with a sealing lid. Three and a half μl of precipitation buffer was added to each of the samples to be sequenced. One hundred μl of 100% ethanol was then added to the sample which was then centrifuged at 4000rpm for 15 minutes at 4°C to pellet the DNA. After the spin, the sealing lid was removed and the plate was spun upside down at 400rpm for 1 minute. Two hundred μl of 70% ethanol was then added to the sample, to wash the pellet, and was centrifuged at 4°C for 10 minutes at 4000rpm. The plate was then spun upside down at 400rpm again and the wash step was repeated. The plate was then spun upside down for a final time and was then left on the worktop until all the residual ethanol had evaporated. 10 μl of formamide (Hi-Di, Applied Biosystems) was added to the DNA sample which was then denatured on a heating block set at 95°C for 5 minutes. The plate was then placed on ice before loading on to the sequencer.

2.2.6 Sequencing analysis

The plate containing the denatured DNA was placed on a AB3730 capillary sequencer (Applied Biosystems), and analysed using Bioedit V7.1.3 (www.mbio.ncsu.edu/bioedit/bioedit.html).

2.3 Cloning

2.3.1 Plasmid constructs

Plasmid maps can be found in section 8.2. UBE2QL1 expression constructs were made by cloning the full length human coding region into the EcoRI-BamHI sites of pcDNA3.1 (Invitrogen), pFLAG-CMV4 (Sigma-Aldrich) and pCMV-myc (Clontech) vectors. All three FBXW7 isoform constructs were kindly given to us by Markus Welcker. The FBXW7 coding regions were cloned into p3XFLAG-myc-CMV-24 (Sigma-Aldrich) at the following sites; FBXW7 α in Hind3-EcoRI, FBXW7 β in EcoRI-Xba1 and FBXW7 γ in Hind3-Xba1. Stop codons were included in the FBXW7 coding regions therefore the myc tag was not incorporated. The Hisx6-Ubiquitin vector was kindly given to us by Dirk Bohmann. Plasmids were verified by sequencing.

2.3.2 Designing cloning primers

Primers were designed to contain specific restriction enzyme sites to produce the correct sticky ends for ligation into the vector. It was important to design the forward primers so the open reading frame (ORF) of the gene was in frame with the epitope tags within the vector. The ORF sequence was run through the webcutter 2.0 software, accessed online, to identify any restriction endonuclease sites within the sequence (www.na.lundberg.gu.se/cutter2). The restriction sites that were chosen for each ORF were ones which would be in the correct orientation for the vector and were not found within the ORF. Forward primers were made to include the initiation (ATG) codon and reverse primers

were made to include the stop codons as all tags used were at the N-terminus of the gene. Primer sequences are shown in appendix 8.1.4.

2.3.3 PCR (pfu taq)

PfuUltra II fusion HS DNA polymerase was used to amplify the open reading frames of genes to be used for expression cloning. Pfu polymerase possesses 3' to 5' proof reading properties and therefore ensures accuracy, preventing the insertion or deletions of incorrect bases during the reaction. The PCR components using pfu DNA polymerase are shown below.

Reaction components*	1 x Volume
10x PfuUltra II reaction buffer	5µl
2mM dNTP mix (1:1:1:1)	5µl
Forward primer 20mM	2µl
Reverse primer 20mM	2µl
PfuUltra II fusion HS DNA polymerase	1µl
dH ₂ O	Up to 50µl
cDNA**	/
* PfuUltra II DNA polymerase and buffer were purchased from stratagene, dNTPs were purchased from Fermetas.**100ng genomic DNA	

Pfu DNA polymerase PCR reactions were carried out in a thermal cycler with a heated lid at the following conditions.

Step	Temperature	Duration	Cycles
Hot start:	95°C	5 minutes	1x
Denaturation step:	95°C	30s	35-45 x
Annealing step:	Touchdown starting at 4 °C above annealing temperature.*	30s	
Extension step:	72 °C	Depends on length of DNA template (~1 minute per kb)	
Final extension step:	72 °C	10 minutes	1x

* Touchdown annealing steps were used to avoid amplifying non-specific sequence. This involves 5 cycles at 4 °C above annealing temperature, 5 cycles at 2 °C above annealing temperature then 35 cycles at annealing temperature.

2.3.4 Site directed mutagenesis

C88A and C88S UBE2QL1 mutants were generated by PCR-based site-directed mutagenesis using the QuikChange Lightning Site-Directed Mutagenesis Kit following manufacturer's instructions. This allows the generation of site-specific mutations using almost any double stranded plasmid as the template. Complementary primers were designed containing the desired nucleotide change along with 12 correct base pairs either side, the primers anneal to the same sequence on opposite strands of the plasmid. Primer sequences are shown in appendix 8.1.5. The mutant strand synthesis PCR reaction components were as follows:

Reaction components*	1 x Volume
10× QuikChange reaction buffer	2.5µl
dsDNA template (plasmid)**	1µl
Forward primer 20mM	1µl
Reverse primer 20mM	1µl
2mM dNTP mix (1:1:1:1)	0.5µl
QuikSolution reagent	0.75µl
QuikChange® Lightning Enzyme	0.5µl
ddH ₂ O	Up to 25µl

* Quickchange reagents were from the QuikChange Lightning Site-Directed Mutagenesis kit from Stratagene, dNTPs were purchased from Fermetas.**100ng plasmid DNA

The mutant strand synthesis PCR reaction was carried out in a thermal cycler with a heated lid with the following conditions.

Step	Temperature	Time	Cycles
Hot start:	95°C	2 minutes	/
Denaturation step:	95°C	20s	18x
Annealing step:	60°C	10s	
Extension step:	68°C	30 seconds/kb of plasmid length*	
Final extension step:	68°C	5 minutes	/

The PCR product is then treated with 2µl of *DpnI* endonuclease (Stratagene) as this specifically digests methylated DNA and as almost all *E. coli* strains contain DNA that is dam methylated the *Dpn I* digest only digests the parental DNA template therefore selecting for the newly synthesised mutated DNA. PCR products were incubated with *DpnI* for 5 minutes at 37°C. *DpnI* treated plasmid DNA was then transformed into XL-1

Blue competent cells (Stratagene), see section 2.3.9. Plasmids were verified by sequencing (section 2.2).

2.3.5 Gel extractions

DNA fragments of correct size were extracted from agarose gels using the QIAquick gel extraction microcentrifuge protocol (Qiagen). The DNA was eluted in 30 μ l of dH₂O.

Briefly, the DNA band was excised from the gel over a UV light using a sharp scalpel. After weighing the gel fragments, 3 volumes of buffer QG was added to 1 volume of gel in a 1.5ml microcentrifuge tube. The tubes were incubated at 50°C until the gel had dissolved then 1 gel volume of isopropanol was added. QIA-quick spin columns were placed in 2ml collection tubes and the samples were applied to the columns. 0.5ml of buffer QG was added to the columns which were then centrifuged for 1 minute at 13,000xg, removing any agarose in the sample. 0.75ml of buffer PE was added to the column which was centrifuged again for 1 minute. The column was centrifuged for an additional minute to remove any residual ethanol. The column was then placed in a 1.5ml microcentrifuge tube and the DNA was eluted in 30 μ l of dH₂O, the column was left for 1 minute before centrifuging at maximum speed for 1 minute.

2.3.6 Restriction enzyme digest

The UBE2QL1 PCR inserts and vectors were restriction digested with restriction enzymes EcoRI and BamHI to create complementary sticky ends. Plasmids were also digested with the same restriction enzymes; these included PCDNA3.1 (Invitrogen), pFLAG-CMV4 (Sigma) and pCMV-myc (Clontech). The restriction digest reaction components are shown below.

Reaction components*	Insert	Vector
EcoRI 12u/μl	2μl	2μl
BamHI 10u/μl	2μl	2μl
10x Buffer E	5μl	3μl
DNA	30μl of PCR product	1μg
10 x BSA (N,O bis(trimethylsilyl)acetamide)	1x	1x
H2O	Up to 50μl	Up to 30μl

* All reagents were purchased from Promega.

Reactions were incubated at 37 °C for 2 hours.

2.3.7 Ligation reaction

The digest reaction products were run out on a 1.5% agarose gel and extracted using the QIAquick gel extraction microcentrifuge protocol and eluted in 30 μl of H₂O.

The products of the gel extraction were then run out again on a 1.5% agarose to determine the amount of insert and vector. This was done by running out 5 μ l of the insert and 1 μ l of the vector next to 0.5 μ g of fermentas generuler 100bp ladder. By comparing the brightness of the bands the estimated concentration (ng) of the vector and insert could be determined and used to estimate the amount needed for a 3:1 ratio using the following equation:

$$\text{Insert length (bp)} \times \text{Vector mass (ng)} / \text{vector length (bp)} = \text{Insert mass (ng)} \text{ 1:1}$$

$$\text{Insert mass (ng)} \text{ 1:1 ratio} \times 3 = 3:1 \text{ insert:vector ratio}$$

For example 1 μ l of vector was estimated to be ~100ng by comparing the vector band on an agarose to the bands on the ladder of known concentration. The vector size was 6,300bp and the insert size was 495bp, therefore using the equation:

$$495\text{bp} \times 100\text{ng} / 6,300\text{bp} = 8\text{ng of insert.}$$

5 μ l of the insert was estimated to be about 40ng therefore 8ng per 1 μ l. Therefore 3 μ l of insert was added to 1 μ l of vector for a 3:1 ratio. T4 DNA ligase was used for the ligation reaction. The reaction conditions are shown on the next page.

Reaction components*	1x Volume
10X ligation buffer	1µl
Plasmid	3:1 ratio
Insert	(plasmid:insert)
T4 DNA ligase 100u	1µl
dH2O	Up to 10µl
* The T4 DNA ligase and 10x ligation buffer were purchased from Promega.	

The ligation reaction was left at 4°C overnight.

2.3.8 pGEM-T easy vector ligation

The pGEM-T easy vector system was used to clone modified DNA PCR products for sequencing and methylation analysis. Taq DNA polymerase adds single 3' A-deoxynucleotide to double stranded DNA. These A tails allow the PCR products to be cloned into the pGEM vector (promega). The pGEM vector was already linearized with EcoRV and a T base is added to the 3' ends.

The PCR products were run out on a 2% gel and gel extracted using the QIAquick gel extraction microcentrifuge protocol described in section 2.3.5. The ligation reactions were then set up as follows on the next page.

Reaction components	1xVolume
2x rapid ligation buffer	5 μ l
pGEM T Easy Vector (50ng)	1 μ l
PCR product	3 μ l
T4 DNA ligase	1 μ l
dH ₂ O	Make Up to 10 μ l

The reaction was mixed by pipetting up and down and then incubated at 4°C overnight.

2.3.9 Transformation

Plasmids were transformed into α -select chemically competent cells (DH5 α) according to manufacturer's instructions (Bioline).

Briefly, 100 μ l of DH5 α cells were added to 10 μ l of ligation reaction which were then incubated on ice for 30 minutes. The cells were heat shocked at 42°C for 45 seconds promoting the uptake of the plasmid, then placed on ice for 2 minutes. 2ml of pre-warmed L-Broth was added to the cells which were then incubated in a rotating incubator set at 220rpm at 37°C for 1 hour. 200 μ l of cells were spread onto LB agar plates

containing either 100µg/ml ampicillin or 25µg/ml of kanamycin. These were then incubated overnight at 37°C.

2.3.10 Minipreps

Colonies were then selected off agar plates and picked off using a pipette tip which was added to 2ml of LB-broth containing either 100µg/ml ampicillin or 25µg/ml of kanamycin. This was then left in a rotating incubator set at 220rpm at 37°C overnight. Plasmid DNA extractions from DH5α cells were performed using the Wizard plus SV miniprep protocol (Promega). The DNA was eluted in 50µl of dH₂O.

1ml of the culture was pelleted by centrifugation at 15000rpm for 15secs. The pellet was resuspended in 250µl of cell resuspension solution. Two hundred and fifty µl of cell lysis solution was added and the cell suspension which was left until clear. Ten µl of alkaline protease solution was then added and the lysate was incubated for 5 minutes at room temperature. Three hundred and fifty µl of neutralization solution was applied and the lysate was then centrifuged for 10 minutes at 14000xg. The cleared lysate was then added to a spin column which was centrifuged at 14000xg for 1 minute. The column was then washed twice with 750µl of diluted column wash solution and then centrifuged for 1 minute at 14000xg. The column was then centrifuged for 2 minutes at 14000xg. The column was placed in a 1.5ml centrifuge tube and the DNA was eluted with 50µl of nuclease free water by centrifuging at 14000xg for 1 minute.

2.3.11 Maxipreps

The plasmids were extracted and purified using QIAfilter plasmid Maxi kits (QIAGEN 2005).

Briefly, 200ml of bacterial cultures were left overnight in a rotating incubator set at 220rpm and 37°C. All of culture was centrifuged at 6000rpm for 10mins. The pellet was resuspended in 10ml of buffer P1 solution. 10ml of lysis buffer (buffer P2) was added to the cell solution and mixed thoroughly; this was then left for 5 minute incubation at room temperature. 10ml of neutralization buffer (buffer P3) was added to the cell solution and the lysate was decanted into the QIAfilter cartridge and incubated at room temperature for 10 minutes. Qiagen-tips were equilibrated by applying 10ml of equilibration buffer (buffer QBT) and allowing the column to empty by gravity flow. The nozzle cap from the QIAfilter cartridge was removed and the plunger was inserted into cartridge filtering the cell lysate into a 50ml tube. The cell lysate was applied to the equilibrated QIAGEN-tip and was left to enter by gravity flow. Two x 30ml of wash buffer (buffer QC) was applied to the Qiagen-tip. The DNA was eluted in 15ml of elution buffer. Ten ml of isopropanol was added to precipitate the DNA, this was centrifuged at 6000rpm for 60 minutes at 4°C. The DNA pellet was washed using 70% ethanol and centrifuging for 10 minutes at 11,000rpm. The pellet was left to dry and then resuspended in 500µl dH₂O.

2.3.12 Glycerol stocks

Glycerol stocks were made from DH5 α cell colonies known to contain the correct plasmid and insert. Two hundred μ l of 100% glycerol was added to 800 μ l of cell culture in a 1.5ml microcentrifuge tube, therefore using a 1:4 ratio. These were then frozen at -80°C.

2.3.13 DNA quantification

DNA concentration and quality was determined by measuring the absorbance at 260nm and 280nm in a spectrophotometer. DNA was diluted in sterile RNase and DNase free water, therefore a reading of 1 unit at 260nm corresponds to 50 μ g of DNA per ml. DNA of good quality was determined by having a 260nm/280nm absorbance ratio value between 1.8 and 2. The calculation used to determine DNA concentration is shown below.

$$[\text{DNA}] \mu\text{g}/\mu\text{l} = \frac{50 \times \text{Absorbance at 260nm} \times \text{Dilution factor}}{1000}$$

2.4 DNA Methylation analysis

2.4.1 Bisulphite DNA modification

DNA methylation occurs on cytosine residues on CpG dinucleotides in regions with a GC content of >55% known as CpG islands. These CpG islands are found at the regulatory regions of gene promoters. One way to determine the methylation status of

genes is to use sodium bisulfite treatment of DNA. This causes the conversion of unmethylated cytosine residues to uracil residues and the methylated cytosines stay unchanged. Therefore the DNA sequence will be different depending on the DNA being methylated or unmethylated. The epitect bisulfite kit (QIAGEN) was used for the conversion of tumour DNA as it provides fast and efficient DNA modification starting with DNA amounts as small as 1ng. An example of how bisulfite treated DNA enables to distinguish between methylated and unmethylated DNA is shown below.

Non-treated DNA	Bisulfite Treated DNA	
Original DNA sequence	Methylated DNA	Unmethylated DNA
<u>C</u> -G-N-N- <u>C</u> -G-N-N- <u>C</u> -G	<u>C</u> -G-N-N- <u>C</u> -G-N-N- <u>C</u> -G	<u>U</u> -G-N-N- <u>U</u> -G-N-N- <u>U</u> -G

DNA was modified using the epitect sodium bisulfite modification kit, the DNA was eluted in 40µl of buffer EB (QIAGEN).

Briefly, the bisulfite mix was prepared by adding RNase free water and vortexing until dissolved. Eighty-five µl of the bisulfite mix was added to ~1µg of DNA in 200µl PCR tubes. Thirty-five µl of DNA protection buffer was added to the reaction and the reaction volume was made up to 140µl using RNase-free water. The bisulfite DNA conversion step was performed using a thermal cycler following the conditions shown on the next page.

Step	Temperature	Time
Denaturation	99°C	5s
Incubation	60°C	25s
Denaturation	99°C	5s
Incubation	60°C	85s
Denaturation	99°C	5s
Incubation	60°C	175s
Hold	20°C	Indefinite

Once the bisulfite conversion step was complete, the reaction mixtures were transferred to 1.5ml tubes and 560µl of buffer BL with 10µg/ml of carrier RNA was added to the reactions which were then transferred to an Epiect spin column. The column was centrifuged for 1 minute at 15,000xg and DNA was then washed using 500µl of buffer BW and centrifuged again. Five hundred µl of buffer BD was then added to desulfonate the DNA and was centrifuged for 1 minute. The wash step with buffer BW

was then repeated and the column was centrifuged for 1 minute to remove any residual liquid. The column was placed in a new 1.5ml centrifuge tube and 40µl of buffer EB was added to the membrane. DNA was eluted by centrifuging at 15,000xg for 1 minute.

2.4.2 Designing non bias primers for methylated and unmethylated DNA

To determine if the CpG island of *UBE2QL1* was methylated in cell lines and tumour samples the COBRA technique was used. Primers needed to be designed, to amplify the CpG island from bisulfite modified DNA, that bound specifically to modified DNA and to not show any bias towards the methylation status. As bisulphite modified DNA converts all non-methylated cytosines (C) to thymines (T) all the C were substituted for T in the primer providing they were not next to guanines (G). Any C next to G in the primer that could not be avoided were substituted for a Y in the forward primer meaning the base could be a C or T and an R in the reverse primer meaning the base could be an A or G. *UBE2QL1* COBRA primers can be found in appendix 8.1.6.

2.4.3 COmbined Bisulphite Restriction Analysis (COBRA)

COBRA was used to determine DNA methylation at the *UBE2QL1* promoter CpG island and consists of sodium bisulfite PCR treatment followed by a restriction digest to identify methylated CpGs.

2.4.3.1 CpG amplification PCR conditions

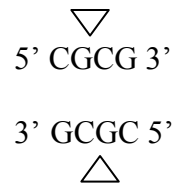
The first PCR reaction included 2µl of bisulfite modified DNA and the *UBE2QL1* COBRA F primer and the *UBE2QL1* COBRA OR primer. Two µl of PCR product from this reaction was then used in a second round of nesting PCR using the same forward primer and the inner reverse primer (*UBE2QL1* COBRA IR). This was to ensure the correct product was amplified. The PCR reactions were set up using the same reagents and concentrations as standard PCR as described in section 2.2.1. The PCR conditions are shown below.

Step	Temperature	Duration
Hot start:	95°C	5 minutes
Denaturation step:	95°C	30s
Annealing step:	Touchdown decreasing 2°C every 2 cycles from 62°C – 58°C Then 56°C for 35 cycles*.	30s
Extension step:	72°C	45s
Final extension step:	72°C	10 minutes

* The PCR machine was set to 56°C for 40cycles after the touchdown in the second round.

2.4.3.2 Restriction Digest

The restriction enzyme BstII cuts at the recognition site shown below:



As only methylated C will stay as C and not be converted to T, the enzyme will only cut at methylated CpGs. Therefore after running the digest products on an agarose gel it was possible to determine which samples had methylated *UBE2QL1* CpG islands. The digest reactions are shown below.

Reaction components*	1x volume
BstUI (Bsh1236I) 10u/μl	0.5μl
1x buffer R	2μl
DNA (PCR product)	12μl
dH ₂ O	Make up to 20μl
* Bsh1236I and 1xbuffer R were purchased from Fermentas.	

The digest reaction was incubated at 37°C for 2 hours. A control plasmid with known CGCG sites was also digested at the same time to ensure the digestion was successful. The digested products were then run out on a 2% agarose gel for analysis.

2.4.3.3 COBRA analysis

Bisulfite modified *UBE2QL1* promoter PCR products, from each tumour, were transformed into DH5 α cells as in section 2.3.9. As the PCR products were bisulfite modified, sequencing each of the clones allowed detection of methylated CpGs within the promoter region. Eight to 12 colonies were picked for each tumour using a pipette tip and were placed in 5 μ l of dH₂O of which 2 μ l was used in a PCR reaction (section 2.2.1) with plasmid specific primers to amplify the plasmid inserts. PCR products for each tumour were then sequenced and analysed (see section 2.2). *UBE2QL1* CpG diagrams were produced using CpGviewer (<http://dna.leeds.ac.uk/cpgviewer/>) to demonstrate the number of CpGs methylated in each of the clones from each tumour.

2.5 DNA deletion analysis

2.5.1 Multiplex Ligation-dependent Probe Amplification (MLPA)

MLPA is a multiplex PCR method which allows detection of abnormal copy numbers of genomic DNA or RNA sequences. MLPA probes contain primer sequences at the 5' and 3' ends that allow a single pair of PCR primers to be used for MLPA amplification, see *Figure 2.1*. The probes hybridise to their target sequence and the primers allow amplification of the probe sequence. Probe binding only occurs if the target sequence is an exact match, differences in one or more nucleotides of the target sequence can affect binding. MLPA has five major stages; DNA denaturation and probe hybridisation, ligation reaction, PCR reaction, separation of products by electrophoresis

and data analysis. All reagents unless specified were purchased from MRC-holland, the reference kit used was SALSA MLPA kit P300-A1 human DNA reference-2.

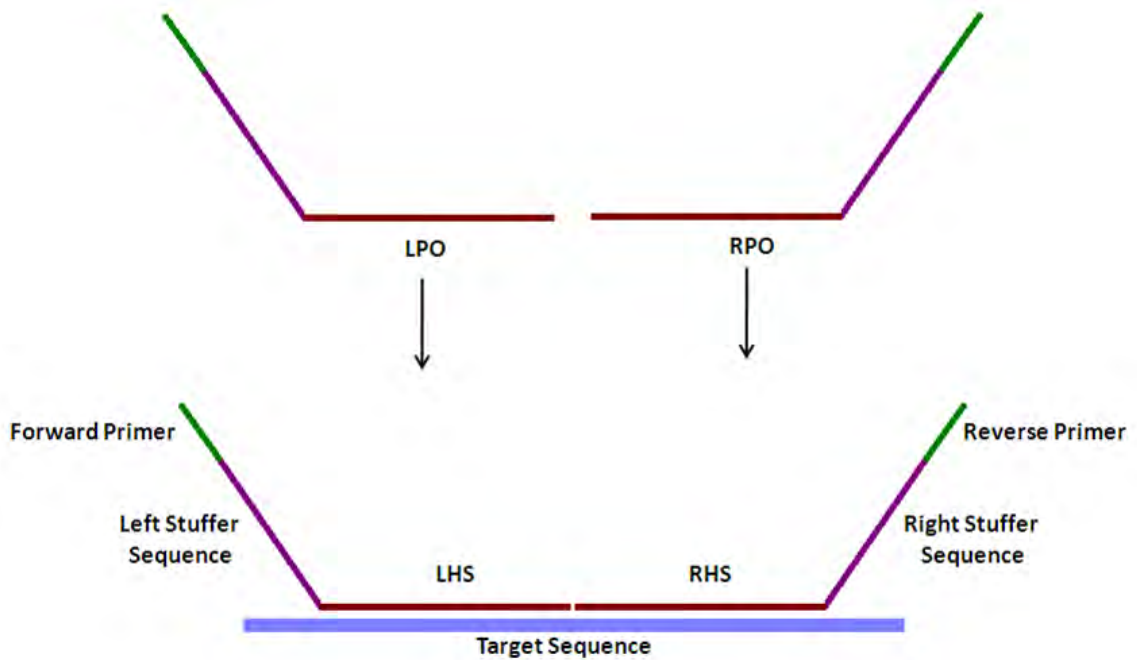


Figure 2.1 schematic diagram of Multiplex Ligation-dependent Probe Amplification (MLPA) Probes.

MLPA probes consist of two separate oligonucleotides named the left probe oligo (LPO) and the right probe oligo (RPO). The LPO consists of the left hybridising sequence (LHS) at its 3' end which binds to the target sequence, an optional stuffer sequence and the forward primer sequence at its 5' end. The RPO contains the right hybridising sequence (RHS) at its 5' end, an optional stuffer sequence and the reverse primer sequence at its 3' end. The RPO is modified with a 5' phosphate to allow ligation of the RPO and LPO during the ligation reaction.

2.5.1.1 Designing MLPA probes

Custom designed probes for *UBE2QL1* are shown in Appendix 8.1.7. Probes were designed using MRC-holland guidelines (www.mrc-holland.com) and the probe designing program alleleID 7 (Premier Biosoft). Probes were designed within the two *UBE2QL1* exons as well as upstream and downstream of each exon. Care was taken to design probes in regions with no known polymorphisms as determined using the single nucleotide polymorphism database from NCBI.

2.5.1.2 Denaturation and hybridisation reaction

Reactions were carried out in a thermal cycler with a heated lid. DNA was diluted to 50-100ng in 2.5µl of buffer TE which was then denatured by heating to 98°C for 5 minutes. The DNA was then cooled to 25°C and 0.75µl of MLPA buffer, 0.5µl of SALSA probe mix and 0.25µl of custom designed probes were added to each tube. Tubes were incubated for 1 minute at 95°C followed by 16 hours at 60°C to allow the hybridisation of probes to their target sequence.

2.5.1.3 Ligation reaction

The samples were cooled to 54°C and 1.5µl of ligase-65 buffer A, 1.5µl of ligase-65 buffer B and 25µl of dH₂O were added to each tube. Samples were then incubated for 15 minutes at 54°C to allow ligation of the RPO and LPO probes. The samples were then heated to 98°C for 5 minutes to inactivate the ligation reaction.

2.5.1.4 PCR reaction

Polymerase mix was made up in new tubes by adding 1µl of SALSA PCR-primers, 1µl of SALSA enzyme dilution buffer, 2.75µl of dH₂O and 0.25µl SALSA polymerase. Two µl of SALSA PCR buffer and 13µl of dH₂O were added to tubes containing 5µl of the ligation reaction. The tubes were placed in a thermal cycler and heated to 60°C, while at 60°C 5µl of the polymerase mix was added to each tube. The following PCR program was then used to amplify the probe products.

Step	Temperature	Duration	Cycles
Denaturation step: Separation of DNA strands to produce single stranded DNA	95°C	30s	Cycle 35x
Annealing step: Anneal primers to single stranded DNA	60°C	30s	
Extension step: Synthesis of new DNA strands complementary to DNA template	72°C	1 minute	
Final extension step:	72°C	20 minutes	/

2.5.1.5 Electrophoresis

The amplification products were separated by electrophoresis using a 3730 DNA analyzer (Applied Biosystems). 1µl of the PCR products were added to a 96 well plate along with 0.2µl of labelled size standard (LIZ-500, applied biosystems) and 9µl of formamide (Hi-Di, applied biosystems).

2.5.1.6 MLPA data Analysis

MLPA data was analysed on Genemapper V3.5 (Applied Biosystems) to visually examine the peak profiles and to calculate the peak area and peak height for each probe. Further calculations were carried out in an excel spreadsheet. Analysis involved block normalisation of all probes by dividing the peak area of each probe by the total peak area of the control reference probes. Further normalisation was achieved by dividing the normalised peak areas with the average of all the normalised peak areas for that probe in control samples. Normalised probe signals that deviated from their neighbouring reference probes by $\geq 25\%$ were highlighted. An average deviation of $\geq 30\%$ from adjacent reference probes for all *UBE2QL1* probes or single exon probes indicated a gene or exon deletion, respectively.

2.5.2 Loss of heterozygosity (LOH)

Microsatellites are segments of DNA, often in non-coding regions, that contain a repeated sequence such as a mono or di nucleotide tract e.g. CACACACA . If an individual is heterozygote for a particular microsatellite marker this can be informative.

Large deletions of DNA often occur in tumours and these can be detected by comparing microsatellite markers in corresponding normal (CN) DNA and tumour DNA. If the marker is heterozygote in the CN but homozygote in the tumour, this suggests that particular locus has been deleted in the tumour. If the CN is homozygote this is said to be non-informative.

2.5.2.1 Microsatellite Markers

Microsatellite markers within the 3p15 locus were found using the NCBI map viewer (www.ncbi.nlm.nih.gov/projects/mapview/). Microsatellite markers within the 3p15 locus with a known heterozygosity of >0.5 , thus likely to be informative, were searched for. Primers were produced to amplify microsatellite markers D5S2505 and D5S2054 both found within the same chromosomal locus as *UBE2QL1*, specifically 3p15. The primers used are shown in appendix 8.1.8.

2.5.2.2 LOH PCR

PCR was used to amplify the microsatellite markers with the conditions shown on the next page.

Reaction components*	1 x Volume
10x PCR reaction buffer	1.5µl
2mM dNTP mix (1:1:1:1)	1.5µl
MgCl	1.5µl
Forward primer 20µM	1µl
Reverse primer 20µM	1µl
Thermoprime taq DNA polymerase 5U/µl	0.1µl
dH2O	Up to 15µl
DNA**	/
* 10x reaction buffer, MgCl and thermoprime taq polyaerase were purchased from Thermo scientific. dNTPs were purchased from Fermetas. **10-200ng genomic DNA	

LOH PCR conditions are shown below.

Step	Temperature	Duration	Cycles
Hot start:	95°C	5 minutes	/
Denaturation step:	95°C	30s	Cycle 30x
Annealing step:	58°C	30s	
Extension step:	72°C	45s	
Final extension step:	72°C	10 minutes	/

Five μl of PCR products were run on a 2% agarose gel to confirm the PCR reaction produced the correct sized products. The PCR products were then diluted 1 in 10. A master mix containing 500 μl of HiDi and 5 μl of LIZ-500 (Applied Biosystems) size standard was prepared. One μl of diluted PCR product was added to 9 μl of master mix. The amplification products were separated by electrophoresis using a 3730 DNA analyzer.

2.5.2.3 *LOH Data analysis*

Data was analysed using Genemapper 4.0 (Applied biosystems). To establish possible LOH candidates the following equation was used:

Determine peak height ratio of tumour or CN:

(Peak area of allele 1 / peak area of allele 2).

LOH was established by dividing the tumour peak height ratio by the CN peak height ratio. A number ≤ 0.5 is due to LOH.

2.6 *RNA analysis*

2.6.1 RNA quantification

RNA concentration and quality was determined by measuring the absorbance at 260nm and 280nm in a spectrophotometer. RNA was diluted in sterile RNase and DNase free water, therefore a reading of 1 unit at 260nm corresponds to 40 μg of RNA per ml.

RNA of good quality was determined by having a 260nm/280nm absorbance ratio value between 1.8 and 2. The calculation used to determine RNA concentration is shown below.

$$[\text{RNA}] \mu\text{g}/\mu\text{l} = \frac{40 \times \text{Absorbance at 260nm} \times \text{Dilution factor}}{1000}$$

2.6.2 Reverse transcription cDNA synthesis

cDNA was produced from 1µg of RNA using superscript II RT and random hexamers following manufacturer's instructions (Invitrogen, 2003). The reaction mixture is shown below.

Reaction components*	1x Volume	[Final]
Random Hexamers 0.5µg/µl	0.5µl	0.25µg
2mM dNTP (1:1:1:1)	2µl	0.25mM
1µg RNA	/	/
RNase free dH ₂ O	Make up to 12µl	/
* All reagents were used from the superscriptII reverse transcriptase kit purchased from Invitrogen.		

The reaction mixture was heated for 65°C for 5 minutes and quickly placed on ice. The following mixture was then added shown on the next page.

Reaction component	1x Volume	[Final]
5 x First Strand Buffer	4 μ l	1x
0.1M DTT	2 μ l	10mM

The reaction mixture was mixed gently using a pipette and then incubated at 25°C for 2 minutes. Then 1 μ l of superscript II RT enzyme was added to the reaction. The following conditions were set in a thermal cycler with a heated lid.

Step	Temperature	Time
Primer annealing	25°C	10 minutes
Extension	42°C	90 minutes
Inactivation of reaction	70°C	15minutes

The cDNA was stored at -20°C.

2.6.3 Reverse transcription PCR (RT-PCR)

RT-PCR was used to measure gene expression by showing the amount of gene specific RNA in a sample in a semi-quantitative manner. The RT-PCR products are run on an agarose gel and viewed under UV light. The strength of the band signal on an

agarose gel was used to determine if there was a loss of gene expression compared to a control.

cDNA was produced using 1µg of RNA from samples of interest. The cDNA was used in a standard PCR reaction to amplify the gene of interest for each sample. GAPDH primers were used as a control to make sure each reaction contained equal amounts of cDNA. RT-PCR reaction components and reaction conditions are shown below and on the next page.

Reaction components*	1 x Volume
10x PCR reaction buffer with 20mM Mgcl ₂	2.5µl
2mM dNTP mix (1:1:1:1)	2.5µl
GC-RICH Solution, 5x conc.	5.0µl
Forward primer 20µM	1µl
Reverse primer 20µM	1µl
Fast start taq DNA polymerase 5U/µl	0.2µl
dH ₂ O	Up to 25µl
cDNA	1 µl
* 10x reaction buffer, 5x GC-rich solution and fast start taq polyaerase were purchased from Roche applied science. dNTPs were purchas ed from Fermetas.	

Step	Temperature	Duration
Hot start:	95°C	5 minutes
Denaturation step:	95°C	30s
Annealing step:	58°C	30s
Extension step:	72°C	45s
Final extension step:	72°C	10 minutes

Ten µl of the RT-PCR products were run out on a 2% agarose gel and analysed under ultraviolet light.

The primers were designed to bind to two separate exons to prevent the amplification of any genomic DNA contaminating the sample, as this would contain an intron between the two exons. All primers used in RT-PCR reactions are shown in Appendix 8.1.9.

2.6.4 Quantitative Real time-PCR

Taqman oligonucleotide probes were used to determine gene expression in real time. Each probe has a fluorescent reporter 6-Carboxyfluorescein (FAM) at the 5' end

and a 3' quencher Tetramethyl-6-Carboxyrhodamine (TAMRA). The probes are designed to bind specifically to RNA/cDNA as they bind within the boundary of two exons, therefore amplification of DNA contamination is avoided. Primers bind to the complementary sequence either side of the probe and taq polymerase extends the primers across the gene of interest. The probe is degraded due to the 5' endonuclease activity of taq polymerase and the fluorescent reporter is released from the quencher emitting fluorescence. Fluorescence is then detected per cycle of PCR allowing quantification of gene expression in real time.

Taqman assays containing probes and primers for UBE2QL1 and β -actin along with taqman universal master mix II were purchased from Applied Biosystems. cDNA samples (1 – 100ng) were loaded in triplicate on a 96 well plate with negative controls containing no cDNA. β -actin probes were used as internal controls and were loaded in triplicate on the same plate for each sample. The reaction components are shown below.

Reaction component*	Volumes per reaction	Final concentrations
Taqman Universal Master Mix II	10 μ l	1X
Taqman assay, 20x	1 μ l	1X
RNase free dH ₂ O	9 μ l	1 – 100ng
Total volume	20 μ l	/
* All reagents were purchased from Applied Biosystems. Universal Master Mix includes 0.05 u/ μ l <i>Taq</i> DNA Polymerase, reaction buffer, 4mM MgCl ₂ and 0.4mM of each dNTP		

A 7500 real-time PCR system (Applied Biosystems) was used set to the following conditions shown on the next page.

Step	Temperature	Duration	Cycles
Hot start:	95°C	10 minutes	/
Denaturation step:	95°C	15s	Cycle 40x
Annealing step:	60°C	1 minute	

2.6.4.1 QRT-PCR analysis

The 7500 fast real-time PCR system (Applied Biosystems) was used to analyse the QRT-PCR data. A threshold is set at a point where PCR products were produced exponentially. Number of PCR cycles undertaken up until the threshold is known as the Ct value. Normalisation of samples is carried out by calculating the ΔCt , which involves subtracting the Ct of the internal control (β -actin) from the Ct of the gene of interest (GOI). Gene expression in tumours was compared to gene expression in corresponding normals (CN) through calculating the $\Delta\Delta Ct$ (ΔCt for GOI – ΔCt for CN). To determine tumour gene expression relative to the CN the following equation was used $2^{-\Delta\Delta Ct}$, presuming the PCR product doubles in log phase.

2.7 Tissue culture

2.7.1 Cell lines and clinical samples

An EBV-transformed lymphoblastoid cell line was established from the index case of the family with the t(5;19)(p15.3;q12) by European Cell and Culture Collection.

RCC cell lines used in this study included KTCL 26, SKRC45, SKRC54, Caki-1, 786-0, KTCL 140, RCC4, SKRC39, SKRC47, SKRC18, UMRC3, RCC48, RCC1, RCC12, A498, ACHN, 769P and CAL 54.

2.7.2 Culture conditions

Cells were grown in 75cm³ flasks with Dulbecco's modified eagle medium (DMEM) containing 10% V/V FBS, 1% L-Glutamine, 1% Penicillin/streptomycin (100 units/ml penicillin, and 100µl/ml streptomycin) (Invitrogen) and 1% MEM non-essential amino acids (all reagents purchased from Sigma unless specified). The t(5;19)(p15.3;q12) EBV-transformed lymphoblastoid cell line was maintained in RPMI 1640 (Invitrogen) supplemented with 10% V/V FBS and 1% Penicillin/streptomycin. Cells were incubated at 37°C and 5% CO².

2.7.3 Transfections

The day before transfection media was removed and the cells were washed with Phosphate buffered saline (PBS) before treatment with 0.25% trypsin (Invitrogen) to resuspend the cells. A haemocytometer was used to count the cells and a cell concentration 3.0×10^5 cells was added to a 6 well dish. A confluency of >80% was achieved overnight. For each transfection 2µg of plasmid DNA was added to 100µl of Opti-MEM medium (Invitrogen). Fugene HD transfection agent (Roche) was then added at a ratio of 2:6 or 2:8 (µg DNA: µl Fugene) depending on the cell line and the

transfection reagent:DNA complex was incubated at room temperature for 15 minutes. The transfection complex was added to the 6 well dish containing the cells, which was then gently rocked to ensure efficient mixing of the transfection complex. Cells were then incubated for 48 hours at 37°C before protein extraction.

2.7.4 Colony formation assays and stable clones

Cells were transfected with either Flag-empty vector or flag-UBE2QL1. The pFLAG-CMV4 (Sigma-Aldrich) plasmid contains the neo gene from Tn5 which allows resistance to G418. Transfected cells were grown in 10cm³ dishes with 10ml of DMEM and 10% FBS plus 1mg/ml G418 an aminoglycoside antibiotic (PAA). Once non-transfected control cells had all died from exposure to G418, transfected cells were seeded in serial dilutions. After 21 days from the initial seeding, the surviving colonies from the colony assays were stained with 0.4% crystal violet (Sigma) in 50% methanol. Replica assays were set up at the same time to produce *UBE2QL1* stably expressing clones. Once colonies were visible by eye at 21-28 days each colony was removed by pipetting up the colony using a p200 pipette and adding the cells to a 6 well dish containing 2ml of DMEM with 10% FBS supplemented with G418. Once cells became >80% confluent they were transferred to a 25ml flask. Protein was extracted from all clones and western blot analysis was used to verify *UBE2QL1* stable expression.

2.7.5 Soft agar colony assays

Soft agar colony assays can be used to determine the ability of a cell line to undergo anchorage independent growth, thus the ability to proliferate suspended in agar. The assays were carried out in 6-well plates and involved adding 2mls of base layer 0.7% agar to each well and then leaving the plates at room temperature to set. Once solidified the agar is placed in a 37°C incubator to equilibrate. SKRC47 flag-UBE2QL1 or flag-empty vector stable clones were counted and prepared to contain $\sim 2 \times 10^4$ cells per 100 μ l. A middle layer of 1ml 0.35% agar was combined with 100 μ l of prepared cells and added to the base agar and allowed to set at room temperature. Once set 2ml of a final layer of 0.7% agar was then added on top of the middle agar layer and allowed to set at room temperature. As soon as the final layer was set the plates were placed in a 37°C incubator for 28 days and were maintained by applying 200 μ l of DMEM supplemented with 10% FCS and 1mg/ml of G418 (PAA) weekly. Each experiment was undertaken 6x simultaneously. Colonies measuring $\geq 100\mu$ m were manually counted under a microscope. Details of the components of 2xDMEM, 1xDMEM, 0.7% agar and 0.35% agar are shown in the tables on the next page.

2X DMEM		
Reaction components	Volumes	Final %
FCS	50ml	20
Penicillin- Streptomycin	5ml	2
L-Glutamine	5ml	2
10x DMEM*	50ml	20
7.5% sodium bicarbonate*	25ml	10
G418 50mg/ml	1ml	0.4
dH ₂ O	Up to 250ml	
*10x DMEM and 7.5% sodium bicarbonate were both purchased from Sigma.		

1X DMEM		
Reaction components	Volumes	Final %
FCS	10ml	10
Penicillin- Streptomycin	1ml	1
L-Glutamine	1ml	1
10x DMEM	10ml	10
7.5% sodium bicarbonate	5ml	5
dH ₂ O	Up to 100ml	

0.7% and 0.35% agar solutions were made up combining different ratios of 1x DMEM, 2x DMEM and 1.4% noble agar (Sigma), as shown in the tables on the next page.

0.7% agar		
Reaction components	Volumes (150ml total)	Final %
2xDMEM	75ml	50
1.4% agar	75ml	50
2xDMEM : 1.4% noble agar = 1:1 ratio		

0.35% agar		
Reaction components	Volumes (80ml total)	Final %
2xDMEM	20ml	25
1.4% agar	20ml	25
1X DMEM	40ml	50
2xDMEM : 1.4% noble agar: 1xDMEM = 1:1:2 ratio		

2.8 Protein Analysis

2.8.1 Antibodies

The following antibodies were used in this study; Monoclonal anti-FLAG M2 (1:2,000 dilution; Sigma), monoclonal anti- β -actin (1:10,000 dilution; Sigma), monoclonal anti-tubulin (1:10,000 dilution; Sigma), anti-C-Myc (1:1,000 dilution; Sigma), anti-6xHis (1:1,000 dilution; Abcam), anti-RBX1 (1:1,000 dilution; Cell Signalling), anti-mtor (1:1,000 dilution; Cell signaling), anti-cyclin E1 (1:1,000 dilution; Abcam).

2.8.2 Protein extraction from cells

Cells were grown in either 6 well dishes or 10cm³ dishes until confluent, they were then washed twice with PBS and 150 μ l – 1ml (depending on the amount of cells) of

lysis buffer* was added. Cells were scraped off into the lysis buffer which was pipetted into 1.5ml tubes and incubated on ice for 20minutes. They were then centrifuged at 15,000 x g for 15 minutes and the supernatant containing the protein was transferred to a clean tube.

* RIPA buffer (50 mM Tris-HCl pH8, 150 mM NaCl, 1 mM EDTA, 1% nonidet NP-40, 0.5% Sodium Deoxycholate, 0.1% SDS) was used for proteins extracted for standard western blot analysis, NETN buffer (50mM Tris-HCl at pH7.5, 150mM NaCl, 1mM EDTA, 1% Nonidet P-40) was used in Co-Immuno-precipitation experiments and His pulldown lysis buffer (50mM Na-phosphate at pH8, 300mM NaCl, 0.01% Tween-20, 1% Triton X-100) was used in Hisx6 pulldown experiments. In all protein extractions a complete mini protease inhibitor cocktail tablet (Roche) was added per 10ml of lysis buffer.

2.8.3 Determining Protein concentration

Protein concentrations were determined using the DC protein assay following manufacturer's instructions (Bio-Rad).

Briefly, 20µl of reagent S was added to every ml of reagent A (an alkaline copper tartrate solution). Protein standards were prepared, 0.2mg/ml – 1.4mg/ml, using BSA (Bovine serum albumin, Invitrogen) in RIPA buffer. Five µl of standards and protein samples were added in duplicate to a 96 well-plate. Twenty-five µl of reagent A (+

reagent S) was added into each of the wells along with 200µl of reagent B (a dilute folin reagent) making sure each of the wells were thoroughly mixed. After 15 minutes at room temperature the OD was measured at 690nm on a Wallac Victor3 fluorometer (Perkin Elmer). A calibration graph was produced from the readings of the protein standards and the regression equation from the graph was used to calculate the concentration of the protein samples.

2.8.4 Western Blot analysis

2.8.4.1 *SDS-PAGE*

Sodium dodecyl sulphate polyacrylamide gel (SDS-PAGE) electrophoresis is used to separate proteins according to their size. Proteins are denatured and given a negative charge due to the SDS detergent. The negative charge per unit mass is identical for each protein; thus once the proteins have been separated on a polyacrylamide gel in an electrical field, specific proteins can be detected due to their size. A protein ladder is run with the samples to determine the size of the protein bands.

The acrylamide gel construct was produced using 0.75mm or 1.5mm glass plates which were assembled and placed in a gel stand. The stacking and resolving mixtures were then prepared, see table on the next page.

Reagents	Stacking	Resolving
Acrylamide/ Bis 30% (W/V)	4%	9 -15% (depending on size of protein)
0.5M TRIS ph 6.8 HCL	1.5ml	-
1.5M TRIS ph8.8 HCL	-	2.5ml
dH₂O	Make up to 7.5ml	Make up to 10ml
10% SDS (Sodium Dodecyl Sulfate)	60µl	100µl
10% APS (Ammonium persulfate)	50µl	50µl
TEMED (Tetramethylethylenediamie)	10µl	10µl

The resolving gel mix was poured between the glass plates this was then covered with 1ml of dH₂O to make sure the top edge of the gel layer set straight. Once the resolving layer had set the water was drained off and the stacking mix was poured on top of the resolving gel and the comb was inserted between the glass plates. After the gel had fully set it was clipped into a gel running tank and 1X SDS running buffer (25 mM Tris, 192 mM glycine, 0.1% w/v SDS, pH 8.3) was poured between two sets of plates and the combs were removed carefully. Five X SDS gel loading buffer (10% w/v SDS, 10mM beta-mercapto-ethanol, 20% v/v glycerol, 0.2M Tris-HCL pH6.8 and 0.05% w/v Bromophenol blue) was added to 10 µg - 30µg of each protein sample which was then loaded onto the gel. Five µl of Fermentas Plus Prestained Protein Ladder was also loaded onto the gel. The gel was electrophoresed at 120V for as long as needed.

2.8.4.2 Wet transfer and blocking

A wet transfer involves the gel and membrane being sandwiched between sponge and paper. Four pieces of filter paper (9cm x 6cm) and two sponges per gel were soaked in transfer buffer (25mM Tris, 192mM Glycine and 20% MeOH). The Polyvinylidene Fluorid (PVDF) membrane was cut to the size needed and activated in 100% methanol (as methanol is a low surface tension liquid it displaces the air in the pore structure of the membrane) and then soaked in transfer buffer. The gel was removed from the tank carefully and the wells cut off using a plastic cutter. The membrane was placed carefully over the gel and both were moved onto the clamping device where the membrane was clamped between filter paper and sponges in the following order; sponge, 2 filter papers, gel, membrane, 2 filter papers, sponge. All were clamped tightly together ensuring no air bubbles formed between the membrane and gel. The sandwich was then submerged in a tank of transfer buffer. An electrical field was then applied at 100V for 1 hour or 50V overnight at 4°C. The negatively charged proteins travel towards the positive electrode therefore the proteins move towards the membrane and binds. To prevent the primary antibody binding to regions of the membrane not bound by proteins, after transfer the membrane was blocked for 45 minutes in 5% w/v dried skimmed milk in PBS or 5% w/v BSA in TBS-T (50M Tris pH7.6, 150mM NaCl, 0.05% Tween 20) depending on the primary antibody.

2.8.4.3 Immunodetection

The primary antibodies were diluted in 5% w/v dried milk in PBS or 5% w/v BSA in TBS-T and incubated with the membrane for 1 hour at room temperature or overnight at 4°C.

Membranes were then washed in PBS or TBS-T 3 x 5 minutes. Secondary-Horse radish peroxidase (HRP) antibodies were diluted in the same buffer used for the primary and incubated with the membrane for 1 hour at room temperature. Amersham ECL western blotting detection agents (GE healthcare) were applied to the membrane making sure the solution was applied evenly across the membrane. This was incubated at room temperature for 5 minutes. The excess solution was drained off the membrane which was then wrapped in cling film making sure no air bubbles were trapped, and was taped onto a film cassette. In the dark room photographic film (Kodak) was exposed to the membrane for as long as required. The film was developed using a SRX-101A medical film processor (Konica Minolta).

2.8.4.4 Membrane stripping

Membranes were stripped of primary and secondary antibodies by boiling in water for 5 minutes. Blocking was repeated to prepare the membrane for further blotting.

2.8.5 Protein synthesis using a Coupled reticulocyte lysate system

UBE2QL1 and UBE2QL1^{C88A} proteins were synthesised and labelled with [35S]-methionine using the TNT Coupled Reticulocyte Lysate System following manufacturer's instructions (Promega). TNT lysate reactions were set up as shown on the next page.

Reaction components*	1 x Volume
TNT Rabbit Reticulocyte Lysate	25µl
TNT Reaction Buffer	2µl
TNT RNA Polymerase (SP6, T3 or T7)	1µl
Amino Acid Mixture, Minus Leucine, 1mM	1µl
Amino Acid Mixture, Minus Methionine, 1mM	1µl
[35S]methionine (1,000Ci/mmol at 10mCi/ml)	2µl
RNasin Ribonuclease Inhibitor (40u/µl)	1µl
DNA Template(s) **	1µl
Nuclease-Free Water to a final volume	Up to 50µl
* All components were purchased from Promega unless stated otherwise. [35S]methionine was purchased from Perkin Elmer. ** 0.5µg/µl of PCDNA3.1 vector (Invitrogen) containing either UBE2QL1 or UBE2QL1 ^{C88A} were used.	

Reactions were incubated at 30°C for 90 minutes. 5µl of reaction mixture was applied to SDS-PAGE and analysed using autoradiography (see sections 2.8.4).

2.9 Pulldowns and Immunprecipiations

2.9.1 Hisx6 ubiquitin pulldown

Pulldowns of Hisx6 tagged ubiquitin were carried out using Dynabeads His-tag isolation and pulldown (Invitrogen). The Dynabeads are coated in a cobalt-based

immobilised metal affinity chromatography chemistry which allows the binding of histidine-tagged proteins.

HEK293 cells were seeded in 10cm³ dishes and transfected with either flag tagged UBE2QL1, UBE2QL1^{C88A} or UBE2QL1^{C88S} along with Hisx6-tagged ubiquitin or Hisx6 empty vector control (sections 2.8.2 and 2.7.3). Cells were lysed with 1x binding/wash buffer (50mM Na-phosphate at pH8, 300mM NaCl, 0.01% Tween-20) containing 1% Triton X-100. The whole-cell lysates obtained by centrifugation for 15 minutes at 12,500rpm, were incubated with 2mg of His tag Isolation and Pulldown Dynabeads (Invitrogen) for 1h at 4°C. The protein bound beads were placed on a magnet and the supernatant was removed. The beads were washed with 1X Pull-down buffer (3.25mM Na-phosphate at pH7.4, 70mM NaCl, 0.01% Tween-20) four times and the bound proteins were then eluted with 50µl of His elution buffer (300mM Imidazole, 50mM Na-phosphate pH8.0, 300mM NaCl, 0.01% Tween-20). Laemmli sample buffer was added to the elutes with or without β- mercaptoethanol (a reducing agent) and applied to SDS-PAGE and western blot analysis (section 2.8.4).

2.9.2 Antibody binding

Dynabeads with protein G coupled to their surface (Invitrogen) were used for Co-immunoprecipitations. The Protein G Dynabeads bind a number of mammalian immunoglobulins including strong binding of human IgGs. As the beads are magnetic the beads along with the bound proteins can be separated from the solution using a magnetic block. To bind the antibody to the beads 50µl of suspended protein G Dynabeads were

added to a 1.5ml tube placed on a magnetic tube rack. The supernatant was removed and the beads were washed twice with Citrate Phosphate Buffer (24.5 mM Citric Acid and 51.7 mM Dibasic Sodium Phosphate, pH=5.0). Ten - 20µg of antibody was diluted in 100µl of PBS then added to the dry beads and incubated for 1 hour. The supernatant was removed and the beads were washed three times with Citrate Phosphate Buffer. The beads were re-suspended in 50µl of PBS and stored at 4°C until required.

2.9.3 Co-immunoprecipitation

Protein was extracted from transfected HEK293 cells grown in 6 well plates (sections 2.8.2 and 2.7.3). Each transfection was repeated in 3 wells and the lysate from all 3 replica wells was combined and added to 50µl of dry antibody bound protein G Dynabeads and was incubated on a roller for 2 hours at 4°C. Twenty µl of the complete lysate was removed before adding to the beads to verify the input. The supernatant was removed from the bead-protein complex using the magnetic rack and the beads were washed 3 times with 200µl of PBS. The beads were re-suspended in PBS one more time and were transferred to a clean 1.5ml tube. The PBS was removed and 30µl of 2x Lamelli sample loading buffer (62.5 mM Tris-HCl pH6.8, 25% Glycerol, 2% SDS, 0.5 % β-Mecaptoethanol, 0.5% Bromophenol blue) was added and the sample was boiled for 10 minutes. The samples were run on a SDS-PAGE gel to undergo western blot analysis (section 2.8.4).

2.10 Immunofluorescence

Immunofluorescence was used for protein localisation experiments in HeLa cells.

2.10.1 Cell fixing

Cover-slips were sterilised by dipping them in 70% ethanol and leaving them to dry on a sterile tissue. Once the ethanol dried, 4 cover-slips were placed in each well of a 6 well plate. HeLa cells were then trypsinized and 3×10^5 cells were seeded into the 6 well dishes and left overnight. Cells were transfected the next day with the appropriate plasmid following the trasfection protocol in section 2.7.3.

After 48 hours media was removed using a vacuum pump, and cells were washed in PBS 3 times. Cells were fixed by adding 2ml of previously chilled 100% methanol to the cells which were then incubated at -20°C for 10 minutes. The cover-slips were washed 3 times with PBS and were blocked by incubating them with 1% BSA in PBS for 30 minutes, this minimises non-specific adsorption of the antibodies to the cover-slips.

2.10.2 Cell staining

The 1% BSA in PBS was removed from the coverslips with a vacuum pump and using tweezers each cover-slip was transferred to a single well in a 24 well dish, making sure the cell side was facing up. Primary antibodies were diluted by the correct amount to a final volume of 1ml. One hundred μl of the diluted antibodies were pipetted onto the cover-slips, which were then incubated for 1 hour at room temperature. Cover-slips were washed 3 times in PBS and 100 μl of the diluted secondary antibody was added to each

cover-slip, which were further incubated for 1 hour at room temperature. Cover-slips were then washed for a final time in PBS.

Microscope slides were labelled and 3 separate drops of 4'-6-Diamidino-2-phenylindole (DAPI) nucleic acid stain (Invitrogen) were dropped on each slide. Cover-slips were removed from the 24 well dish using tweezers and placed cell side down onto the drops of DAPI. Slides were placed in a slide holder covered in tinfoil and left overnight. The next day cells were viewed using a fluorescence light microscope, Axiovert 200 (Zeiss). Secondary antibodies used were goat anti-mouse IgG Alexa Fluor 594 and goat anti-rabbit IgG Alexa Fluor 488 purchased from Invitrogen.

2.11 Protein degradation assay

Cycloheximide (CHX) is an antibiotic that inhibits protein translation in eukaryotic cells and therefore can be used to determine a protein's half life when added to cells in a time-course experiment.

HeLa and SKRC47 cells were transfected with either myc-UBE2QL1 or myc-empty vector (EV) (section 2.7.3). At 24 hours post-transfection cells were treated with 100µg/ml of cyclohexamide (Sigma-Aldrich) and collected at specific time intervals. Cells were lysed and whole-cell extracts were prepared (section 2.8.2). The protein concentration for each sample was determined (section 2.8.3) and 10µg of protein were

analysed by SDS-PAGE and immunoblotting with the indicated antibodies (section 2.8.4).

**Chapter Three:
Characterisation of the
 $t(5;19)(p15.3;q12)$ breakpoints**

3.1 Introduction: A novel familial constitutional translocation, $t(5;19)(p15.3;q12)$, associated with RCC

A constitutional translocation, $t(5;19)(p15.3;q12)$, was found to be associated with a familial predisposition to RCC in one family. No mutations were detected in known RCC genes *VHL* and *FLCN*. The index case developed both oncocytoma and chromophobe RCC at age 35 years and her sister presented with clear cell and chromophobe RCC at age 36 years and then developed multiple oncocytomas at age 38 years. The $t(5;19)(p15.3;q12)$ was shown to be present in both sisters. Their maternal aunt was reported to have died from an RCC, age unknown and their deceased mother was reported to have developed a carcinoid tumour at age 44 years. The $t(5;19)(p15.3;q12)$ was not detected in the two brothers of the index case and they have not developed RCC or any other cancer type. As the $t(5;19)(p15.3;q12)$ positively segregated with the emergence of RCC within this family, it was deduced that the translocation was responsible for the onset of RCC tumourigenesis. It was decided that further characterisation of the $t(5;19)(p15.3;q12)$ breakpoints and investigation of the surrounding genes was necessary to establish the cause of RCC within this family and potentially identify a novel RCC candidate gene (*Figure 3.1*).

3.1.1 Aims

Characterisation of the $t(5;19)(p15.3;q12)$ breakpoint region was carried out to determine the exact breakpoint position on both derivative chromosomes and to elucidate

the genetic consequences of the breakpoint i.e. if there was loss or gain of genetic material within the breakpoint regions. Candidate RCC genes within the breakpoint regions could then be identified and investigated further.

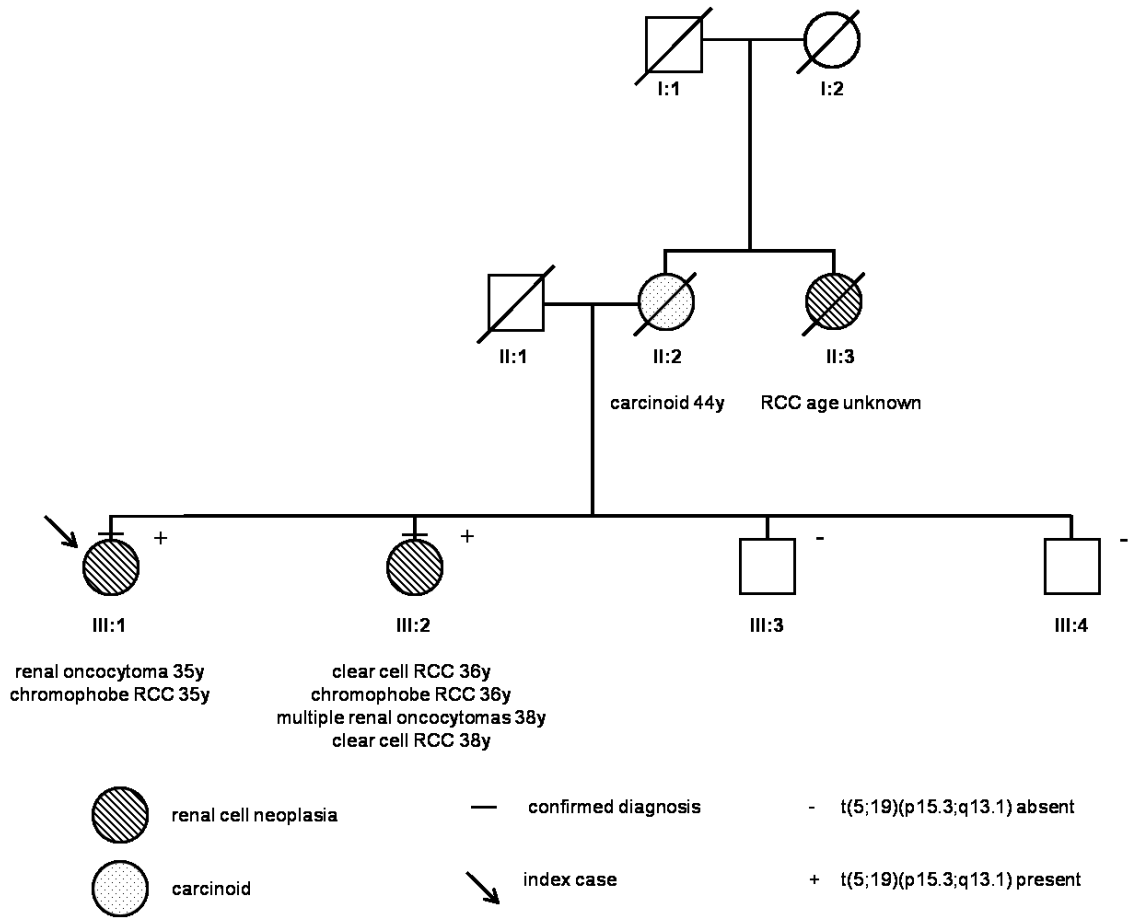


Figure 3.1 Pedigree of family with a constitutional $t(5;19)(p15.3;q13.1)$ and predisposition to renal cell carcinoma (RCC).

Affected family members with the constitutional $t(5;19)(p15.3;q13.1)$ and RCC (or carcinoid) are indicated as shown in the figure legend. Females are illustrated by a circle and males by a square and deceased individuals are indicated by a diagonal line across the respective symbols. III:1 represents the index case.

3.2 Results

3.2.1 Mapping of the t(5;19)(p15.3;q12) breakpoint region

CGH arrays were undertaken by the Wellcome Trust Sanger Institute and Nimblegen prior to the start of this project. Initially, an EBV-transformed lymphoblastoid cell line was established from the index case of the family with the t(5;19)(p15.3;q12) by the European Cell and Culture Collection. To map the t(5;19)(p15.3;q12) breakpoints, derivative (der) chromosomes extracted from the lymphoblastoid cell line were separated by flow cytometry and hybridised onto a whole genome tiling path array at the Wellcome Trust Sanger Institute, which allowed mapping of the breakpoints to within a few megabases (Fiegler et al. 2003). Data from the whole genome arrays showed the breakpoint spanning clone on der(5) was chr5tp-10A3 that corresponded to chromosome region 6,580,618bp and the breakpoint spanning clone on der(19) was chr19tp-1B2 that corresponded to position 35,029,739bp (hg18). Breakpoints were then further refined by Nimblegen where the derivative chromosomes were hybridised onto a custom designed oligonucleotide CGH array that spanned the region of the predicted breakpoint from the whole genome tiling array (*Figure 1.5*). Using the raw data from the oligonucleotide arrays from Nimblegen the breakpoint positions were predicted to be where the Cy5/Cy3 ratio changed from positive to negative (or vice versa), thus showing an intermediate ratio. The probes that showed an intermediate ratio were at 34,971,050bp for der(19) and 6,509,950bp for der(5) and thus were predicted to be where the translocation breakpoints occurred (hg18) (*Figure 3.2*).

3.2.2 Sequence of t(5;19)(p15.3;q12) derivative breakpoints

DNA was extracted from the t(5;19)(p15.3;q12) lymphoblastoid cell line and primers were designed 500bp either side of the predicted breakpoint positions as determined by the CGH array. The breakpoints were then amplified using PCR and subsequently sequenced to determine the exact breakpoint positions of the derivative chromosomes. Sequences revealed the chromosome 19 breakpoint positions to be at 30,279,438bp on der(19) and at 30,279,436bp on der(5) and the chromosome 5 breakpoint at 6,456,990bp on der(19) and at 6,456,998bp on der(5) (hg19). The origin of four bases, CCTG, on the der(19) breakpoint could not be assigned as they were common to both the chr19q and chr5p breakpoint regions. Depending on the origin of the four common bases chr19 showed a duplication of either GGACCTG or GGA and chr5 displayed a deletion of either CAGGGCT or GCT (*Figure 3.3*).

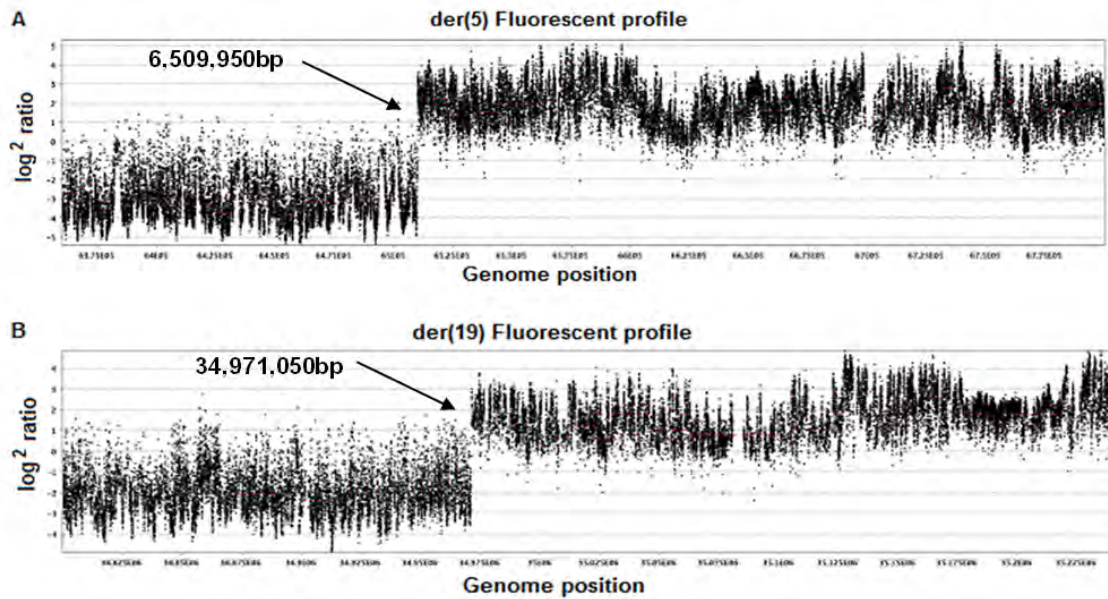


Figure 3.2 Custom designed oligonucleotide array painting of der(5) and der(19)
 The fluorescent profiles of both der(5) (A) and der(19) (B) from the *t(5;19)(p15.3;q12)* are shown. The Y axis represents cy5/cy3 ratio and the X axis shows genome position. Breakpoint positions are indicated by the arrow and estimated breakpoint positions (bp) determined from the array raw data are shown (figure supplied by Nimblegen).

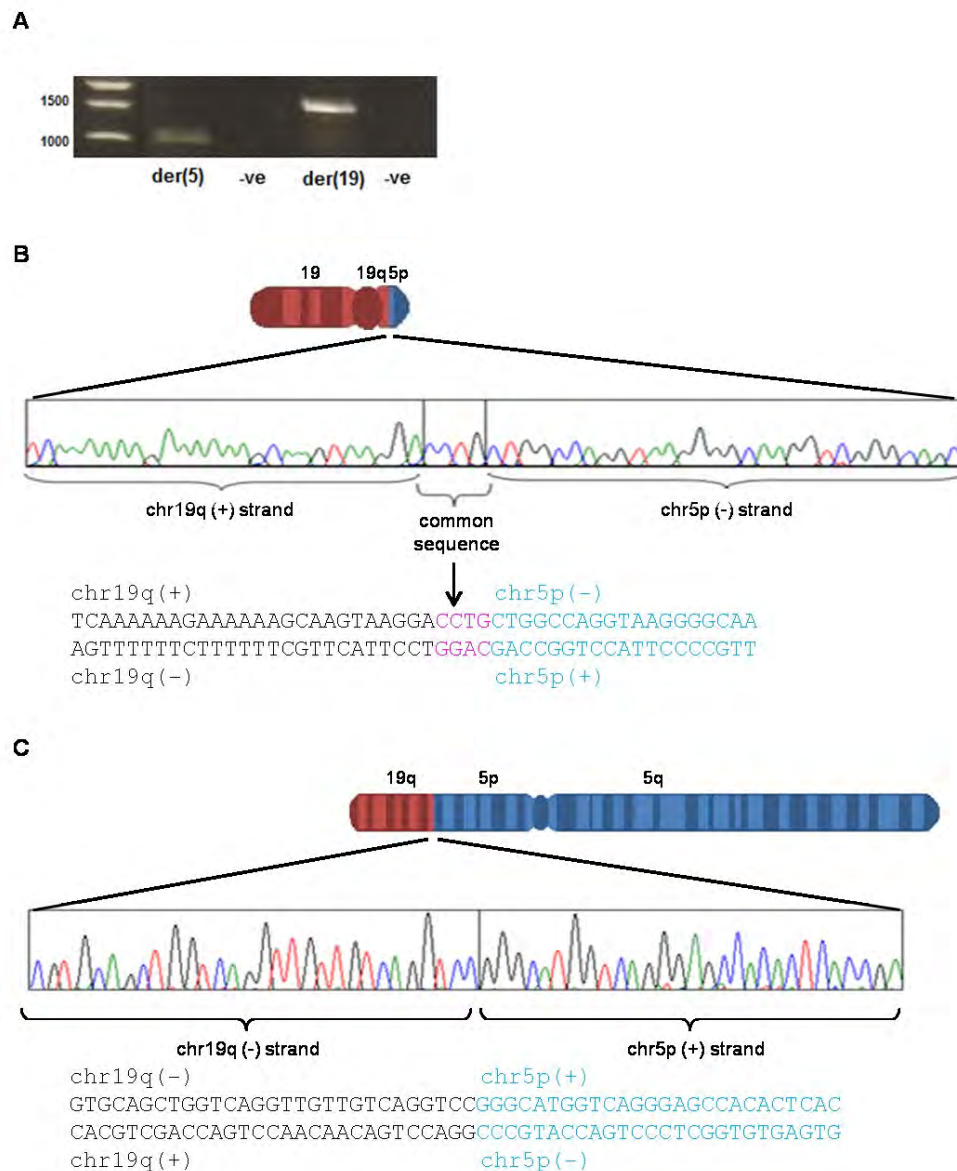


Figure 3.3 Characterisation of the t(5;19) breakpoints.

Nimblegen oligonucleotide array data was used to design primers 500bp either side of the predicted breakpoint positions. **A**, Products of der(5) and der(19) breakpoint amplification from PCR (-ve control contains no DNA). PCR products were gel extracted and sequenced using Sanger sequencing. **B**, Illustration of the der(19) chromosome with the sequence of the der(19) breakpoint below. **C**, Illustration of the der(5) chromosome with the sequence of the der(5) breakpoint below. Bases originating from chr19 are shown in black and from chr5 in blue. It was not possible to ascribe the chromosomal origin for four bases shown in pink, (CCTG). Depending on the origin of the four common bases a duplication of either GGACCTG (30,279,436-30,279,442) or GGA (30,279,436-30,279,438) occurred on chr19 and a deletion of either CAGGGCT (6,456,991-6,456,997) or GCT (6,456,995-6,456,997) occurred on chr5. (-) = DNA reverse strand (+) = DNA positive strand.

3.2.3 Map of genes within breakpoint vicinity

Once the breakpoint had been sequenced a map of the genes within the vicinity of the breakpoint could be established using the Ensemble Genome Browser (www.ensembl.org) (*Figure 3.4*). The der(5) breakpoint was shown to disrupt the only intron of an uncharacterised gene, *UBE2QL1*. The 5' end, including exon 1, and part of the intron of *UBE2QL1* were translocated onto der(19); no genes on chromosome 19 were disrupted. The 3' end of *UBE2QL1*, including exon 2 and part of the intron remained on der(5). No other genes were in the breakpoint vicinity for 23.5kb on der(5) and 73kb on der(19) thus *UBE2QL1* was the only candidate gene within the breakpoint region (*Figure 3.5*).

3.2.4 Existing knowledge on *UBE2QL1*

Research was carried out to determine any existing knowledge on *UBE2QL1* using a number of distinguished scientific websites including Ensemble Genome Browser: www.ensembl.org/index.html, National Center for Biotechnology Information (NCBI): www.ncbi.nlm.nih.gov/, Exome Variant Server: evs.gs.washington.edu/EVS/, Catalogue Of Somatic Mutations In Cancer (COSMIC): www.sanger.ac.uk/genetics/CGP/cosmic/ and PubMed: www.ncbi.nlm.nih.gov/pubmed. There were six main elements that were researched for up to date knowledge on *UBE2QL1*: genomic structure of the gene, predicted protein size, gene homology, evolutionary conservation, expression data and published literature.

UBE2QL1 can be found at position 6,448,736-6bp-6,495,022bp (hg19) on the chromosome 5 forward strand in humans. It consists of two exons separated by a large intron of 41,969bp. Exon 1 consists of 118aa and exon 2 of 43aa contributing to the full sized protein of 161aa (see appendix figure 8.3) with a predicted molecular weight of 18KDa, which was confirmed in this study. *UBE2QL1* is highly homologous to the E2 ubiquitin conjugating family 1 (see section 6.1 for detail) thus is named *UBE2QL1* (Ubiquitin-Conjugating Enzyme E2Q family-Like 1) due to this homology. *UBE2QL1* is highly conserved throughout evolution with 100-99% sequence alignment with primates, 99% sequence alignment with chicken, mouse, rat and guinea pig and 91-95% sequence alignment with zebrafish, fugu and xenopus (see appendix figure 8.4). Human *UBE2QL1* also exhibits high intra-species conservation as little genetic variation has been detected within the protein coding regions or splice sites, with no *UBE2QL1* nonsynonymous single nucleotide polymorphisms (SNPs) and only 3 rare synonymous SNPs been detected by dbSNP, 1000 genomes and variant server (see appendix figure 8.5). Very recently data for *UBE2QL1* in COSMIC (Catalogue Of Somatic Mutations In Cancer) has become available with 2 *UBE2QL1* mutations detected; one synonymous mutation in a breast cancer tissue: c.C480T, p.D160D, and one nonsynonymous mutation in an endometrium cancer tissue: c.C400A, p.R134S. No further functional data was carried out to determine if these mutations affected *UBE2QL1* protein function and if they were involved in cancer initiation and/or progression. *UBE2QL1* expression data from RNAseq (Illumina Body Map 2.0) consisting of expression data from a number of human tissues demonstrated high *UBE2QL1* expression in the brain, heart muscle, skeletal

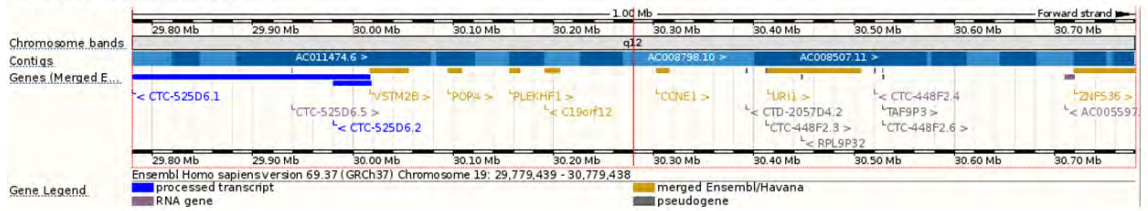
muscle and thyroid, medium expression in the colon, kidney, liver, lung, adipocyte, adrenal gland, breast, ovary, testis and prostate and low expression in white blood cells. No expression was detected in the bone marrow, spleen, thymus, small intestine, pancreas, skin, uterus and cervix. A literature search identified only one peer reviewed paper on *UBE2QL1* research which identifies a number of gene promoter regions that are rich in short tandem repeats (STR) and that lack the conventional motifs for the TATA, and TATA-less promoters, and thus suggests these novel rich STR promoters may possess functional roles in gene expression (Darvish et al. 2011). No published studies or data on *UBE2QL1* protein function were found thus *UBE2QL1* was an uncharacterised protein at the start of this study.

3.2.5 Loss of *UBE2QL1* second allele

To ascertain if *UBE2QL1* functions as a TSG the Knudson ‘two hit’ model of tumourigenesis was applied (see section 1.1.2), thus if the second allele of *UBE2QL1* was disrupted in the tumours (the first allele being disrupted by the t(5;19)(p15.3;q12)) this would suggest *UBE2QL1* was a likely RCC TSG candidate. MLPA was used to investigate if the second *UBE2QL1* allele had been deleted in the t(5;19)(p15.3;q12) tumours with probes being designed within each exon and at the 5’ and 3’ ends of each exon (six probes in total). MLPA confirmed an intragenic deletion of *UBE2QL1* exon 1 in an oncocytoma from patient III:2 with exon 1 probes showing an average loss of peak area by 31% compared to an unrelated normal renal DNA sample. Exon 1 probe deviation from reference probes within the same sample was shown to be significant

using the two tailed t-test ($P < 0.01$) confirming a *UBE2QL1* exon deletion in patient III:2 (Figure 3.6). As both *UBE2QL1* alleles were shown to be disrupted in patient III:2 thus complying with Knudson's TSG two-hit model, *UBE2QL1* was hypothesised to function as a potential RCC TSG.

der(19) breakpoint region



der(5) breakpoint region

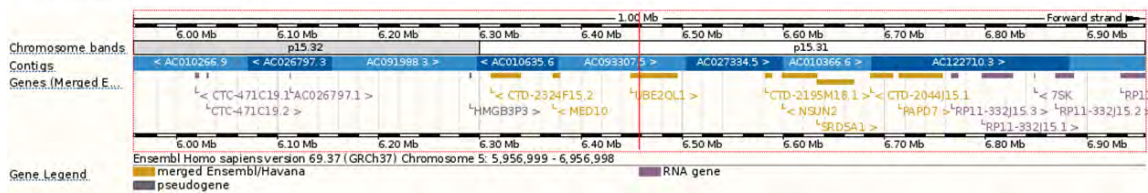


Figure 3.4 Derivative chromosome breakpoint maps

Schematic breakpoint maps of der(5) and der(19) from the $t(5;19)(p15.3;q12)$ created using ensemble genome browser (www.ensembl.org). Red lines indicate the breakpoint positions. Scale is shown in megabases (Mb). der(19) demonstrates no genes within the vicinity of the breakpoint for 73kb (upper panel) and der(5) breakpoint demonstrates disruption of *UBE2QL1* (lower panel).

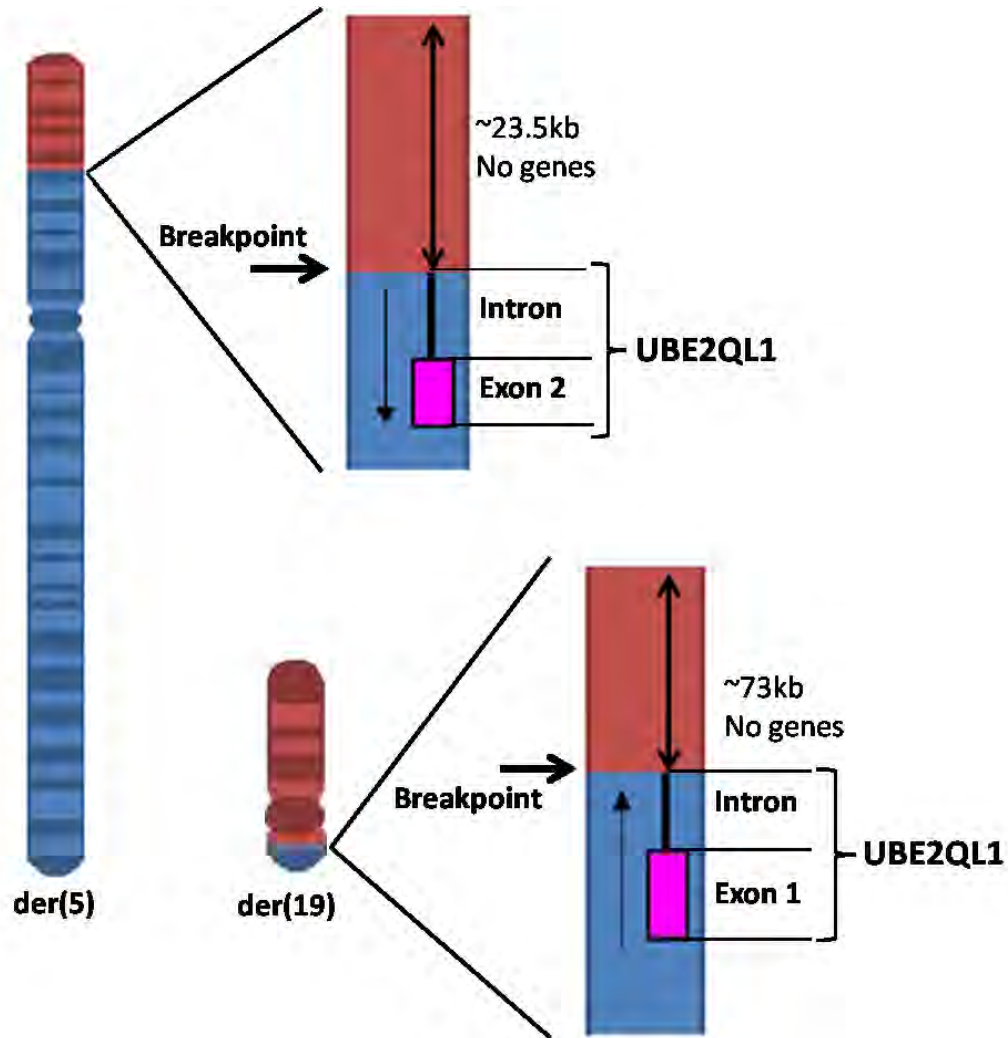


Figure 3.5 *t(5;19)(p15.3;q12)* derivative breakpoints

*Schematic illustration of $t(5;19)(p15.3;q12)$ derivative breakpoints. Chromosome material originating from chromosome 19 is shown in red and from chromosome 5 in blue. *UBE2QL1* on chromosome 5p was disrupted by the translocation leaving exon 2 and part of the intron on *der(5)* and exon 1 and part of the intron translocated to *der(19)*. There were no other genes within the vicinity of the breakpoint for 23.5kb on *der(5)* and 73kb on *der(19)*. Arrows within the chromosomes indicate the normal direction of transcription. Breakpoint positions are indicated in the diagram.*

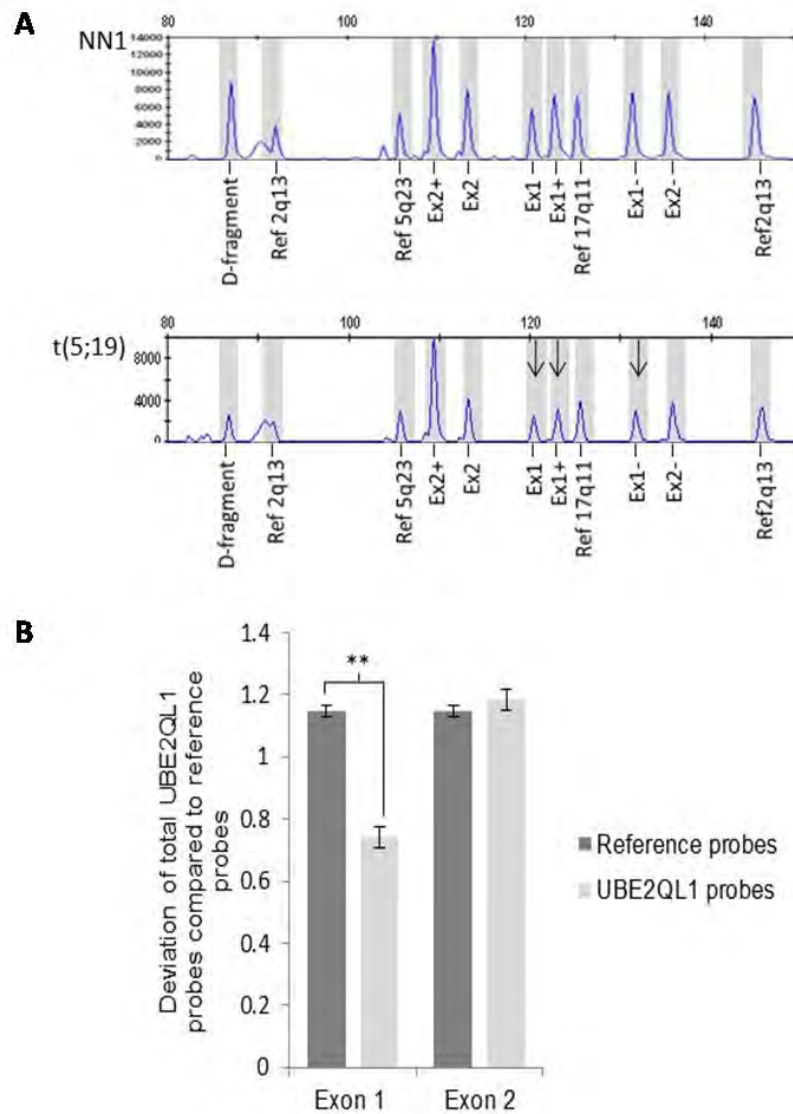


Figure 3.6 MLPA deletion analysis of UBE2QL1 exon 1 in t(5;19) patient III:II

A, MLPA (Multiplex Ligation-dependent Probe Amplification) trace for 6 UBE2QL1 probes. All 3 UBE2QL1 exon 1 probes show an average loss of 31% (arrowed) in a t(5;19)(p15.3;q13.1) associated oncocyoma from patient III:2 as compared with unrelated normal renal tissue, NN1. UBE2QL1 probe locations: Ex1/2 = within exon, Ex1/2+ = 3' of exon, Ex1/2- = 5' of exon. Reference probes are labelled. **B**, UBE2QL1 MLPA probe deviation from reference probes for exons 1 and 2. Deviation of exon 1 probes is significant indicating a deletion of exon 1. Unpaired t test, $P=0.0048$, Error bars= SEM, **= $P<0.01$.

3.2.6 Expression analysis of HIF-1/2 targets in t(5;19)(p15.3;q12) renal tumours

As explained in section 1.3 *VHL*-associated renal tumourigenesis involves the deregulation of HIF and subsequently HIF target genes. To investigate if *UBE2QL1* RCC tumourigenesis was associated with HIF deregulation, expression analysis of the HIF-1 and HIF-2 target genes; carbonic anhydrase 9 (CA9) and Cyclin D1 (CCND1) respectively, was undertaken. Immunohistochemical staining of three t(5;19)(p15.3;q12) associated renal tumours from individuals III:1 and III:2 (two oncocytomas and one chromophobe RCC) for HIF target genes CA9 and CCND1 was kindly undertaken by Dr Anne-Bine Skytte. None of the tumours displayed up-regulation of CA9 or CCND1 when compared to sporadic ccRCCs with known HIF deregulation, thus if *UBE2QL1* does function as an RCC TSG than it likely causes RCC tumourigenesis via novel mechanisms (*Figure 3.7*).

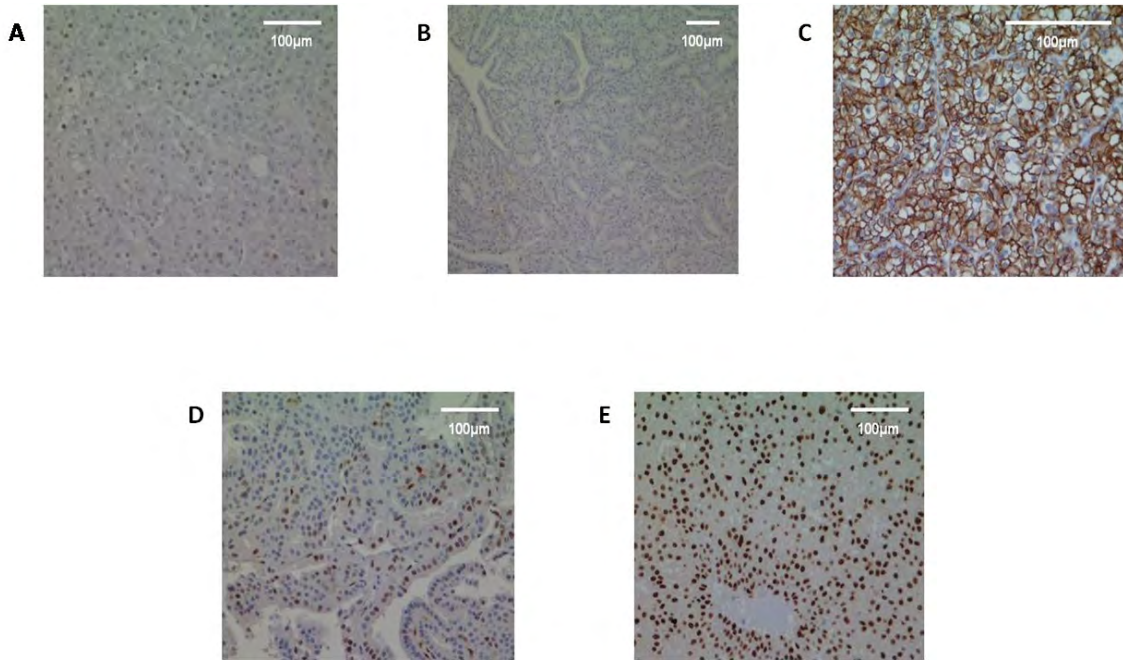


Figure 3.7 *HIF-1/2 target gene immunohistochemistry on $t(5;19)(p15.3;q13.1)$ tumours carried out by Anne-Bine Skytte*

*Immunohistochemistry (IHC) of HIF targets on three $t(5;19)(p15.3;q13.1)$ associated renal tumours. **A**, Carbonic anhydrase (CA9) IHC in a $t(5;19)(p15.3;q13.1)$ oncocytoma. **B**, Carbonic anhydrase (CA9) IHC in a $t(5;19)(p15.3;q13.1)$ chromophobe renal tumour. Both **A** and **B** show no CA9 up-regulation as compared to **C**, CA9 up-regulation shown in a sporadic clear cell RCC through IHC. **D**, IHC of cyclin D1 (CCND1) in a $t(5;19)(p15.3;q13.1)$ chromophobe renal tumour showing no up-regulation compared to **E**, a sporadic chromophobe RCC showing up-regulation of CCND1.*

3.3 Conclusion

Characterisation of the t(5;19)(p15.3;q12) breakpoint region allowed the identification of a disrupted uncharacterised gene *UBE2QL1*. As the t(5;19)(p15.3;q12) was associated with RCC in one family and a *UBE2QL1* exon 1 deletion was detected in an oncocytoma in one of the t(5;19)(p15.3;q12) patients, this suggested *UBE2QL1* could be the causative gene within this family following Knudson's two hit model. As *UBE2QL1* possibly functions as a novel RCC TSG it was essential to determine if *UBE2QL1* functioned within the same pathway as VHL thus initiating RCC tumourigenesis through the same means. VHL-dependent RCCs (and familial RCC associated with *FH* and *SDHB*) are caused by the dysregulation of HIF-1/2 leading to upregulation of HIF-1/2 target genes, therefore VHL-dependent RCCs show a dramatic increase in expression of HIF-1/2 target genes such as *CA9* and *CCND1* on immunohistochemistry. t(5;19)(p15.3;q12) oncocytoma and chromophobe slices showed no upregulation of HIF targets *CA9* and *CCND1* thus suggesting *UBE2QL1* tumourigenesis initiation may function through an alternative pathway to that of VHL.

Chapter Four: Genetic and epigenetic analysis of *UBE2QL1* in RCC

4.1 Introduction: Is *UBE2QL1* inactivated in other familial and sporadic RCCs?

UBE2QL1 was the only gene within the vicinity of the t(5;19)(p15.3;q12) breakpoints and a second hit in the wildtype (wt) *UBE2QL1* allele was identified in a t(5;19)(p15.3;q12) associated tumour. This suggested *UBE2QL1* maybe a novel TSG responsible for RCC tumourigenesis in the t(5;19)(p15.3;q12) family. It was therefore necessary to identify if *UBE2QL1* is a novel RCC TSG in other familial and/or sporadic RCC cases. There are a number of mechanisms including chromosomal translocations that can lead to the deregulation of TSGs in cancers; gene mutations, gene deletions and promoter methylation (see section 1.1.2 for details). All three mechanisms of TSG inactivation were investigated for *UBE2QL1* in sporadic RCCs to determine if, like *VHL*, *UBE2QL1* was important for the tumourigenesis in both sporadic and familial cases.

4.1.1 Aims

UBE2QL1 mutation, promoter methylation and gene deletion analysis were undertaken in sporadic RCC cell line and tumour samples to determine if *UBE2QL1* gene deregulation was occurring in other RCC cases.

4.2 Results

4.2.1 *UBE2QL1* mutation analysis in RCCs

Mutation analysis of the exons and exon/intron boundaries of *UBE2QL1* was undertaken by direct sequencing in (i) 116 sporadic RCC tumours; (ii) 17 RCC derived cell lines; and (iii) lymphocyte derived DNA from 71 individuals with a genetic predisposition to the development of RCC, the nature of which is not known. No mutations or polymorphisms were detected. As no polymorphisms were detected in the protein coding region or splice sites and only 3 rare synonymous polymorphisms have been detected by dbSNP, 1000 genomes and variant server (see section 3.2.4), it was deduced that *UBE2QL1* is a highly conserved gene. This therefore suggests there is strong negative selection during *UBE2QL1* evolution due to functional constraint, thus any harmful variants of *UBE2QL1* would diminish an individual's capacity to succeed reproductively thus causing removal of deleterious alleles from the population, this is also known as purifying selection. It was also shown in section 3.2.4 that *UBE2QL1* has remained highly conserved during its evolution, thus evidence suggests *UBE2QL1* may be an important gene in organism viability, though further studies in animal models would need to be carried out to test this hypothesis.

4.2.2 UBE2QL1 CpG island

CpG islands can be identified as a 200bp stretch of DNA with GC content of $\geq 50\%$ and an observed CpG/expected CpG ($\text{Obs}_{\text{CpG}}/\text{Exp}_{\text{CpG}}$) ratio of ≥ 0.60 . The ($\text{Obs}_{\text{CpG}}/\text{Exp}_{\text{CpG}}$) ratio is calculated using the following formula: number of (CpGs/ (number of Cs x number of Gs)) x total number of nucleotide (Han & Zhao 2009). To determine if *UBE2QL1* contains a promoter CpG island and therefore could undergo deregulation via promoter hyper-methylation in tumours the promoter and 5' UTR of *UBE2QL1* was examined using the UCSC genome browser (<http://genome.ucsc.edu/>). A 250bp region 5' to the transcription start of *UBE2QL1* showed a CpG content of 66% and a ($\text{Obs}_{\text{CpG}}/\text{Exp}_{\text{CpG}}$) ratio of 0.8 suggesting *UBE2QL1* transcription could be regulated by promoter methylation (*Figure 4.1*).

4.2.3 UBE2QL1 expression and methylation analysis in RCC cell lines

RT-PCRs (reverse transcriptase-PCR) were carried out to determine if *UBE2QL1* expression was deregulated in RCC cell lines. Complete loss of *UBE2QL1* expression was shown in 11/18 RCC cell lines thus suggesting *UBE2QL1* may be deregulated (Figure 4.2). Promoter methylation is a common mechanism of TSG inactivation in many cancers including RCC (see section 1.1.4). One method to detect gene inactivation due to promoter methylation within cell lines is to extract protein from the cell lines before and after incubation with the de-methylating agent 5-Aza-2'-deoxycytidine (5-Aza). 5-Aza is a nucleoside analog which becomes incorporated into the cell's DNA, it inhibits methyltransferases due to stable complexes forming between the 5-Aza residues in the DNA and the methyltransferases. mRNA expression analysis pre and post 5-Aza can help determine if a gene has been inactivated due to promoter methylation as it would show loss (or reduced) expression pre 5-Aza and increased expression post 5-Aza due to the inhibition of promoter methylation within the cells. RCC cell line mRNA was extracted pre and post 5-Aza treatment courtesy of Dr. Mark Morris. Eleven RCC cell lines showed decreased *UBE2QL1* mRNA expression via RT-PCR. After 5-Aza treatment re-expression of *UBE2QL1* was observed in 6/11 RCC cell lines suggesting epigenetic silencing of *UBE2QL1* by promoter methylation was taking place in these cell lines (Figure 4.2).

To confirm *UBE2QL1* promoter methylation within the RCC cell lines, COBRA (COmbined Bisulfite Restriction Analysis) was undertaken. COBRA involves the

bisulfite modification of the cell line DNA leading to changes in the DNA sequence depending on whether the DNA is methylated or unmethylated. Methylated cytosines remain as cytosines and unmethylated cytosines become thymines. A restriction enzyme (BstUI) that recognises the restriction site 'CGCG' can then be used in a digest reaction to cut any CpGs within the amplified promoter region. Only methylated CpGs will be cut and therefore only methylated *UBE2QL1* promoter regions will show digested products when run on an agarose gel, see section 2.4 for details. *UBE2QL1* methylation was confirmed by COBRA in 5/5 RCC cell lines that showed reduced expression (*Figure 4.2*).

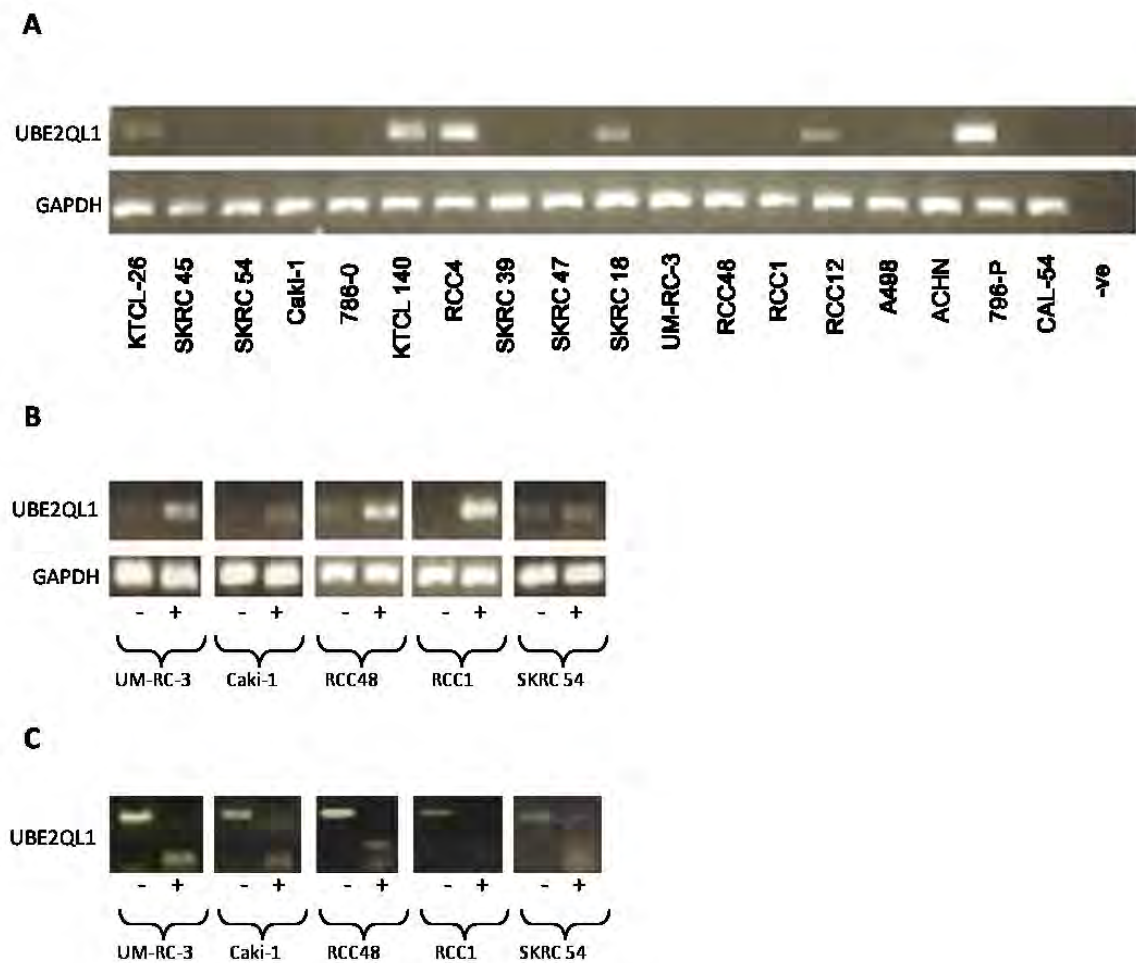


Figure 4.2 *UBE2QL1* expression, pre and post 5-aza and methylation results in RCC cell lines

A, Reverse transcriptase (RT) – PCR shows complete loss of *UBE2QL1* expression in 11/18 RCC cell lines (upper band). *GAPDH* expression levels are shown to verify the same amount of RNA was used for each RCC cell line (lower band). –ve = negative control with no RNA added to the RT-PCR reaction. *B*, RT-PCR of RCC cell lines grown without 5-aza (-) and with 5-aza (+). 5 RCC cell lines that showed increased expression of *UBE2QL1* post 5-Aza are presented (upper band) along with the *GAPDH* expression levels shown as a positive control (lower band). *C*, Bisulphite modified DNA was used to amplify the *UBE2QL1* CpG island and subsequently used in a *Bst*UI digest reaction. The PCR products are shown with no *Bst*UI added (-) and with *Bst*UI added (+).

4.2.4 Expression and methylation analysis of *UBE2QL1* in sporadic RCCs

As *UBE2QL1* was shown to be regulated by promoter methylation in RCC cell lines this suggested it may also be deregulated in RCC sporadic tumours. Expression analysis of *UBE2QL1* was undertaken in 28 sporadic RCC tumours compared to corresponding normal kidney tissue from the same patients by quantitative real-time PCR (QRT-PCR). *UBE2QL1* demonstrated reduced mRNA levels (>40% loss) in 22/28 (78.6%) sporadic RCCs compared to the corresponding normals (CN) (*Figure 4.3*). Both promoter methylation and *UBE2QL1* exon deletions had previously been detected as mechanisms of *UBE2QL1* gene deregulation, it was therefore deduced these mechanisms were likely the cause of *UBE2QL1* decreased expression in sporadic RCCs.

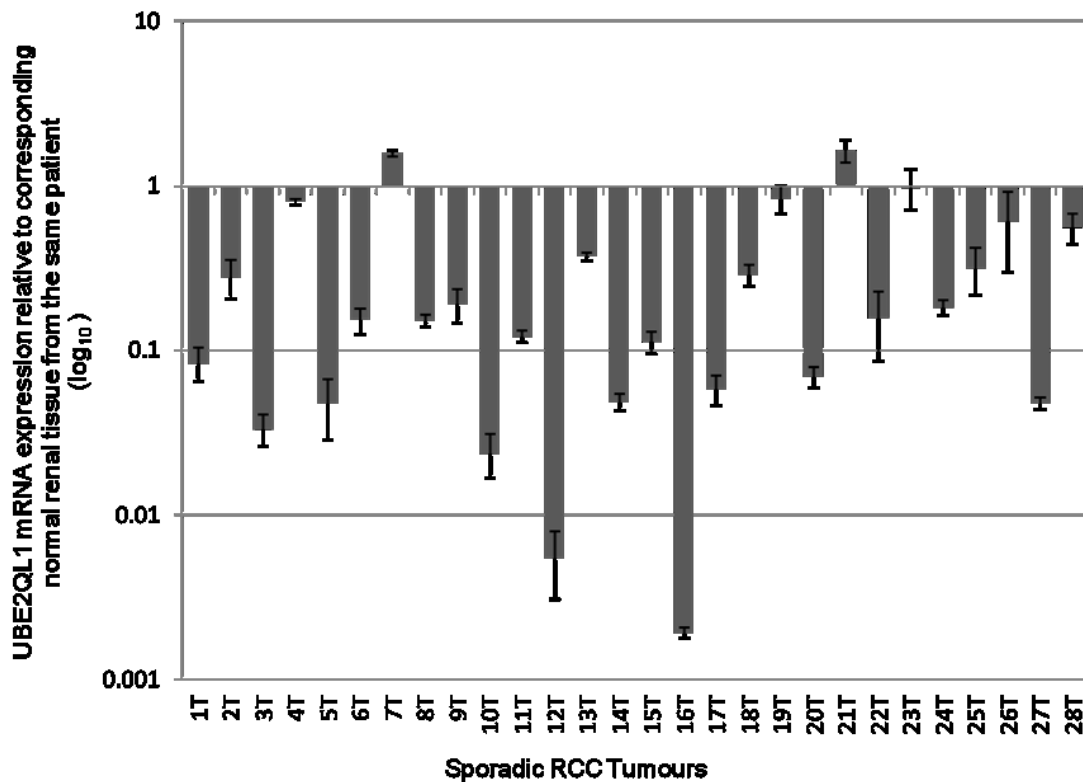


Figure 4.3 Expression analysis of UBE2QL1 in sporadic RCCs

Quantitative Real-Time PCR (QRT-PCR) results showing the mean values of UBE2QL1 expression for 28 sporadic RCCs compared with matched corresponding normal (CN) renal tissue. 1 = 100% expression compared to CN. All samples were normalised to β -actin. $n = 3$ independent assays run in triplicate for all samples. Error bars represent \pm standard error of the mean (SEM).

As *UBE2QL1* showed decreased mRNA expression in RCC tumours COBRA analysis was undertaken to determine if CpG island promoter methylation was the mechanism for this deregulation in expression. *UBE2QL1* promoter methylation was detected in 14/66 (21.2%) sporadic RCC tumours. CNs from the same patient and 5 unrelated normal renal tissues did not show promoter methylation (*Figure 4.4*). *UBE2QL1* QRT-PCR data was available for 8 of the methylated sporadic RCCs (1T, 2T, 5T, 13T, 17T, 18T, 20T and 22T) (no RNA was available for the other sporadic RCC cases) all demonstrating a $\geq 60\%$ decrease in expression compared to matched CNs (*Figure 4.3*). To determine the extent of promoter methylation within the sporadic RCC tumours the methylation index (MI) was calculated. This involves calculating the total methylated CpGs and dividing by the total number of CpGs sequenced. Single *UBE2QL1* alleles were cloned and sequenced by cloning the bisulfite modified *UBE2QL1* CpG island into pGEM-T vectors and extracting the DNA from positive clones which were subsequently sequenced. Each RCC tumour had 8-12 clones sequenced to determine the extent of *UBE2QL1* methylation within the tumour. Forty-seven CpGs were identified within the *UBE2QL1* CpG island and were labelled 1-47 (*Figure 4.1*). The sequencing data from each clone was used to produce representative *UBE2QL1* CpG island figures showing both methylated and unmethylated CpGs for all the clones for each tumour. Four/eleven *UBE2QL1* methylated RCC tumours showed an MI of $>40\%$ and were therefore determined to be hypermethylated, a further 6/11 showed an MI of 10-40% suggesting partial promoter methylation. One tumour presented an MI of $<10\%$. MI

analysis was not carried out for 3 tumours due to lack of DNA from these tumours
(*Figure 4.5*).

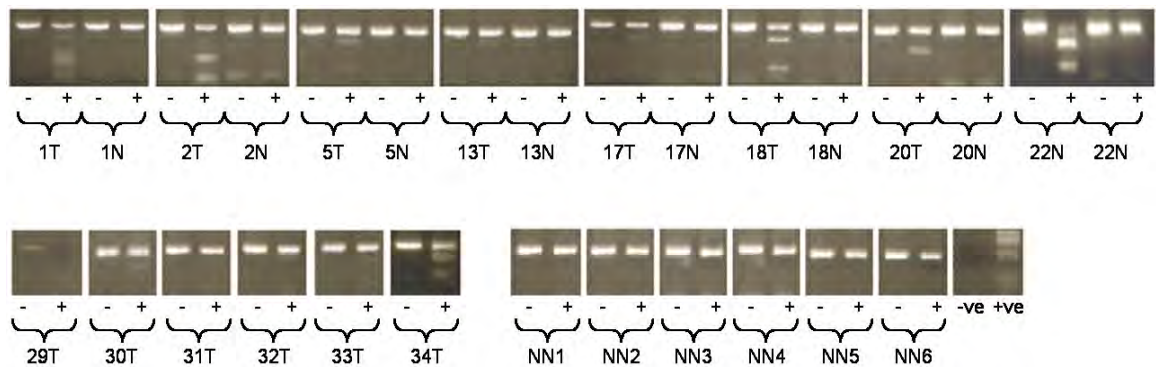


Figure 4.4 *BstUI* digest of bisulphite modified *UBE2QL1* CpG island in sporadic RCCs.

BstUI digests of bisulphite modified *UBE2QL1* CpG island for 14 sporadic RCCs that showed promoter methylation. Eight tumours (T) with matched corresponding normals (N) (top panel) and 6 tumours without Ns (bottom left panel) are shown. Six normal renal tissues (NN) demonstrate no promoter methylation (bottom right panel). The PCR products are shown with no *BstUI* added (-) and with *BstUI* added (+). *BstUI* digested products signify promoter methylation. Negative control (-ve) = no DNA template added and positive control (+ve) = *PCDNA3.1* plasmid to demonstrate the digestion reaction worked.

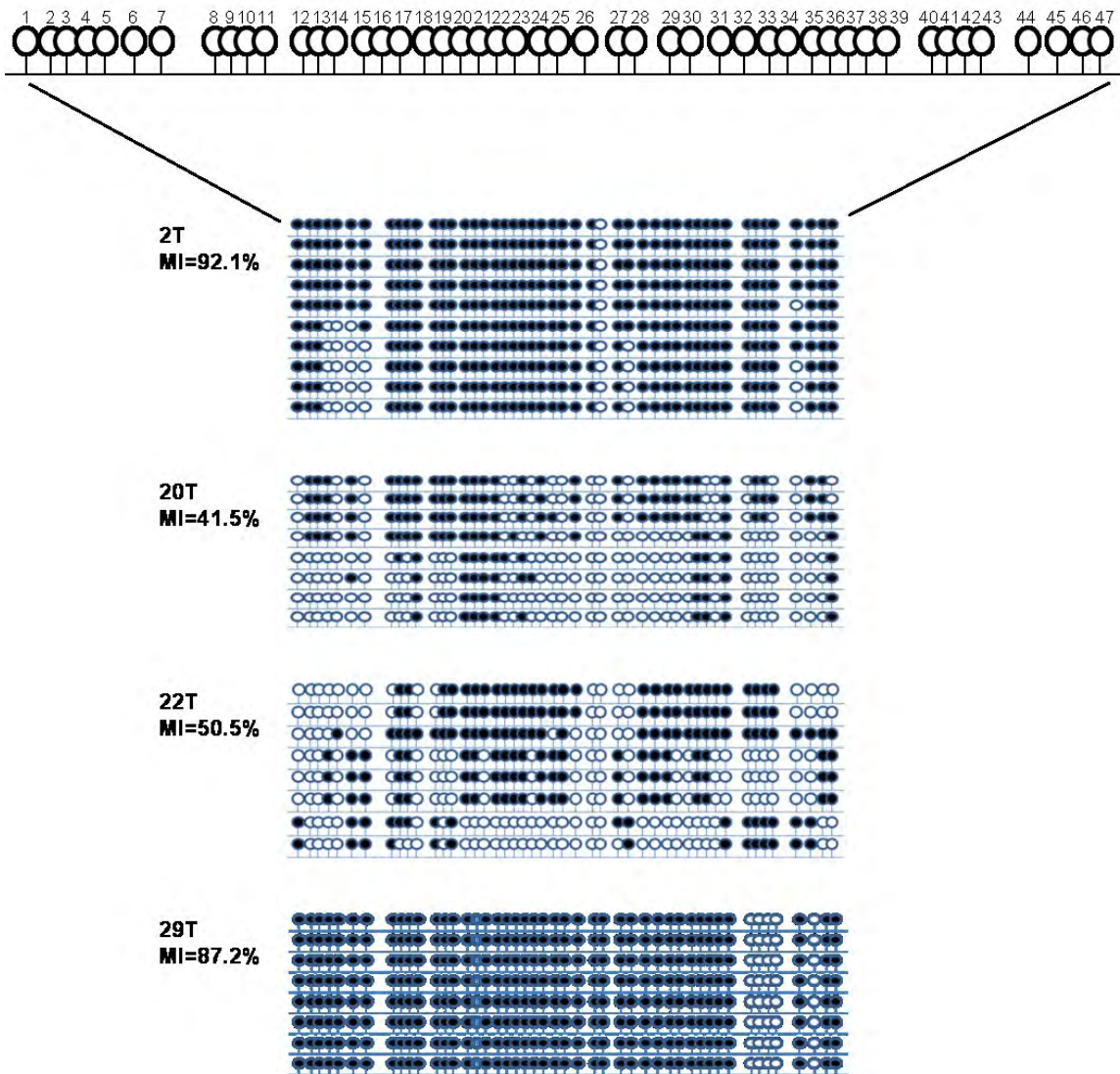


Figure 4.5 Schematic diagram representing UBE2QL1 CpG island clones for 4 sporadic RCCs.

Bisulfite modified UBE2QL1 CpG islands were cloned for 11/14 methylated sporadic RCCs. The analysed CpG dinucleotides are number 1-47 and are represented as individual circles as shown on the top panel. Each horizontal line of 47 CpG dinucleotides represents one clone for that particular sporadic RCC. Black circles signify methylated CpGs and white circles unmethylated CpGs. Four sporadic RCCs (2T, 20T, 22T and 29T) that demonstrated hypermethylation with an MI >40% are shown. MI is calculated as a percentage of total methylated CpGs for one RCC tumour / total number of CpGs sequenced for the same tumour.

4.2.5 LOH (Loss of heterozygosity) of 5p15.3 in sporadic RCCs

Microsatellite marker analysis is a technique used to determine if a region within the genome has undergone loss of heterozygosity (LOH). Microsatellites are short tandem repeat sequences that can be from 2-7 nucleotides, for example the dinucleotide repeat CACACA. The number of repeat sequences within a microsatellite can be highly variable, resulting in different length microsatellites. Allelic variation of microsatellite lengths can be highly informative when determining LOH of chromosomal regions when comparing tumour DNA and CN DNA. NCBI map viewer (<http://www.ncbi.nlm.nih.gov/projects/mapview/>) was used to identify known, characterised microsatellite markers found within the same chromosomal band as *UBE2QL1*, specifically 5p15.3, with a known LOH frequency of >60%. Two microsatellite markers were identified that met the correct criteria; D5S2505 (5,869,996 - 5,870,453bp) and D5S2054 (5,944,886 – 5,945,198bp) (hg19) both found within the 5p15.3 chromosomal band. Primers were designed to amplify the microsatellite markers by PCR and products were separated by electrophoresis. Markers that were heterozygous for an individual in the CN were labelled as informative as a loss of heterozygosity in the tumour could be identified by a loss of one of the markers. Homozygote markers are non-informative as a loss of one allele cannot be detected. To establish possible LOH candidates, the peak height ratio was calculated for both the matched CN and tumour using the following equation: Peak area of allele 1 divided by peak area of allele 2. The peak height ratio of the tumour was then divided by the CN peak height ratio and a

number ≤ 0.5 was concluded to be due to LOH of that particular allele. The microsatellite marker D5S2505 was found to have LOH in 3/28 informative sporadic RCC tumours. LOH was confirmed in two of these tumours with the D5S2054 marker while the third tumour was non-informative for this marker (*Figure 4.6*).

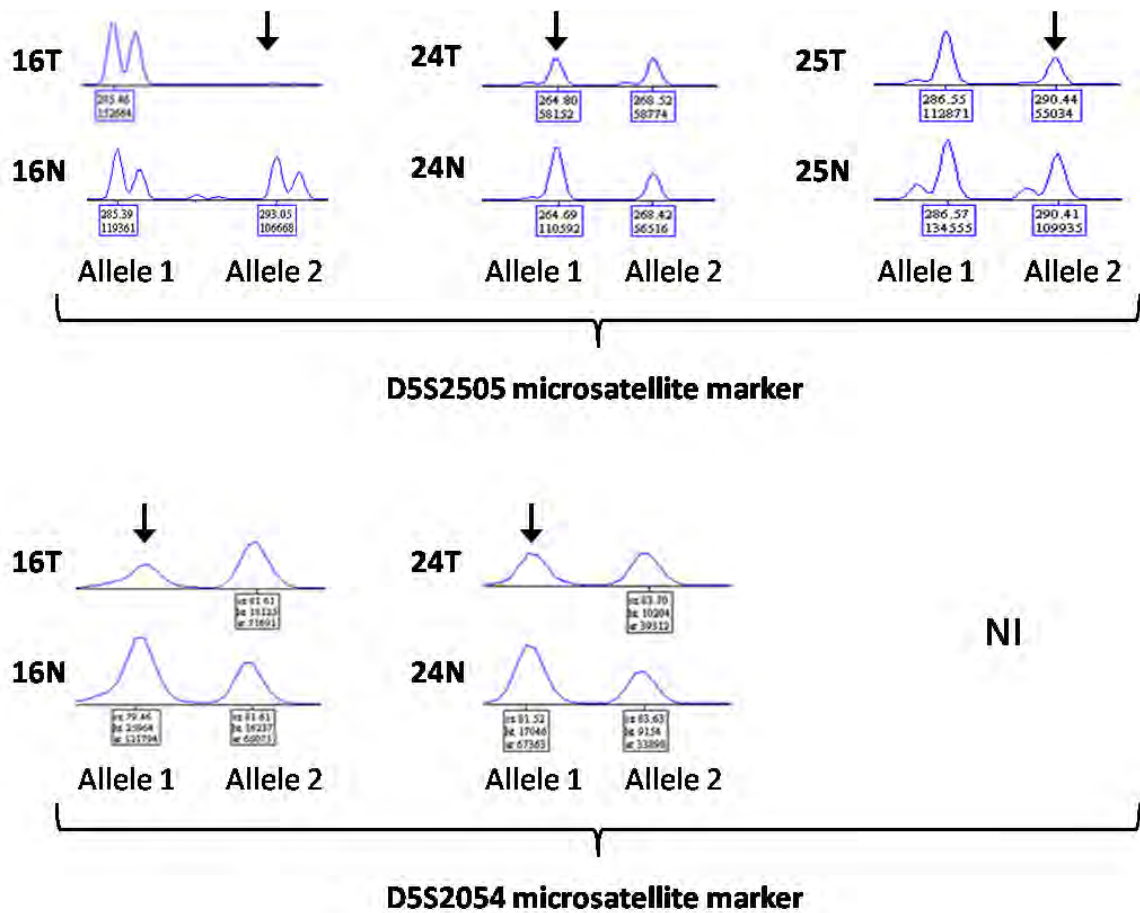


Figure 4.6 Microsatellite marker analysis for 5p13.3 in sporadic RCC tumours

Microsatellite traces for 3 tumours (16T, 24T and 25T) showing loss of marker D5S2505 and 2 tumours (16T and 24T) showing loss of D5S2054, both markers reside at chromosome position 5p15.3. T = Tumour, N = normal kidney tissue from the same individual, NI = non-informative due to homozygosity of marker. The peak height ratio for the tumour and normal was calculated (Peak Height (PH) of allele 1 / PH of allele 2) and loss of heterozygosity was established by dividing the tumour peak height ratio by the normal peak height ratio. A number ≤ 0.5 was due to LOH.

4.2.6 Multiplex Ligation-dependent Probe Amplification (MLPA) of UBE2QL1 in sporadic and familial RCCs

As the microsatellite marker analysis suggested there was LOH of 5p15.3 for 3 sporadic RCC tumours this suggested *UBE2QL1* could be deleted presuming the entire chromosomal band was lost. Smaller gene deletions can also occur in tumours leading to the complete or partial deletion of TSGs (see section 1.1.2). To analyse if *UBE2QL1* was deleted in the tumours showing 5p15.3 LOH and if smaller gene deletions of *UBE2QL1* had also occurred in sporadic RCCs, specific *UBE2QL1* probes were designed for MLPA analysis. MLPA allows the detection of abnormal copy numbers of very small targets (50-70 nucleotides) thus allowing the detection of single exon aberrations within a gene (for details see section 2.5.1). Probes were designed for *UBE2QL1* with exons 1 and 2 and both 5' and 3' of each of the exons making a total of 6 probes. Peak heights of *UBE2QL1* probes were compared to control reference probes for each sample and an average deviation of $\geq 30\%$ from adjacent reference probes were regarded for all *UBE2QL1* probes or single exon probes indicating a whole gene or exon deletion respectively. *UBE2QL1* deletions were demonstrated in 8/49 (16.3%) sporadic RCC tumours with confirmed *UBE2QL1* deletions in the three tumours that demonstrated LOH of 5p15.3, see section 4.2.5 (*Figure 4.7*).

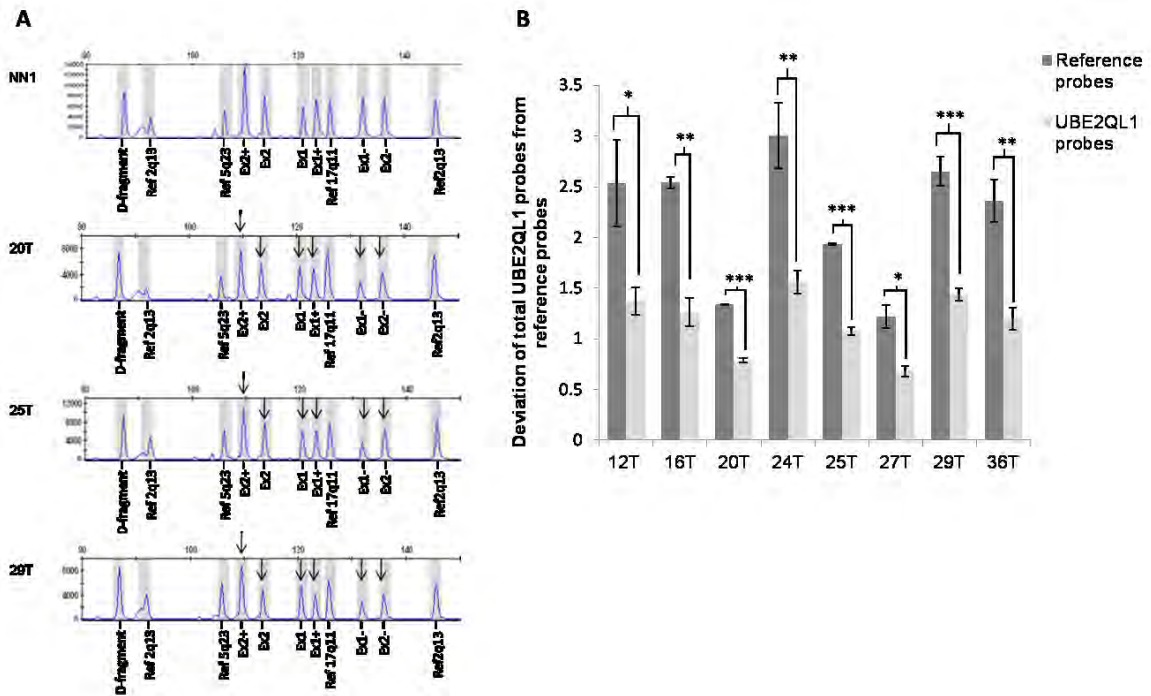


Figure 4.7 UBE2QL1 deletion analysis via MLPA in sporadic RCCs

A, MLPA (Multiplex Ligation-dependent Probe Amplification) traces of 3 sporadic renal tumours (20T, 25T and 29T) compared to a normal renal tissue (NN1). Probe loss indicating UBE2QL1 deletions are shown by an arrow. 20T showed an average peak loss of 30.5% across all the UBE2QL1 probes, 25T an average peak loss of 32.3% and 29T an average peak loss of 35.7%. UBE2QL1 probe locations: Ex1/2 = within exon, Ex1/2+ = 3' of exon, Ex1/2- = 5' of exon. Reference probes are labelled. **B**, Total UBE2QL1 probe deviations from reference probes for 8 sporadic RCCs. All tumours show a significant deviation of all UBE2QL1 probes compared to reference probes signifying a complete gene deletion of UBE2QL1 (unpaired *t* test). Error bars = SEM, * = $P < 0.05$, ** = $P < 0.01$, *** = $P < 0.001$.

4.3 Conclusion

UBE2QL1 was shown to be disrupted in sporadic RCC by promoter hypermethylation and LOH of the *UBE2QL1* locus with *UBE2QL1* deregulation demonstrating in 37% of sporadic RCCs. One sporadic tumour (20T) was confirmed to have both *UBE2QL1* with both promoter methylation and gene loss been detected, thus following Knudson's two hit model, suggesting *UBE2QL1* is an important TSG in RCC tumourigenesis. 78.6% of sporadic RCCs showed a >40% loss of *UBE2QL1* expression compared to the CN; therefore not all mechanisms of *UBE2QL1* deregulation were detected. This suggests other, possibly indirect mechanisms, have led to *UBE2QL1* deregulation including aberrations of regulators of *UBE2QL1* or disruptions in pathways upstream of *UBE2QL1* expression. No intragenic *UBE2QL1* mutations were detected, yet lack of coding region polymorphisms suggests *UBE2QL1* has undergone strong negative selection during evolution suggesting it has an important role in organism viability. Although no mutations were detected this observation is reminiscent of *RASSF1A* a TSG which is often inactivated by methylation/allele loss in sporadic RCC and intragenic mutations are rarely detected (see section 1.3.4). The detection of *UBE2QL1* aberrations in sporadic cases of RCC has demonstrating that the study of inherited forms of RCC has provided important insights into the pathogenesis of the more common sporadic forms of RCC.

**Chapter Five: UBE2QL1
suppresses RCC cell line
proliferation and colony formation**

5.1 Introduction: Does UBE2QL1 functions as a tumour suppressor?

UBE2QL1 was found to be disrupted by the constitutional t(5;19)(p15.3;q13.1) associated with familial RCC and an intragenic deletion of *UBE2QL1* exon 1 was detected in an oncocytoma of a t(5;19)(p15.3;q13.1) patient (section 3.2). It was also established that *UBE2QL1* showed decreased expression of >40% in 78.6% of sporadic RCCs compared to CN and in 21.2% and 16.3% of cases this deregulation was due to promoter methylation and gene deletions, respectively (section 4.3). This data suggests *UBE2QL1* was likely to function as a novel RCC tumour suppressor gene as it was found to be disrupted in both sporadic and familial RCCs by a number of mechanisms. To determine if *UBE2QL1* exhibited growth suppressor properties both colony formation assays and soft agar growth assays were carried out using *UBE2QL1* silenced RCC cell lines.

Colony formation assays involve the introduction of a tumour suppressor or oncogene into a cell line via plasmid transfection. Cells containing the plasmid can be selected for as the plasmids contain an antibiotic resistance gene such as the neomycin resistance gene. Treating cells with Geneticin (G418) an aminoglycoside antibiotic similar in structure to neomycin, enables only cells resistant to G418, and therefore containing the plasmid, to survive. Control experiments involve the transfection of the empty vectors containing only the antibiotic resistant gene. Two weeks after transfection surviving cells are seeded for colony formation assays and the number of colonies that

have grown to a size $\geq 100\mu\text{m}$ after 4 weeks determined. The growth of colonies in the presence of a tumour suppressor gene would normally be significantly reduced compared to the control. Soft agar growth assays are carried out in a similar manner to colony formation assays, the difference being the cells are grown in soft agar as opposed to being grown on a tissue culture dish, thus measuring the ability of the cells to grow in an anchorage-independent manner. The process of transformation of normal cells to neoplastic cells produces a population of cells that proliferate independently of external and internal signals that would normally inhibit growth. Anchorage-independent growth is the most common method for detecting cell transformation as this measures the ability of cells to proliferate in a semisolid culture media (soft agar). Cancer cell lines have already undergone this transformation and are often capable of efficiently undergoing anchorage-independent growth; the introduction of a tumour suppressor gene into these cancer cell lines should therefore hinder their ability of anchorage-independent growth thus producing fewer and smaller colonies after the incubation period.

5.1.1 Aims

Colony formation assays and soft agar growth assays were carried out using a naturally occurring *UBE2QL1* silenced RCC cell line(s) transfected with either *UBE2QL1* or empty vector to determine if *UBE2QL1* possessed tumour suppressor gene properties, such as proliferation and anchorage-independent growth inhibition, thus reversing the effects of neoplastic cell transformation.

5.2 Results

5.2.1 UBE2QL1 colony formation assays

To determine if the function *UBE2QL1* allowed the suppression of growth of RCC cells, the *UBE2QL1* silenced RCC cell lines SKRC47 and SKRC39 were transfected with FLAG tagged wild-type *UBE2QL1* expression plasmids or FLAG empty vector plasmids, which after two weeks of selection were subsequently seeded at varying densities to carry out colony formation assays. *UBE2QL1* re-expression produced a 57.5% (P<0.0001, SEM 2.556) and a 54.6% (P<0.0001, SEM 0.87) reduction in colonies compared with those transfected with empty vector in SKRC47 and SKRC39 cell lines, respectively. This data suggests *UBE2QL1* possesses growth suppressive functions in renal cancer cells (*Figure 5.1*).

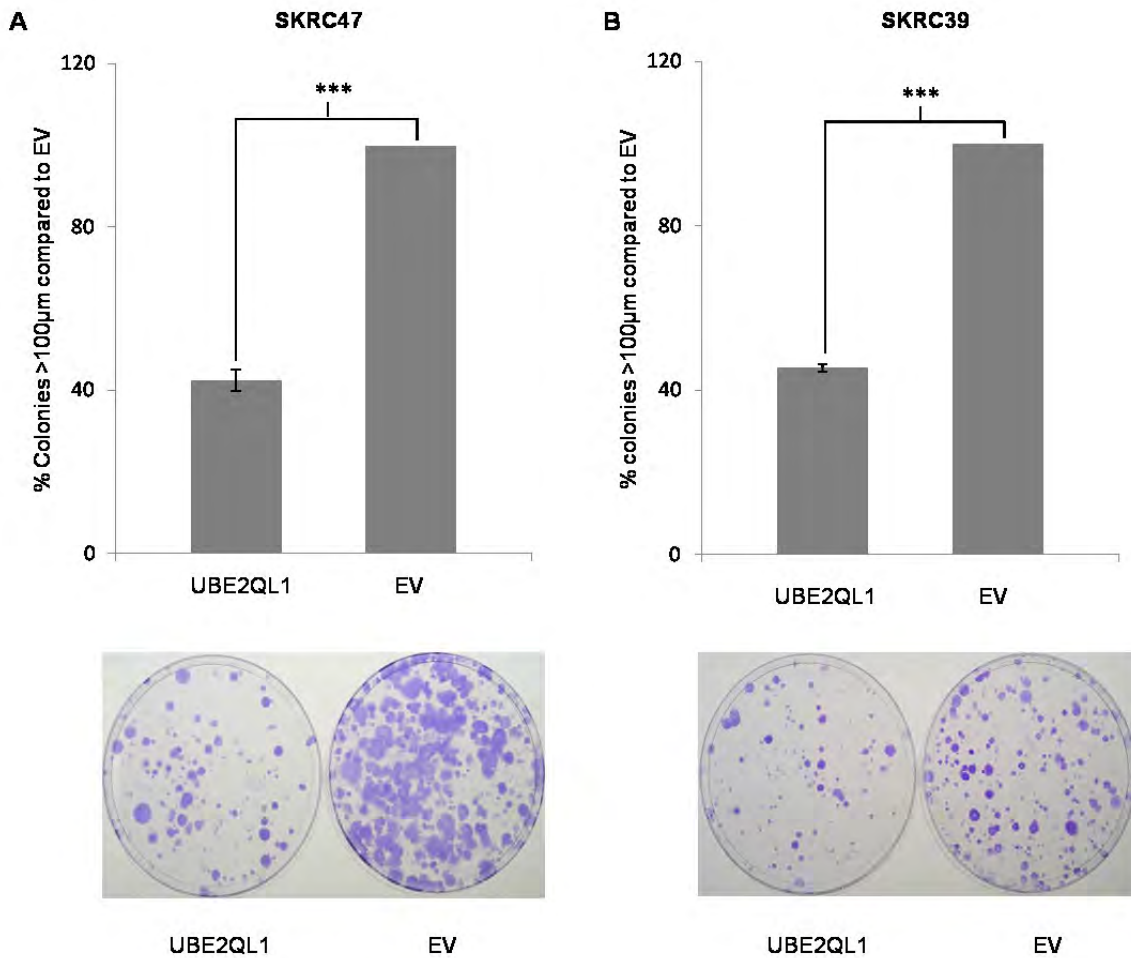


Figure 5.1 Colony formation assays to assess *UBE2QL1* growth suppression function in RCC cell lines.

Equal amounts of G418 resistant empty vector (EV) pFLAG-CMV-4 and pFLAG-CMV-4-wt*UBE2QL1* were transfected into SKRC47 and SKRC39 cell lines which after 2 weeks of selection and seeding, were incubated in media containing G418. After four weeks plates were stained with 0.4% crystal violet and manually counted blindly using an average of 3 counts ($n = 3$). **A**, (Top panel) chart demonstrating the percentage of SKRC47 colonies (>100µm) for cells expressing *UBE2QL1* compared to cells expressing EV. Error bars represent standard error of the mean (SEM). ($t = 22.5199$, $SEM = 2.556$, $*** = p < 0.0001$). **B**, (Top panel) chart demonstrating the percentage of SKRC39 colonies (>100µm) for cells expressing *UBE2QL1* compared to cells expressing EV. (unpaired t -test: $t = 62.5977$, $SEM = 0.87$, $*** = p < 0.0001$). (Bottom Panel) Photographic image of representative plates showing colony growth for *UBE2QL1* (left) expressing cells compared to EV (right) after 4 weeks for SKRC47 (**A**) and SKRC39 (**B**) RCC cell lines.

5.2.2 Stable *UBE2QL1* expressing SKRC47 clones

To produce SKRC47 clones stably expressing *UBE2QL1* or empty vector (EV) cells were initially transfected with EV pFLAG-CMV-4 and pFLAG-CMV-4-*wtUBE2QL1*. Transfected cells were selected for using G418 antibiotic as plasmids contained a neomycin resistant gene. Selected cells were seeded and 12 colonies were selected and grown in separate dishes. Western blot analysis was used to determine if clones stably expressed Flag-UBE2QL1 after a four week period. One clone was shown to stably express Flag-UBE2QL1 and was subsequently used in the soft agar assays (*Figure 5.2*).

5.2.3 UBE2QL1 soft agar assays

The ability of *UBE2QL1* to inhibit anchorage independent growth in soft agar was assessed by soft agar growth assays. Flag-UBE2QL1 or Flag-EV stably expressing SKRC47 clones were seeded in six well dishes in soft agar and compared following five weeks of incubation. There was a statistically significant 77% reduction in colony growth (number of colonies $\geq 100\mu\text{m}$) for *UBE2QL1* expressing cells compared to EV ($p < 0.0001$, SEM 17.252) (*Figure 5.2*). This result verified the ability of UBE2QL1 to inhibit anchorage independent growth and therefore suggests UBE2QL1 potentially inhibits the transforming abilities of neoplastic cells by functioning as a tumour suppressor.

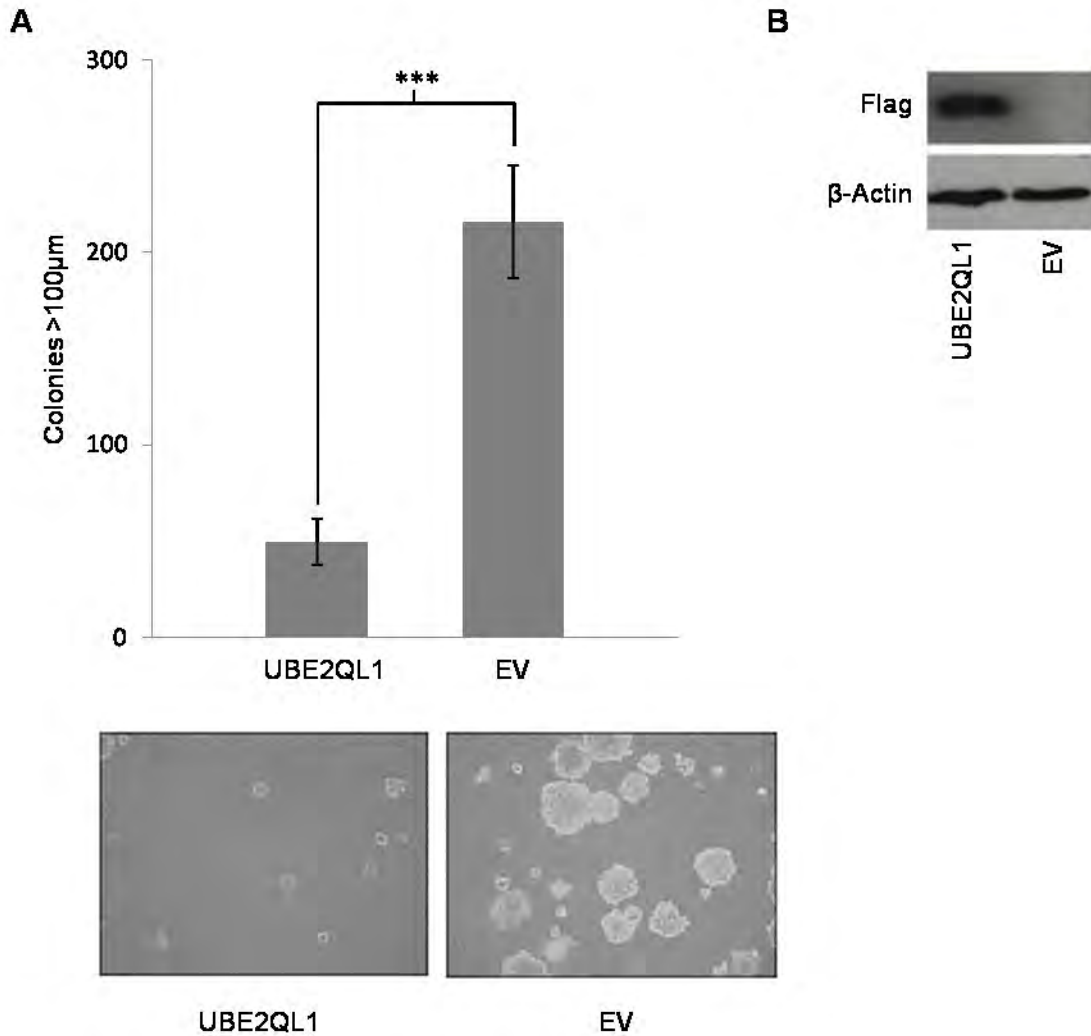


Figure 5.2 Soft agar growth assays to assess *UBE2QL1* inhibition of anchorage independent growth.

Clones of SKRC47-pFLAG-CMV-4-wt*UBE2QL1* and empty vector (EV) pFLAG-CMV-4 were seeded at the same density into soft agar and incubated for five weeks after which colonies (>100µm) were blindly counted with a light microscope (n = 6). **A**, Chart demonstrating the number of colonies (>100µm) grown in an anchorage-independent manner after 4 weeks for clones expressing *UBE2QL1* compared to cells expressing EV. Error bars represent standard error of the mean (SEM). (unpaired t-test: $t = 9.6319$, $SEM = 17.252$, $*** = p < 0.0001$). **B**, Representative microscope images (x100 magnification) of clones following five weeks of incubation expressing either *UBE2QL1* (left) or EV (on the left), showing the difference in number and size of colonies. **C**, Western blot analysis of protein extracted from Flag-*UBE2QL1* stably expressing SKRC47 clone and Flag-EV clone to confirm expression for soft agar assays. Blots were probed with anti-Flag (top panel) and anti-β-actin to confirm equal loading (bottom panel).

5.3 Conclusion

UBE2QL1 re-expression in *UBE2QL1* silenced RCC cell lines demonstrated significant suppression of colony growth suggesting UBE2QL1 has anti-proliferative function thus demonstrating tumour suppressor properties. This was further supported by the ability of UBE2QL1 to diminish colony formation of an RCC cell line in soft agar, as anchorage independent growth represents a hallmark of tumourigenesis. These results along with the genetic and epigenetic evidence of *UBE2QL1* dysregulation in sporadic and familial RCC, supports the notion that *UBE2QL1* is a novel RCC tumour suppressor gene. Although components of E3 ubiquitin complexes (e.g. VHL and FBXW7) have clearly been implicated in tumourigenesis (see section 1.5) there is very little information regarding the potential role of E2 ubiquitin conjugating enzymes, although increased expression of some (e.g. UbcH10 and E2-EPF) has been described in some cancers (Okamoto et al. 2003b, 2003b; Tedesco et al. 2007; Roos et al. 2011; Seghatoleslam et al. 2012). Thus it was determined important to investigate the function and role UBE2QL1 plays in the cell to determine the mechanism of its tumour suppressor properties.

Chapter Six: UBE2QL1 ubiquitin conjugation, E3 binding partners and protein substrates

6.1 Introduction: UBE2QL1 is part of the ubiquitin cascade

UBE2QL1 was an uncharacterised protein with an unknown function and therefore to understand the mechanism involved that allows UBE2QL1 to function as a novel RCC tumour suppressor gene it was important to determine the normal function of UBE2QL1 in the cell. The UBE2QL1 amino acid (aa) sequence shows homology to the family of ubiquitin conjugating enzymes known as E2 enzymes, these are characterized by a ~150aa ubiquitin conjugating domain (UBC) which contains a conserved active-site cysteine (C) residue that binds ubiquitin via a thioester bond (see section 1.4.1 for detail) (*Figure 6.1*). E2s form an important component of the ubiquitin cascade as they interact with an E3 ubiquitin ligase to ubiquitylate the protein substrate with substrate fate being determined by the nature of the ubiquitin chain(s) formed by the E2 enzyme (see section 1.4). As UBE2QL1 showed homology to the family of E2 enzymes it was necessary to determine if UBE2QL1 functioned as an E2 conjugating enzyme. Alignment of UBE2QL1 with the UBC domain of E2 conjugating enzymes allowed the identification of a possible active cysteine (C88) which could be hypothesised to bind ubiquitin via a thioester bond (*Figure 6.1*). To determine if UBE2QL1 binds ubiquitin at residue C88 mutant forms of UBE2QL1 that were predicted to affect the binding of ubiquitin were created. It has been shown that mutating the active C residue of E2 enzymes to an alanine (A) produces an E2 enzyme that lacks the capacity to bind ubiquitin as the thioester bond can no longer be formed (Sung et al. 1990). Point mutations of the active C residues of E2 conjugating enzymes to a serine (S) residues have been demonstrated to bind

ubiquitin and ubiquitin-like proteins with a much more stable oxy-ester bond as opposed to the normal thioester bond (Wada et al. 2000). As the normal thioester created between an E2 active C and ubiquitin is often disrupted during normal lysis procedures a C-S mutant creating a more stable oxy-ester bond formation would potentially enhance ubiquitin binding and allow identification of ubiquitin binding to an E2 *in vivo* under normal lysis conditions (Jin et al. 2007). Due to the aforementioned properties of E2 conjugating active cysteine C-A and C-S mutants, UBE2QL1 C88A and C88S mutants were created to investigate the potential binding of ubiquitin at the C88 residue and were used in subsequent ubiquitin binding assays, along with wild-type UBE2QL1, *in vitro* and *in vivo*.

Once ubiquitin is bound to an E2 ubiquitin conjugating enzyme the ubiquitin protein is transferred to a substrate leading to substrate ubiquitylation. This process is often facilitated via an E3 ligase complex which binds both the substrate and E2 enzyme (see section 1.4). Initially a yeast-2-hybrid was carried out by the German Cancer Research Centre using UBE2QL1 as bait to identify potential E3 protein binding partners. Only one potential binding partner was identified which was isolated only once: SUGT1 (suppressor of G2 allele of SKP1), yet this interaction could not be confirmed via co-immunoprecipitation or mass spectrometry and was therefore deduced to be a false positive. The interaction of E2 enzymes and E3 ligases are often weak as this allows for efficient E2 dissociation from the E3 enzyme after the transfer of the ubiquitin to make way for a new E2-ubiquitin molecule. It is also important to note E3 ligases often only

bind to E2 enzymes already thioesterified with ubiquitin, and not to the naked E2 proteins. It is often the case that many E2-E3 interactions are not discovered using normal methods to detect protein interactions, such as yeast-2-hybrids and pulldown assays, this is thought to be because the weak binding of E2 enzymes to E3 ligases is often disrupted in the wash steps of such assays, or the input E2 protein is non-thioesterified with ubiquitin thus would not likely bind to its E3 partner (Deshaies & Joazeiro 2009). Although VHL is an E3 ligase enzyme and is the most frequently mutated gene in ccRCC, it was determined that it was not likely that UBE2QL1 partners with VHL to ubiquitinate VHL substrates, as staining of t(5;19)(p15.3;q12) renal tumours showed no HIF target gene deregulation, thus suggesting UBE2QL1 functions in a different pathway to that of VHL/HIF α .

As mentioned above following initial failed attempts to identify a UBE2QL1 E3 ligase binding partner, an *in silico* search using the full length UBE2QL1 protein sequence to identify potential binding motifs within the protein was performed using ELM (The Eukaryotic Linear Motif resource for Functional Sites in Proteins). This revealed a phosphodegron consensus sequence, VTPPVS at positions 154-159, which was proposed to act as an FBXW7 recognition motif (Nash et al. 2001) (*Figure 6.2*). FBXW7 is an F-box protein that provides substrate recognition to the CUL1-SKP1-RBX1 SCF ubiquitin ligase (SCF^{FBXW7}) complex, is inactivated in a variety of cancers and was previously found to be disrupted in a case of clear cell RCC associated with a

constitutional t(3;4)(q21;q31) (see section 1.5.1 and 1.5.2). Therefore it was important to ascertain the possible interaction between UBE2QL1 and FBXW7.

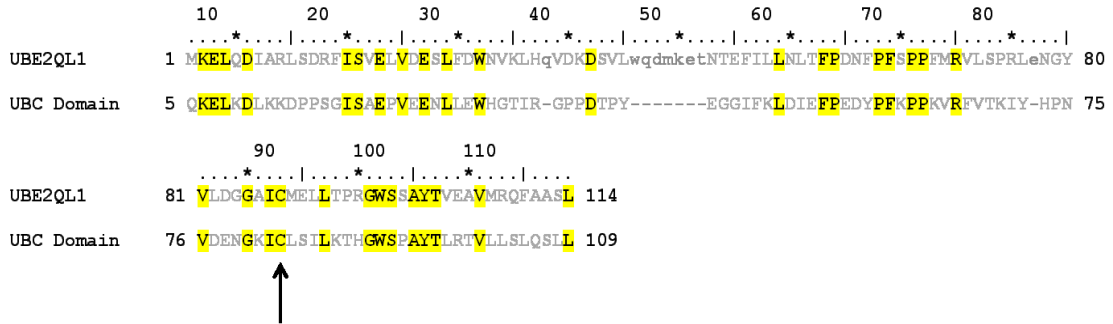


Figure 6.1 UBE2QL1 amino acid alignment with the ubiquitinating conjugating (UBC) domain.

Alignment showing homology of UBE2QL1 and the UBC domain. Homologous amino acids are shown in yellow. The UBC domain active cysteine is indicated by an arrow showing homology to a C88 on UBE2QL1.

6.1.1 Aims

UBE2QL1 plasmid constructs expressing mutants $UBE2QL1^{C88A}$ and $UBE2QL1^{C88S}$, were used in an *in vitro* transcription/translation rabbit reticulocyte lysate system that supports ubiquitin conjugation and in His pull down assays, along with wild type *UBE2QL1*, to determine if *UBE2QL1* binds ubiquitin at amino acid position C88. As *UBE2QL1* was shown to contain a consensus sequence proposed to act as an FBXW7 recognition motif, both immunoprecipitations and co-localisation experiments were undertaken with *UBE2QL1* and $FBXW7\alpha/\gamma$ to establish if the proteins interacted *in vivo*. Degradation assays were performed to ascertain if *UBE2QL1* re-expression increased the rate of FBXW7 substrate degradation.

6.2 Results:

6.2.1 UBE2QL1 ubiquitin binding

Wild-type UBE2QL1 (wtUBE2QL1) and UBE2QL1^{C88A} were synthesised using an *in vitro* transcription/translation rabbit reticulocyte lysate system that incorporates L- α -[³⁵S]-methionine into the proteins. The rabbit reticulocyte lysate contains all the machinery for ubiquitylation (E1 ubiquitin-activating enzyme, ubiquitin and ATP) and therefore supports ubiquitin conjugation. The reticulocyte UBE2QL1 protein synthesis products, when run on an agarose gel and detected using x-ray film, showed UBE2QL1^{C88A} migrated to the expected UBE2QL1 size of 18KDa whereas wtUBE2QL1 migrated to a size of 26KDa. As it was predicted that UBE2QL1 binds ubiquitin at residue C88 and ubiquitin itself runs to a size of 8KDa, the results suggest this increase in size of wtUBE2QL1 was due to bound monoubiquitin. UBE2QL1^{C88A} was likely unable to bind ubiquitin by inhibiting the formation of a thioester bond.

With this indication that UBE2QL1 contains a central active-site cysteine residue (C88) involved in ubiquitin binding, it was determined important to investigate whether UBE2QL1 binds ubiquitin directly *in vivo*. HEK293 cells were transfected with expression plasmids encoding Hisx6–ubiquitin (His-Ubq) or Hisx6 empty vector (His-EV) and either wtUBE2QL1, UBE2QL1^{C88A} or UBE2QL1^{C88S}. His pull-downs were carried out in both the presence and absence of β -mercaptoethanol, which is predicted to

reduce thioester bonds thus breaking the bond between E2 enzymes and ubiquitin. In the absence of β -mercaptoethanol, wtUBE2QL1 and UBE2QL1^{C88S} were both shown to bind ubiquitin with UBE2QL1^{C88S} showing enhanced avidity for ubiquitin relative to wtUBE2QL1. In the presence of β -mercaptoethanol, and consistent with observations for some other E2 enzymes, wtUBE2QL1 was no longer shown to bind ubiquitin, whilst UBE2QL1^{C88S} retained its ability to bind ubiquitin. This is most likely due to the reduction of the thioester bond produced between wtUBE2QL1 and ubiquitin. UBE2QL1^{C88S} most likely produced an oxy-ester bond with ubiquitin which is a much more stable bond able to withstand the reducing abilities of β -mercaptoethanol. UBE2QL1^{C88A} was unable to bind ubiquitin in either the presence or absence of β -mercaptoethanol as was shown with the reticulocyte lysate protein synthesis kit. In all cases of UBE2QL1 binding ubiquitin only the binding of mono-ubiquitin was detected. Together these results indicate that UBE2QL1 is monoubiquitinated *in vivo* at an active-site cysteine residue C88.

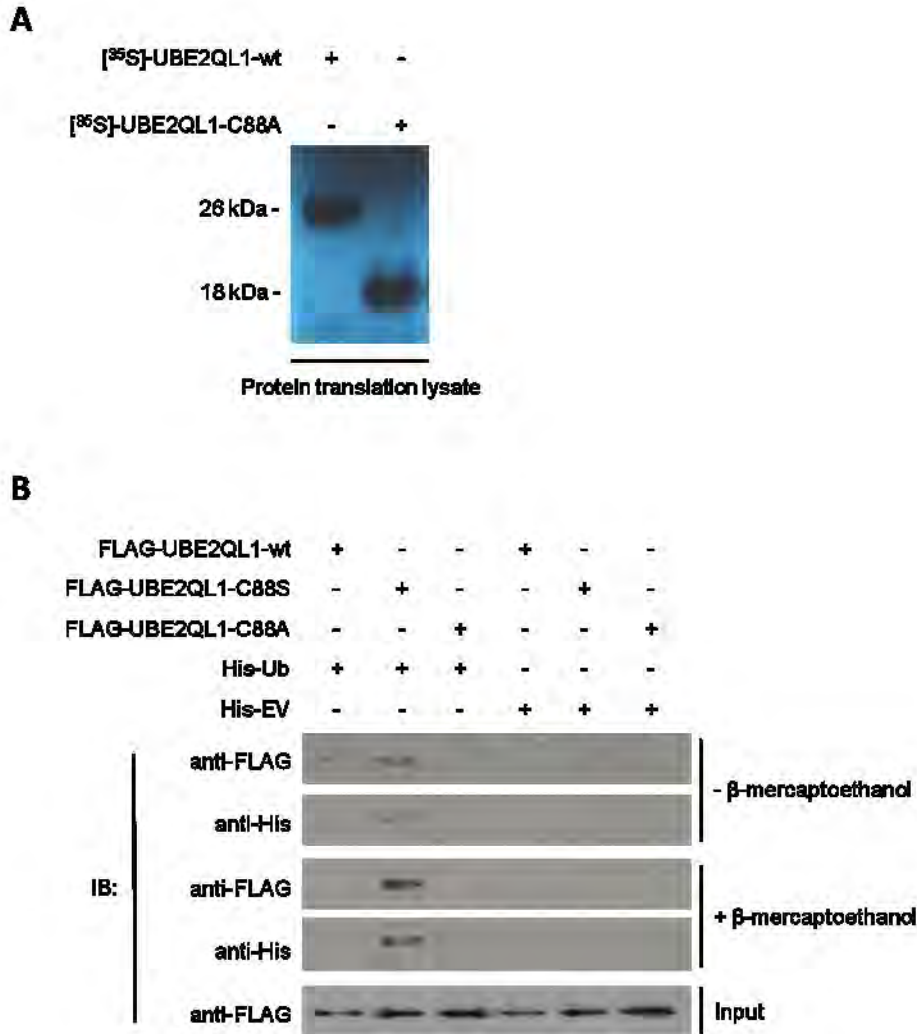


Figure 6.3 UBE2QL1 binds ubiquitin via an active cysteine, C88.

A, wtUBE2QL1 and UBE2QL1^{C88A} were synthesised with the incorporation of [³⁵S]-methionine using an *in vitro* reticulocyte lysate transcription/translation kit that supports ubiquitin conjugation. UBE2QL1^{C88A} migrated to the correct protein size of 18KDa. wtUBE2QL1 migrated to a size 26KDa. As ubiquitin has a molecular weight of 8KDa this suggested the increase in size of wtUBE2QL1 was due to mono-ubiquitylation. *B*, HEK293 cells were transfected with FLAG-wtUBE2QL1 or FLAG-UBE2QL1^{C88S} or FLAG-UBE2QL1^{C88A} mutants and His₆-ubiquitin or His-EV (as indicated). Ubiquitin binding was assessed with His pull-downs using dynabeads in the presence (+) and absence (-) of β-mercaptoethanol and probed with anti-FLAG and anti-HIS. Input bands were detected at a size of 18KDa (UBE2QL1 M_r = 18KDa). All other bands were detected at a size of 26KDa due mono-ubiquitination of UBE2QL1 and UBE2QL1^{C88S}.

6.2.2 UBE2QL1 and FBXW7 protein interaction

As a number of attempts to identify a UBE2QL1 protein binding partner(s), including a yeast 2 hybrid carried out by the German Cancer Research Centre and immunoprecipitations followed by mass spectrometry, produced no UBE2QL1 binding partner candidates, an ELM (Eukaryote Linear Motif) search was undertaken. ELM is an open access website (<http://elm.eu.org/>) that uses a comprehensive database of validated motifs to predict functional motifs within a protein of interest, including ligand motifs, post-translational modification sites, subcellular targeting sites and cleavage sites. These linear motifs are short modules within proteins that allow low-affinity interactions providing a level of protein regulation within the cell and are important in targeting protein localisation, directing protein turnover and regulating cell signalling (Puntervoll et al. 2003; Dinkel et al. 2012). A UBE2QL1 ELM search identified two linear motifs outside of the UBC globular domain; globular domain filtering is undergone as functional sites must be accessed and therefore don't often reside in globular domains with most true motifs being present in the exposed loops (*Table 6.1*). One motif identified was the FBXW7 binding motif (*Figure 6.2*), FBXW7 is one of the many F-box proteins that functions as a substrate recognition component for the E3 ligase complex SCF. In one study *FBXW7* was found to be disrupted by a familial constitutional translocation associated with RCC and was shown to be mutated in small number of sporadic cases of RCC, thus suggesting FBXW7 may play a role in RCC tumourigenesis (see section 1.5.2). FBXW7 has also been shown to regulate the degradation of mTOR and as the

mTOR pathway has been demonstrated to be an important pathway in RCC tumourigenesis, this along with the aforementioned points indicated it was important to determine if UBE2QL1 and FBXW7 interacted *in vivo* (see section 1.5.1 and 1.5.2).

Table 6.1 Linear motifs identified in the UBE2QL1 protein sequence by ELM

Linear motifs were detected using the ELM (Eukaryote Linear Motif) website. After taxonomic range, cell compartment, structure and globular domain filtering two linear motifs were found within UBE2QL1; a phosphothreonine motif that binds FHA domains and an FBXW7 phosphodegron motif. Key: . = any amino acid, [...] = amino acids listed are allowed, {min, max} = specified range of amino acids; min required and max allowed, (...) = Used to mark positions of specific interest; e.g. the amino acid being covalently modified, or used to group parts of the expression. A probability score is calculated which is a low number for strictly annotated regular expressions and a high number for degenerate ones. This score reflects the probability of the regular expression to be found by chance in a given protein sequence and helps limit the number of predicted degenerate motif instances. The motif probability cut-off was set to 0.1.

Elm Name	Instances (Matched Sequence)	Positions (aa)	Elm Description	Cell Compartment	Motif	Probability score
LIG_FHA_1	WVTPPVS	153-159	Phosphothreonine motif binding a subset of FHA domains that show a preference for a large aliphatic amino acid at the pT+3 position.	nucleus	..(T)..[ILV]	0.0087
LIG_SCF_FBW7_1	VTPPVS	154-159	The TPxxS phospho-dependent degron binds the FBXW7 F box proteins of the SCF (Skp1_Cullin-Fbox) complex.	cytosol, nucleus	[LIVMP].{0,2}(T)P..([ST])	0.0007

Immunofluorescence studies to determine UBE2QL1 cell expression were carried out using both FLAG and MYC tagged UBE2QL1 constructs in HeLa, Hek293 (data not shown) and SKRC47 (data not shown) cell lines. As an antibody was not available to detect endogenous UBE2QL1 only exogenous expression could be detected using expression constructs. UBE2QL1 appears to localise in small clusters within the nucleus (*Figure 6.4*). From analysing the DAPI (4',6-diamidino-2-phenylindole) stains these small clusters do not appear to be in the nucleoli as these are displayed as black spots within the nucleus, this is due to little DNA residing within the nucleoli and DAPI only binding to double stranded DNA (*Figure 6.4*). These UBE2QL1 clusters would therefore most likely be localised to specific subdomains known as nuclear bodies found within the nucleus. There are a number of nuclear bodies that have been characterised including Cajal bodies, PML bodies, Gems (gemini of Cajal bodies), cleavage bodies, clastosomes and nuclear speckles (Spector 2001; Spector & Lamond 2011; Lafarga et al. 2002). Many of these nuclear bodies contain specific machinery for particular tasks within the nucleus, for example nuclear speckles are enriched in pre-mRNA splicing factors and clastosomes are composed of components of the ubiquitin-proteasome pathway. Further investigations using specific nuclear body markers would need to be carried out to confirm which nuclear body UBE2QL1 resides in.

Immunofluorescence and co-immunoprecipitation experiments were undertaken to determine if UBE2QL1 and FBXW7 interacted within the cell. FBXW7 has three known isoforms that are produced by alternative splicing (FBXW7 α , β and γ). The three isoforms are differentially regulated and FBXW7 α is expressed at much greater levels

than FBXW7 β and FBXW7 γ , in most human and primary cell lines (Welcker & Clurman 2008). All three isoforms have been shown to localise to specific areas within the cell, with FBXW7 β exhibiting cytoplasmic localisation and both FBXW7 γ and FBXW7 α localising to the nucleus with some clustering to specific domains within the nucleus (Welcker & Clurman 2008). Immunofluorescence of FLAG-FBXW7 α , β , and γ in HeLa cells demonstrated similar localisation patterns to what has previously been reported, suggesting the FBXW7 constructs and immunofluorescence protocol were producing normal expression and staining of the FBXW7 proteins (*Figure 6.5*).

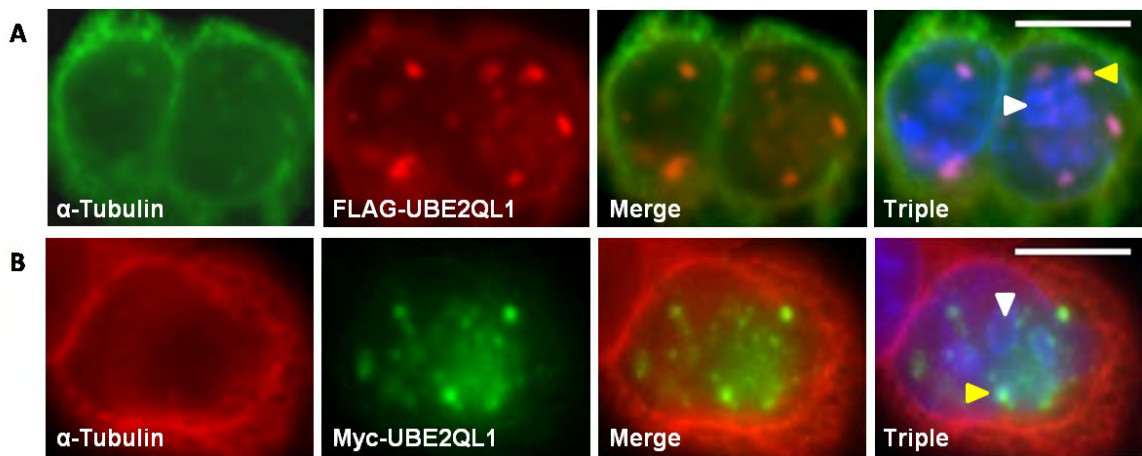


Figure 6.4 FLAG and MYC tag UBE2QL1 immunofluorescence in HeLa cells

A, HeLa cells were transfected with FLAG-UBE2QL1 and blotted with anti-FLAG (mouse) and anti- α -tubulin (rabbit) and labelled with secondary antibodies anti-mouse (red) and anti-rabbit (green). **B**, HeLa cells were transfected with MYC-UBE2QL1 and blotted with anti-MYC (rabbit) and anti- α -tubulin (mouse) and labelled with secondary antibodies anti-mouse (red) and anti-rabbit (green). The nucleus was labelled using the nuclear stain DAPI (blue). Both MYC and FLAG labelled UBE2QL1 shows speckled nuclear staining (yellow arrow) suggesting domain localisation within the nucleus. This speckled appearance is not due to nucleoli localisation as no UBE2QL1 staining occurred within any of the nucleoli (white arrow). scale bars = 13 μ m.

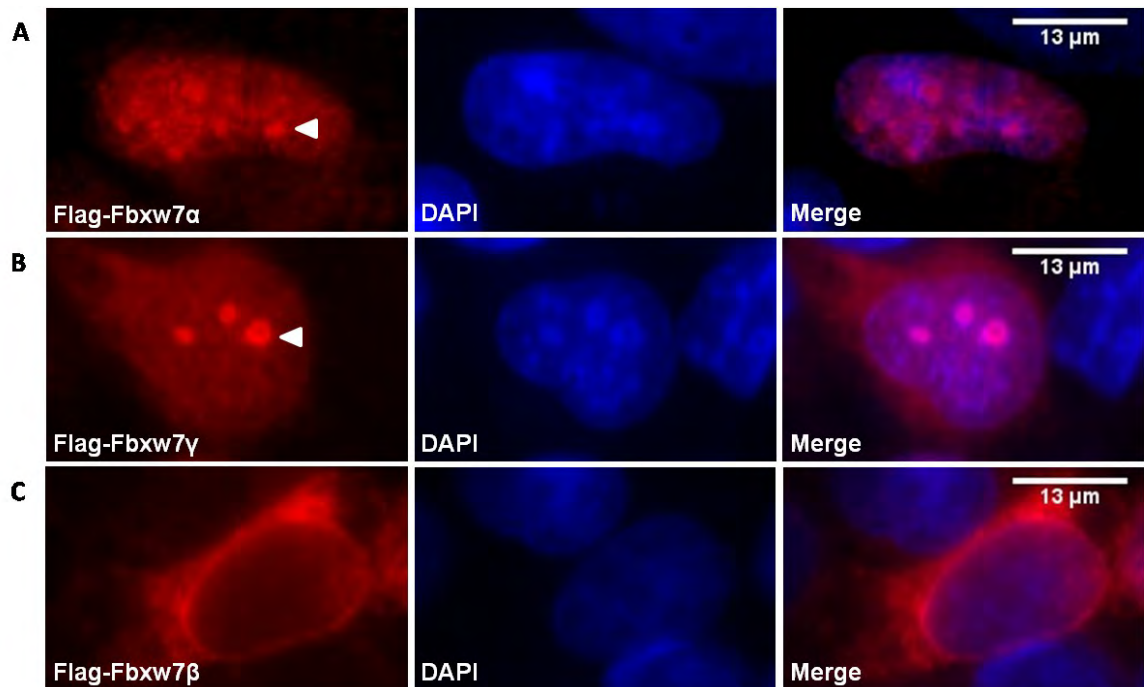


Figure 6.5 *FBXW7* α , β and γ isoform localisation staining within HeLa cells.

HeLa cells were transfected with *FLAG-FBXW7* α (A), *FLAG-FBXW7* γ (B) and *FLAG-FBXW7* β (C). Cells were blotted with anti-FLAG and labelled with anti-mouse (red). Both *FBXW7* α and γ showed nuclear localisation with staining in specific domains within the nucleus (white arrows) and *FBXW7* β displayed cytoplasmic localisation. The nucleus was labelled using the nuclear stain DAPI (blue), scale bar = 13 μ m.

As α and γ isoforms of FBXW7 were shown to reside in specific clusters within the nucleus similar to that of UBE2QL1, immunofluorescence was undertaken to determine if FBXW7 α and/or FBXW7 γ co-localised with UBE2QL1. HeLa cells were co-transfected with FLAG-FBXW7 α/γ and MYC-UBE2QL1 and cells were stained with fluorescently labelled anti-MYC and anti-FLAG antibodies as well as DAPI to indicate the nucleus. These experiments demonstrated UBE2QL1 and FBXW7 α/γ partially co-localised within specific clusters in the nucleus of the cell (*Figure 6.6*), thus suggesting an interaction between UBE2QL1 and FBXW7 α/γ may occur *in vivo*.

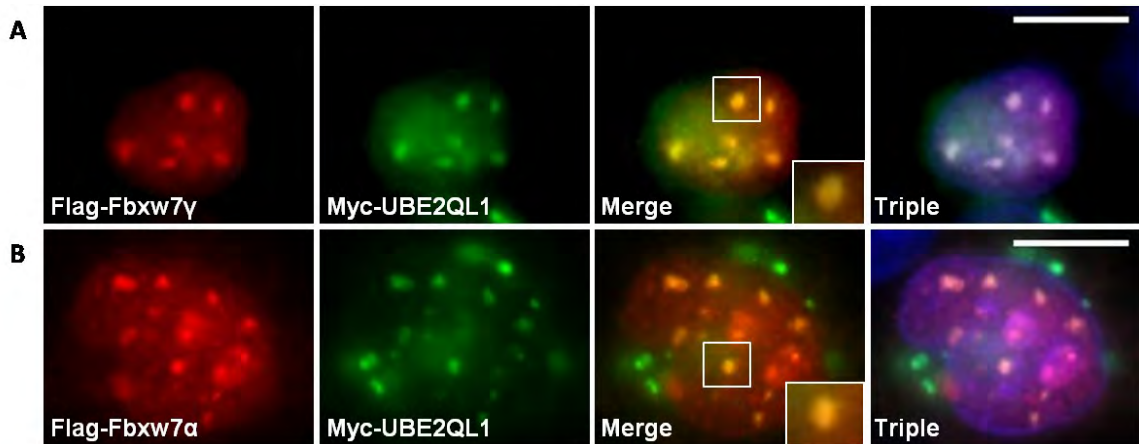


Figure 6.6 *UBE2QL1 and FBXW7 α/γ co-localisation in HeLa cells*

HeLa cells were transfected with FLAG-FBXW7 γ (A) or FLAG-FBXW7 α (B) and MYC-UBE2QL1. Cells were labelled with anti-FLAG (red) and anti-MYC (green) along with the nuclear stain DAPI (blue). Both FBXW7 α/γ and UBE2QL1 demonstrated staining of the same specific domains within the nucleus producing a speckled appearance. Partial co-localisation is visualised as a yellow stain due to the overlay of red and green stains (white box shows a zoomed in image of co-localisation). Merge = labelled with anti-MYC (green) and anti-FLAG (RED), Triple = labelled with anti-MYC (green), anti-FLAG (red) and DAPI (blue). Scale bar = 13 μ m.

Co-immunoprecipitations were undertaken to demonstrate protein binding of UBE2QL1 and FBXW7 α/γ . As there were no antibodies available for UBE2QL1 and no FBXW7 antibodies that could be used successfully for immunoprecipitations (IPs), all IPs were undertaken using tagged expression plasmids. MYC-UBE2QL1 and FLAG-FBXW7 (α or γ) were transfected into HEK293 cells and IPs were carried out using magnetic Dynabeads (Invitrogen) that had been conjugated with either anti-FLAG or anti-MYC antibodies. When UBE2QL1 was immunoprecipitated with MYC Dynabeads and immunoblotted with anti-FLAG, FLAG-FBXW7 bands were present demonstrating protein binding. IPs of FBXW7 isoforms using anti-FLAG Dynabeads also demonstrated protein binding with bands present for MYC-UBE2QL1 after blotting with anti-MYC (*Figure 6.7*). Controls transfected with empty vector (EV)-MYC and FBXW7 or EV-FLAG and MYC-UBE2QL1 showed no bands for MYC-UBE2QL1 or FLAG-FBXW7 respectively, demonstrating proteins were not binding to the FLAG or MYC tags or weren't binding to the antibody bound dynabeads (*Figure 6.7*). Thus both immunofluorescence co-localisation studies and Co-IP experiments demonstrated UBE2QL1 and FBXW7 α/γ interaction *in vivo*.

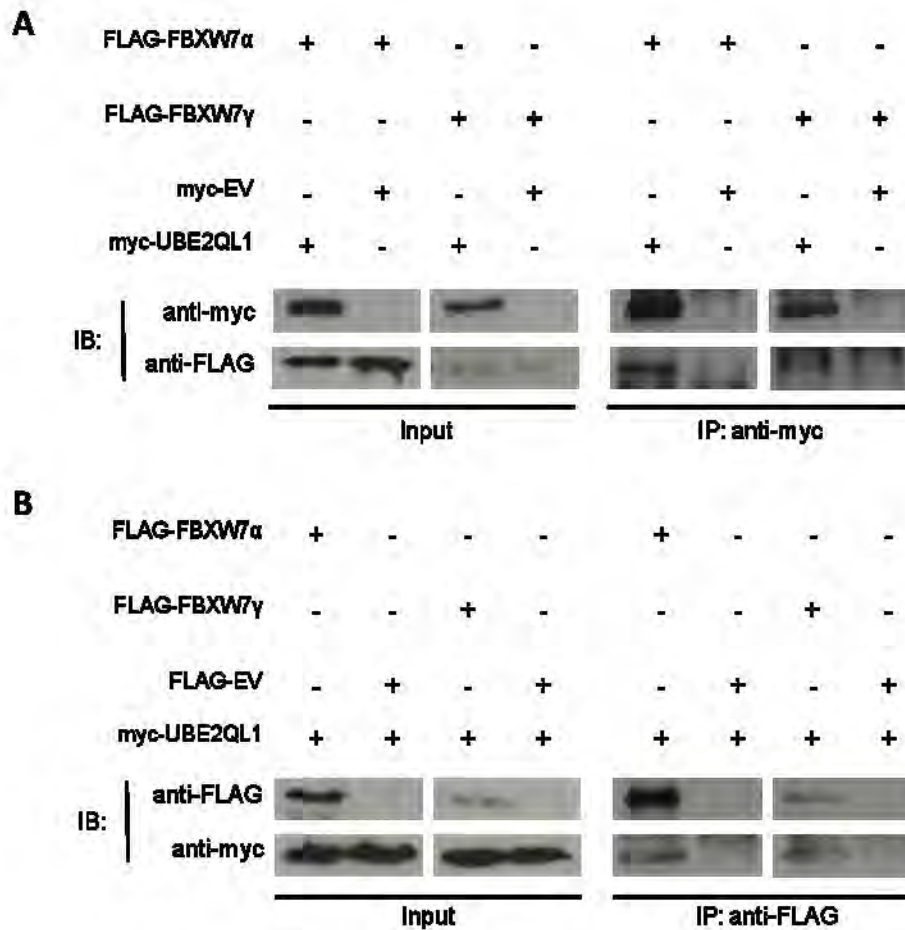


Figure 6.7 UBE2QL1 and FBXW7 α/γ co-immunoprecipitations

A, HEK-293 cells were transfected with either empty vector (EV)-MYC or MYC-UBE2QL1 and FLAG-FBXW7 α/γ as indicated. Immunoprecipitation (IP) of MYC-UBE2QL1 followed by immunoblot (IB) analysis with anti-FLAG identified FBXW7 α and FBXW7 γ as UBE2QL1 interacting proteins (right panel). *B*, HEK-293 cells were transfected with either EV-FLAG or FLAG-FBXW7 α/γ and MYC-UBE2QL1 as indicated. IP of FLAG-FBXW7 α and FLAG-FBXW7 γ followed by IB analysis with anti-MYC confirmed FBXW7 α and FBXW7 γ as UBE2QL1 interacting proteins (right panel). 10 μ g of cell lysates are shown to indicate input levels of FBXW7 α , FBXW7 γ and UBE2QL1 (*A* and *B* left panels).

6.2.3 Does FBXW7 target UBE2QL1 for proteasome degradation?

The FBXW7 recognition motif identified in UBE2QL1 acts as a phosphodegron motif that has been demonstrated to target FBXW7 substrates, such as cyclin E1 and mTOR, to the SCF^{FBXW7} complex leading to substrate ubiquitylation and often targeted proteasome degradation (Nash et al. 2001; Bai et al. 1996) . It was therefore important to investigate whether FBXW7 facilitated UBE2QL1 proteasome degradation. SKRC47 cells were transfected with UBE2QL1 and EV-FLAG, or UBE2QL1 and FBXW7 and a degradation assay was carried out with protein levels been measured at serial time points following the addition of the protein synthesis inhibitor, cyclohexamide. There was no increase in UBE2QL1 protein degradation with the addition of FBXW7 detected (*Figure 6.8-A*). The E2 ubiquitin conjugating CDC34 has been shown to be recruited to the SCF^{βTRCP} E3 complex leading to the ubiquitylation of substrates such as IκBα (Read et al. 2000). Following an *in silico* search (<http://elm.eu.org/>) using the full length CDC34 protein sequence (NP_004350), the presence of a βTRCP phosphodegron motif, DSGTEES, was detected within CDC34 at amino acid residues 230-236 (*Figure 6.9*) and studies have shown CDC34 is degraded by the SCF^{βTRCP} complex under specific cellular conditions, thus E2 conjugating enzymes can be ubiquitylated by the same E3 ligase complexes that they interact with to ubiquitylate their substrates (Fernandez-Sanchez et al. 2010; Sadowski et al. 2007). It was therefore speculated that although UBE2QL1 may be ubiquitylated by SCF^{FBXW7}, due to the presence of its FBXW7 phosphodegron, which most likely occurs under unknown specific cellular conditions, UBE2QL1 may also

functioning as an E2 conjugating enzyme for SCF^{FBXW7}. It is widely accepted that SCF E2 conjugating enzymes interact to the E3 complex via the ring-finger protein RBX-1 (Jin & Harper 2002; Spratt et al. 2012). We therefore determined whether UBE2QL1 and RBX1 interacted within the cell by co-immunoprecipitation, which demonstrated an interaction *in vivo* (Figure 6.8-B) thus suggesting UBE2QL1 may interact with FBXW7 via RBX-1 within the SCF complex.

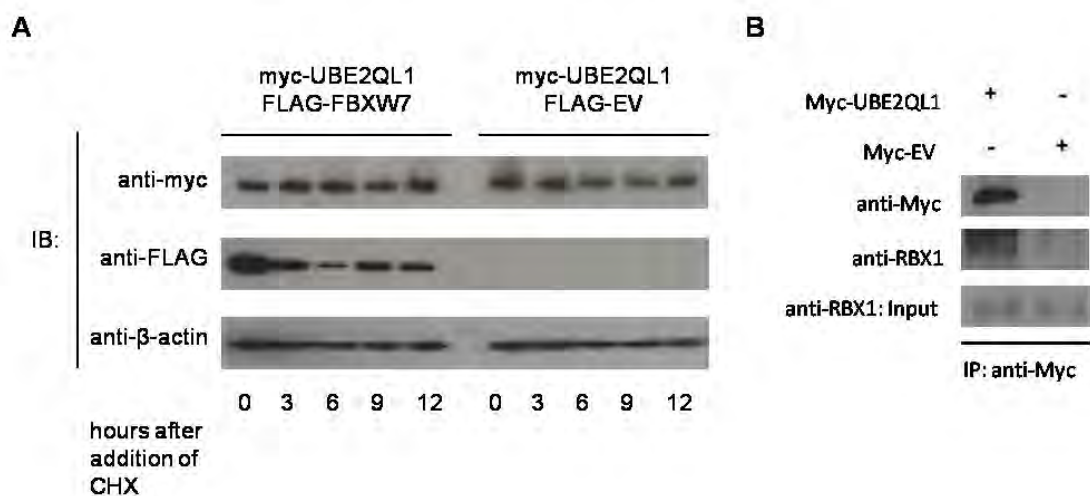


Figure 6.8 *FBXW7* does not facilitate the degradation of *UBE2QL1* under normal cellular conditions and *UBE2QL1* interacts with endogenous *RBX-1*

A, SKRC47 Cells were transfected with indicated plasmids treated with 100µg/ml cyclohexamide (CHX) 24hrs post transfection and collected at the indicated times. IB analysis was undertaken with the indicated antibodies. Anti-β-actin was used as loading control, n=3. **B**, Immunoprecipitation (IP), in HEK293 cells transfected with EV-MYC or MYC-UBE2QL1, with anti-MYC along with immunoblot (IB) analysis with anti-RBX-1 and anti-MYC demonstrated UBE2QL1 and RBX-1 protein interaction. 10µg of protein lysate was immunoblotted with anti-RBX-1 (input).

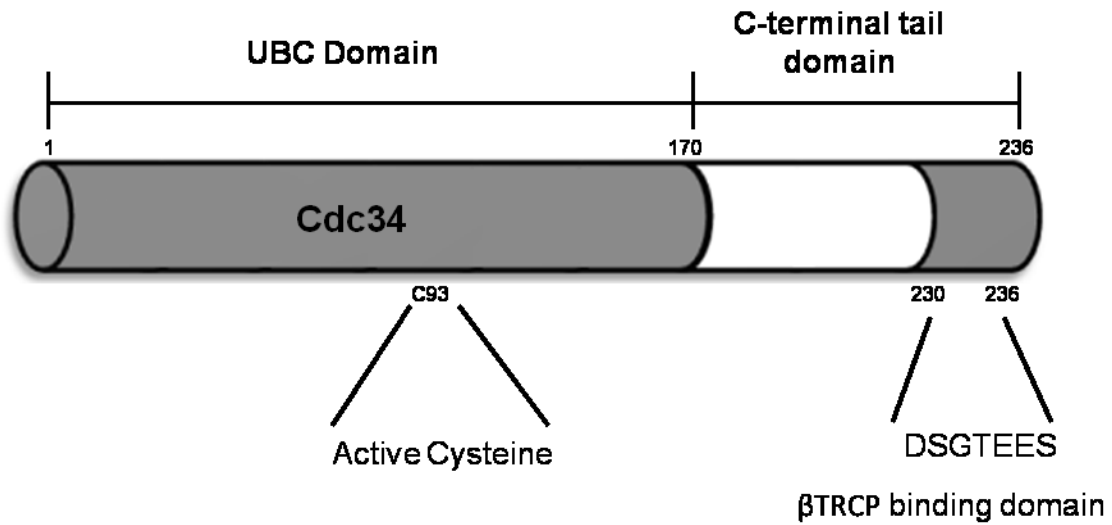


Figure 6.9 Schematic illustration of Cdc34 protein domains

Cdc34 is an E2 conjugating enzyme for the SCF^{βTRCP} E3 complex. It consists of a 170aa core UBC domain containing an active cysteine residue at (C93) and an acidic c-terminal tail domain shown to be important in its interaction to the E3 complex. A βTRCP phosphodegron binding domain was detected at residues 230-236.

6.2.4 FBXW7 substrate degradation assays

Given the association between UBE2QL1, FBXW7 and RBX-1 this suggested UBE2QL1 may function as an E2 conjugating enzyme for the SCF^{FBXW7} E3 ligase complex contributing to the ubiquitylation of its protein substrates. Although a number of outcomes can occur from substrate ubiquitylation depending on the ubiquitin linkages formed by the E2 enzyme (*Figure 1.7*), it was decided to initially determine if SCF^{FBXW7} protein substrate proteasomal degradation was enhanced by UBE2QL1. A UBE2QL1 stably expressing RCC cell line was used to determine if re-expression of UBE2QL1 caused a decrease in SCF^{FBXW7} substrate half life, thus suggesting UBE2QL1 may be targeting the substrates for proteasomal degradation. Protein lysates from the UBE2QL1 or EV stably transfected SKRC47 and SKRC39 cell lines were used to compare protein expression levels of mTOR and cyclin E1 as these have both been shown to be targeted for proteasomal degradation via the SCF^{FBXW7} complex (see section 1.5). UBE2QL1 stably expressing cells displayed a marked decrease of both cyclin E1 and total mTOR expression compared to EV controls (*Figure 6.10*). To determine if this decrease in mTOR and cyclin E1 expression was due to enhanced protein degradation and not another mechanism such as a change in transcriptional regulation, a degradation assay was carried out which involved exposing UBE2QL1 or EV transfected SKRC47 cells to the protein synthesis inhibitor cycloheximide and extracting cells at serial time points. mTOR and cyclin E1 protein levels were measured at serial time points following the addition of cycloheximide twenty four hours post transfection. A significant serial

reduction in both cyclin E1 and mTOR levels in cells transfected with myc-UBE2QL1 compared with cells transfected with myc-EV was detected indicating that degradation of these FBXW7 targets is enhanced by UBE2QL1 (*Figure 6.11*).

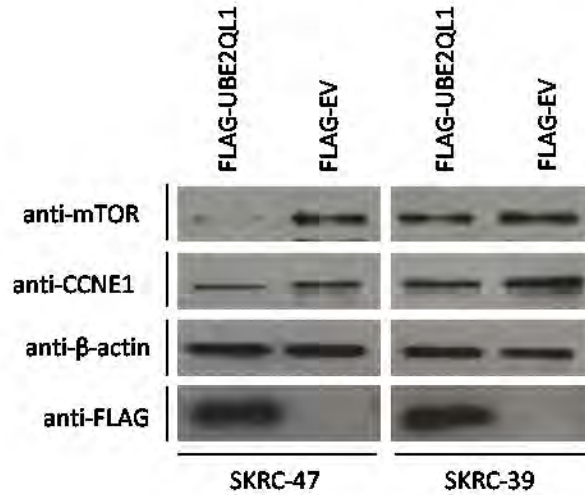


Figure 6.10 *UBE2QL1* stable clones demonstrate decreased cyclin E1 and *mTOR* expression compared to controls

Protein lysate was extracted from SKRC47 and SKRC39 stable clones expressing FLAG- *UBE2QL1* (*UBE2QL1*) and FLAG-EV (EV) and 10 μ g of protein was immunoblotted with the indicated antibodies. Anti- β -actin was used as a loading control.

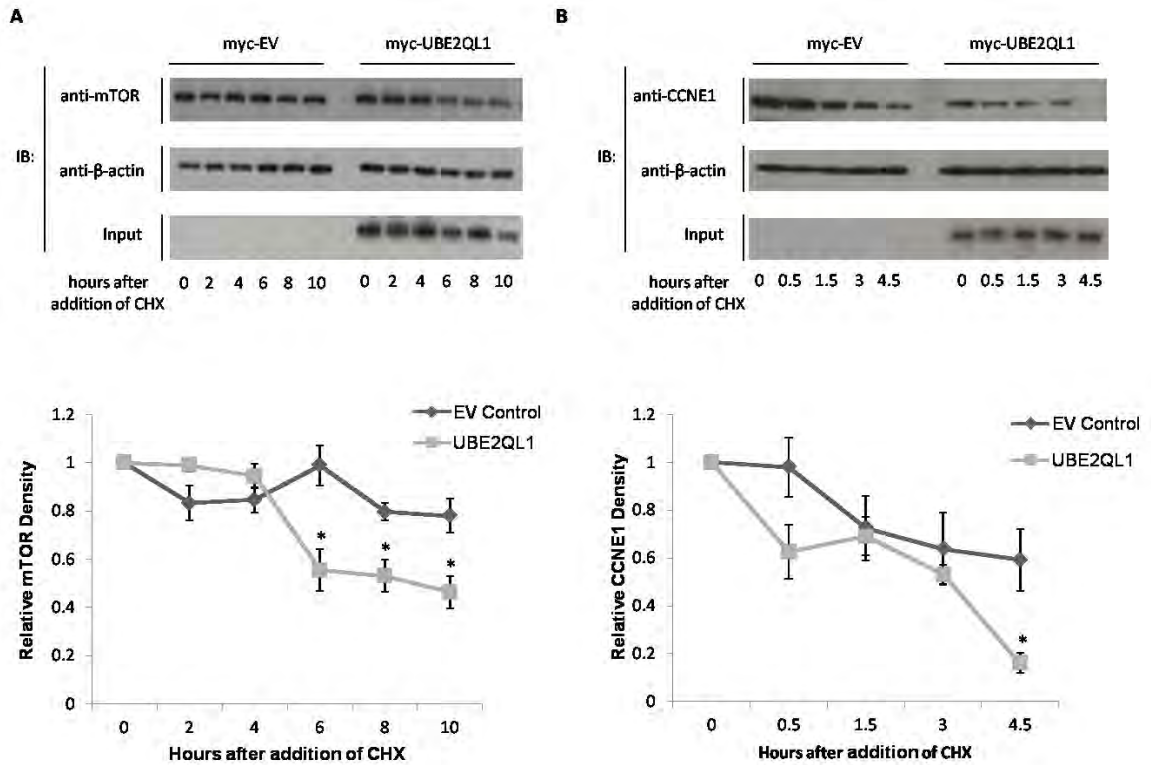


Figure 6.11 UBE2QL1 enhances mTOR and cyclin E1 degradation

SKRC47 Cells were transfected with myc-UBE2QL1 and myc-EV and were treated with 100µg/ml cyclohexamide (CHX) 24hrs post transfection and collected at the indicated times. Upper panels, 10µg of protein was immunoblotted with anti-mTOR (A) and anti-cyclin E1 (B). Anti-β-actin was used as loading control. Lower panels, relative densities of mTOR (left) and cyclin E1 (right) to β-actin by densitometry, normalised to time point zero. (unpaired t-test, error bars = SEM, n = 3, * P<0.05).

As these experiments suggested *UBE2QL1* is involved in the regulation of cyclin E1 expression, t(5;19)(p15.3;q12) associated renal tumours from individuals III:I and III:II (two oncocytomas and one chromophobe RCC) were stained for cyclin E1 expression in immunohistochemistry experiments by Dr Anne-Bine Skytte and increased cyclin E1 expression (compared to normal kidney) was detected (*Figure 6.12*) thus demonstrating *UBE2QL1* is likely involved in the regulation of cyclin E1 expression.

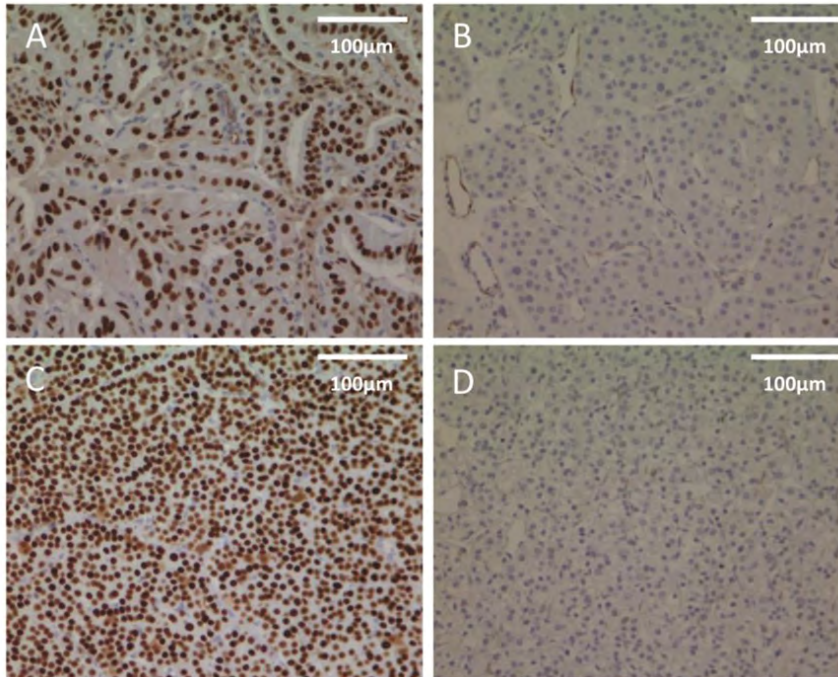


Figure 6.12 Immunohistochemistry with cyclin E1 (cyclin E1) in *t(5;19)(p15.3;q13.1)* associated renal tumours carried out by Anne-Bine Skytte
 (A) cyclin E1 immunohistochemistry (IHC) in a *t(5;19)(p15.3;q13.1)* associated renal oncocytoma showing up-regulation. (B) cyclin E1 IHC in a sporadic renal oncocytoma showing no evidence of up-regulation to compare to (A). (C) cyclin E1 IHC in a *t(5;19)(p15.3;q13.1)* associated chromophobe RCC showing up-regulation. (D) cyclin E1 IHC in a sporadic clear cell RCC showing no evidence of up-regulation to compare with (A) and (C). All images are at x10 magnification.

6.3 Conclusion

UBE2QL1 shows homology to the class I of E2 ubiquitin conjugating enzymes as it only consists of the catalytic core domain (UBC domain) while class II and class III E2 conjugating enzymes contain additional N- or C- terminal extensions and class IV contain both (Wijk & Timmers 2010). The UBC domain contains an active cysteine in all active E2 ubiquitin conjugating enzymes that bind ubiquitin via a thioester bond prior to the interaction with their E3 ligases. It was demonstrated that UBE2QL1 bound ubiquitin via a predicted active cysteine residue C88. The UBE2QL1-ubiquitin interaction was disrupted by β -mercaptoethanol capable of reducing thioester bonds thus suggesting UBE2QL1 bound ubiquitin at C88 through the formation of a thioester bond, confirming its likely function as an E2 conjugating enzyme. The majority of E2 enzymes require the interaction to an E3 ligase to facilitate the ubiquitylation of the substrate protein (see section 1.4). An FBXW7 phosphodegron was identified in UBE2QL1 and an interaction was demonstrated between UBE2QL1 and FBXW7 isoforms α and γ *in vivo* as the proteins partially co-localised within the cell and were co-immunoprecipitated. It was also demonstrated that UBE2QL1 interacts with endogenous RBX-1, the RING-finger protein shown to bind E2 conjugating enzymes within the SCF complex, therefore it may be that the UBE2QL1 interaction with FBXW7 isoforms is via the SCF complex.

The FBXW7 phosphodegron motif has only been identified in FBXW7 substrates, targeting these substrates for ubiquitylation via the SCF^{FBXW7} complex, it was therefore initially thought that UBE2QL1 was likely an SCF^{FBXW7} substrate. Initial degradation assays did not suggest UBE2QL1 was targeted for degradation by FBXW7 under normal cellular conditions and further experiments demonstrated that UBE2QL1 was involved in the targeted degradation of FBXW7 substrates cyclin E1 and mTOR. This was further confirmed with both a t(5;19)(p15.3;q13.1) oncocyoma and chromophobe demonstrating cyclin E1 up regulation compared to normal kidney. It is also interesting to note that CDC34 an E2 ubiquitin conjugating enzyme for the SCF complex shown to function with the SCF^{βTRCP} complex leading to the degradation of substrates such as IκBα and β-catenin, also contains an F-box phosphodegron motif that targets substrates to the βTRCP F-box. CDC34 has been shown to be targeted for proteasomal degradation by the SCF^{βTRCP} complex under specific conditions, thus E2 conjugating enzymes are often regulated by the same E3 ligase complexes that they bind to ubiquitylate substrates (Fernandez-Sanchez et al. 2010; Sadowski et al. 2007). This suggested that although the UBE2QL1/FBXW7 interaction was initially identified due to the presence of the FBXW7 motif within UBE2QL1, studies have suggested it likely also functions as a ubiquitin conjugating enzyme for the SCF complex. Studies here did not suggest UBE2QL1 was targeted for degradation by FBXW7 under normal cellular conditions and it is likely that a specific stimulus is needed to induce FBXW7-dependent proteasomal degradation similar to that of βTRCP-dependent degradation of CDC34. Further experiments to determine if the decreased degradation of FBXW7 substrates, mTOR and cyclin E1,

detected in UBE2QL1 expressing cell lines, along with the up regulation of cyclin E1 in UBE2QL1 deficient tumours, is either due to UBE2QL1 functioning as an E2 ubiquitin conjugating enzyme for the SCF^{FBXW7} complex or an alternative mechanism, and whether or not this plays a role in the tumour suppressor function of UBE2QL1 (see section 7.4).

Chapter Seven: Discussion

7.1 *UBE2QL1 is a novel RCC TSG gene and E2 conjugating enzyme*

The characterisation of a constitutional translocation, t(5;19)(p15.3;q12), associated with a familial predisposition to RCC, led to the identification of a novel candidate RCC gene, *UBE2QL1*. It was determined that *UBE2QL1* demonstrated TSG activity and was inactivated in 37% of sporadic RCC by promoter region hypermethylation and/or allele deletions. Disruption of both *UBE2QL1* alleles were identified in one sporadic RCC and in an oncocytoma in one of the t(5;19)(p15.3;q12) patients thus following Knudson's 'two hit' model and reinforcing the evidence that *UBE2QL1* functions as a TSG (see section 1.1.2). The absence of frequent intragenic mutations of *UBE2QL1* is reminiscent of *RASSF1A*, a known TSG often inactivated by methylation and/or allele loss in sporadic RCC (see section 1.3.4). The function of *UBE2QL1* had not previously been characterised though it shows homology to the class of E2 ubiquitin conjugating enzymes and was demonstrated to contain an active cysteine residue (C88) that binds ubiquitin similar to that of other E2 conjugating enzymes. Recently a number of components of the ubiquitin-mediated proteolysis pathway (UMPP) were found to be mutated in RCC, though at a very small frequency (1-3%) when not including *VHL* (Guo et al. 2011). It is interesting that *UBE2QL1* is another member of the UMPP pathway with deregulation detected in 37% of sporadic RCCs thus substantiating the importance of the UMPP pathway in RCC. UMPP pathway components are often capable of regulating numerous proteins involved in different pathways. It can therefore be seen why the disruption of components of the UMPP

pathway is a common mechanism of tumourigenesis in a number of cancers including RCC, as a number of important regulatory pathways can be disrupted from the genetic and/or epigenetic dysregulation of a single UMPP component. Many of the UMPP components that are disrupted in RCC are often involved in the mTOR, HIF and/or Wnt/ β -catenin pathways, for example VHL has been demonstrated to regulate components of both the HIF and Wnt/ β -catenin pathways, suggesting dysregulation of these pathways play an important role in RCC tumourigenesis (see section 1.5.2).

7.2 *UBE2QL1 regulates oncogenes mTOR and cyclin E1*

Although the mechanism of tumour suppression of several inherited RCC genes (e.g. *VHL*, *FH*, and *SDHB*) have been linked to HIF-1/2 related pathways, evidence of HIF target dysregulation in t(5;19)(p15.3;q12) associated renal tumours was not identified and there was no relationship between *UBE2QL1* status and the presence or absence of a *VHL* mutation in sporadic RCC. *UBE2QL1* was demonstrated to interact with FBXW7 α/γ isoforms and the SCF component RBX-1 suggesting it may play a role within the SCF^{FBXW7} complex. It was demonstrated that *UBE2QL1* potentially regulates FBXW7 substrates, cyclin E1 and mTOR and with both of these proteins demonstrating oncogenic properties in numerous cancers, it could therefore be speculated that the mechanism of *UBE2QL1* tumour suppression activity involves that regulation of these oncogenic products. Investigations showed *UBE2QL1* stably expressing cell lines demonstrating a significant decrease in anchorage independent growth also exhibited a marked decrease in both mTOR and cyclin E1 expression, and two t(5;19)(p15.3;q12)

tumours demonstrated a dramatic cyclin E1 up-regulation compared to normal kidney. cyclin E1 is essential for the control of the cell cycle and accumulates during G1-S phase (Koff et al. 1992; Möröy & Geisen 2004). Over-expression of cyclin E1 has been observed in many tumours and results in chromosome instability contributing to tumourigenesis (Donnellan & Chetty 1999). mTOR activation is common in sporadic RCC, though in many cases the exact mechanism of this deregulation is unknown, and mTOR inhibitors have shown promise in clinical trials for the treatment of metastatic RCC (Anandappa et al. 2010; Gerullis et al. 2010; Marín et al. 2012). *VHL*-inactivated RCC are invariably clear cell, yet those associated with germline *FLCN* mutations (causing Birt-Hogg-Dubé syndrome) represent a variety of histopathological subtypes (similar to that of the t(5;19)(p15.3;q12)) and interestingly the *FLCN* gene product has been implicated in mTOR pathway regulation (Baba et al. 2006; Chen et al. 2008; Hasumi et al. 2009). Thus impaired degradation of mTOR may contribute to the development of RCC associated with *UBE2QL1* inactivation.

7.3 E2 ubiquitin conjugating enzymes in cancer

There is relatively little information regarding the potential role of E2 conjugating enzymes in cancers with only a few reports of increased E2 enzyme expression in some cancers (e.g. UbcH10 and E2-EPF) (Okamoto et al. 2003b, 2003b; Tedesco et al. 2007; Roos et al. 2011; Seghatoleslam et al. 2012). *UBE2QL1* is the first E2 conjugating enzyme shown to demonstrate TSG activity. It was originally depicted that E3 enzymes were the only components that brought substrate specificity to the ubiquitin cascade with

E1 and E2 enzymes functioning as ubiquitin carriers (see section 1.4.1), thus the tumour suppressor or oncogenic properties of E3 ligases could be easily recognised due to their specific nature (Ardley & Robinson 2005) and many components of E3 ligase complexes have been implicated in numerous cancers (Sun 2003; Sun 2006; Bernassola et al. 2008). With recent research demonstrating E2 conjugating enzymes also playing an important role in the biological outcome of a substrate as the length and type of ubiquitin chain(s) assembled can affect the fate of the substrate(s) thus providing another level of specificity, it could be speculated that E2 enzymes may play a more important role in disease and cancer than originally contemplated (see section 1.4.1).

CDC34 is the most well characterized E2 for SCF, mainly because experiments have been undertaken in yeast which specifically uses Cdc34 only (Schwob et al. 1994; Mathias et al. 1998). Although it is thought that human SCF can use alternate E2s, limited data only exists for members of the UBCH5 family (Gonen et al. 1999; Popov et al. 2010). Interestingly, it has been suggested that the choice of E2 may influence substrate outcome by virtue of the ubiquitin chains formed. Thus CDC34 promotes substrate degradation through its promotion of K48 linked ubiquitin chains necessitated by its acidic loop and has been shown to promote the degradation of c-myc by SCF^{FBXW7} whereas the E2 UBCH5, promotes stabilization of c-myc by SCF^{βTRCP} through the formation of heterotypic linked ubiquitin chains (Popov et al. 2010; Petroski & Deshaies 2005). It was demonstrated that UBE2QL1 carries monoubiquitin, but it is not clear whether UBE2QL1 acts alone to build a polyubiquitin chain by sequential transfer of

single ubiquitins, as described for CDC34 (Kleiger et al. 2009; Pierce et al. 2009) or whether UBE2QL1 acts in concert with another E2 to promote chain assembly. UBE2QL1 lacks the acidic tail of CDC34 which has been demonstrated to be essential for poly-ubiquitination of substrates of the SCF complex, but not for the initial mono-ubiquitination (Gazdoiu et al. 2007) and it may be that UBE2QL1 provides the rate limiting step to enable initial transfer of monoubiquitin prior to the efficient transfer of subsequent ubiquitins by another E2, for example CDC34. Further investigations are required to elucidate the precise function of UBE2QL1 and the relationship between UBE2QL1 growth suppression, E2 activity and FBXW7 function (see section 7.4).

7.4 Future experiments

7.4.1 Investigations of UBE2QL1 function within the cell

As expression of UBE2QL1 promoted the degradation of mTOR and cyclin E1, both substrates of FBXW7 and preliminary co-immunoprecipitations suggested UBE2QL1 does bind to RBX-1 (the E2 binding component of the SCF complex) *in vivo*, this suggested UBE2QL1 may function as an E2 conjugating enzyme for the SCF^{FBXW7} complex. A standard *in vitro* ubiquitin assay could be performed which includes all purified components of the SCF^{FBXW7} complex (RBX-1, CUL-1, SKP1 and FBXW7) along with the human E1 – activating enzyme, ubiquitin (often GST or His tagged), E2 conjugating enzyme (UBE2QL1) and FBXW7 substrates cyclin E1 and mTOR. Other FBXW7 substrates may also be ubiquitylated by UBE2QL1 and could therefore also be investigated. The reaction involves incubating all the protein components with a specific ubiquitination buffer including ATP as the reaction is ATP dependent. Controls include reactions in the absence of the E1 enzyme, E2 enzyme and ubiquitin. Samples would be loaded onto SDS-PAGE gels and blotted with the respective antibodies to detect substrates and ubiquitin (Choo & Zhang 2009). *In vivo* ubiquitin assays could also be carried out to confirm any *in vitro* results. These would involve transfecting a UBE2QL1 null cell line with UBE2QL1 and an epitope tagged ubiquitin (i.e. His tag). After 48 hours cells would be lysed and protein extracted. Immunoprecipitations and/or pulldown assays would be undergone to extract ubiquitin and substrate proteins from the protein

lysate. SDS-PAGE would be used to confirm substrate ubiquitylation using the respective antibodies. Controls would include substituting UBE2QL1 with empty plasmid. These assays can also be undertaken using the proteasome inhibitor, MG-132, thus preventing substrate proteasomal degradation.

Further work would also be required to determine how exactly UBE2QL1 causes substrate ubiquitination and whether this also requires other E2s (i.e.CDC34) and, if so, which one(s). The *in vitro* and *in vivo* ubiquitination assay described above would help determine if UBE2QL1 substrates are mono or poly ubiquitinated. Commercial antibodies are now available that can detect specific ubiquitin linkages, for example antibodies that specifically detect K48-linked ubiquitin chains only (Boston Biochem), thus allowing detection of the specific ubiquitin linkages UBE2QL1 attaches to its substrates.

7.4.2 UBE2QL1 tumour suppressor activity

UBE2QL1 stable expression in a UBE2QL1 null expressing cell line demonstrated tumour suppressor activity with decreased anchorage independent growth and decreased proliferation. *UBE2QL1* knockdown experiments in a UBE2QL1 expressing cell line such as HEK293 would help confirm this data, as these would be predicted to show increased proliferation and anchorage independent growth in colony growth assays and soft agar assays respectively, compared to the UBE2QL1 expressing cell lines. Attempts were made to knockdown *UBE2QL1* using the only available (non-

verified) silencer select siRNA (Invitrogen). As no antibody was available for UBE2QL1, knockdowns had to be verified using QRT-PCR. A knockdown of only 20% was demonstrated thus would not be sufficient to determine UBE2QL1 knockdown affects in the cell. A more successful method may be to use UBE2QL1 shRNA vectors that can be used to produce stable knockdowns of proteins as these vectors contain an antibiotic resistant gene and thus shRNA transfected cells can be selected for leading to stable integration of the shRNA expression cassette into the host genome. As many assays such as soft agar and colony assays require a long incubation period stable knockdowns are an advantage as siRNA often only produces a knockdown for up to 5-7 days.

To determine if mTOR deregulation is one of the key mechanisms involved in *UBE2QL1* TSG activity, the activity of the mTOR inhibitor, rapamycin, could be assessed using *UBE2QL1* knockdown cell lines along side *UBE2QL1* expressing controls (Yip et al. 2010). Thus if rapamycin treatment on *UBE2QL1* null cell lines reversed the knockdown affects on the cells, this would suggest *UBE2QL1* regulation of mTOR is an important aspect of its TSG activity.

UBE2QL1 has been shown to act as a novel tumour suppressor gene in RCC, it would be interesting to determine if its TSG function is specific to RCC or if it acts as a general TSG and therefore would be disrupted in other cancers. To assess this UBE2QL1

promoter methylation, gene deletion and mutation analysis could be carried out on a panel of other sporadic tumours.

7.5 Conclusion

Due to recent advances and affordability in genome sequencing technology, the majority of investigations to identify novel disease genes are now being initiated through exome or whole genome sequencing of patients, and though this research has greatly increased the rate at which disease associated genes are identified, it is important to note that *UBE2QL1*, like *RASSF1A*, would not have been identified through exome sequencing (Peters et al. 2007; Loginov et al. 2009). This demonstrates that although exome sequencing studies have become a fundamental tool in identifying causative genes it is important that other methods of gene identification continue to be utilized to allow a complete analysis of the causative genetic and epigenetic abnormalities within a disease.

This research has illustrated how the analysis of rare inherited forms of RCC can allow the identification of candidate RCC TSGs involved in the more common sporadic forms of the disease. The findings in this thesis have increased the knowledge of familial and sporadic RCC tumorigenesis and have confirmed recent reports of the importance of the UMPP pathway in RCC. This research also presents a novel finding in which a component (*UBE2QL1*), other than an E3 ligase, of the ubiquitin cascade has been shown to function as a TSG, thus warranting further investigations to determine *UBE2QL1* function and specificity within the cell.

Chapter Eight: Appendices

8.1 *Primer sequences*

8.1.1 PCR and sequencing primers

Product	Direction	Primer sequence
UBE2QL1 Ex1	F	AGCAACACTGCACGCAGGT
	R	GTGAGCAGCTCCATGCAGAT
UBE2QL1 Ex2a	F	GACCAACACCGAGTTCATCC
	R	CGCTGGTGTAGTCAGAGCAG
UBE2QL1 Ex2b	F	AGACATCAGAAATCCCCACG
	R	ATTCAGGATGCAGTTCTGGC
VHL Ex1	F	AGTCCGGCCCCGGAGGAACT
	R	TGCTGGGTCTGGGCCTAAGC
VHL Ex2	F	CACCGGTGTGGCTCTTTAACAA
	R	ACATCAGGC AAAAATTGAGA ACTGG
VHL Ex3	F	CCTTG TACTGAGACCCTAGTCTGCCACT
	R	CAAGACTCATCAGTACCATCAAAAAGCTG

8.1.2 t(5;19)(p15.3;q12) primers

Derivative breakpoint	Purpose	Direction	Primer sequence
der(5)	PCR	F	TGTTGCAGTTCTTTTCAGTTTCG
	PCR	R	AACAAAGTGTGGACATTTAGCAAA
der(5)	Seq	F	TGTTGCAGTTCTTTTCAGTTTCG
	Seq	R	TTTAGAGGAGCCATGCAGGT
der(19)	PCR	F	AGTGGGAAATAGCTCTAGGAATGG
	PCR	R	GCCAAGTGGCTTCACAAGTATCT
der(19)	Seq	F	ACTTAACAGACTGCCCTGGTG
	Seq	R	TCATTCACTGAGCACTGTAGTGAC

8.1.3 Vector sequencing primers

Vector	Direction	Primer sequence
pFLAG-CMV4	F	AATGTCGTAATAACCCCGCCCC GTTGACGC
	R	TATTAGGACAAGGCTGGTGGG CAC
pCMV-myc	F	TATTAGGACAAGGCTGGTGGG CAC
PGEM-T Easy	F	TAATACGACTCACTATAGGG
	R	ACACTATAGAATACTCAAGC
pcDNA3.1	F	TAATACGACTCACTATAGGG
	R	GCCTCGACTGTGCCTTCTA

8.1.4 Cloning primers

Gene	Direction	Primer sequence
UBE2QL1	F	GG AAT TCA CTC ATG AAG GAG CTG CAG GAC
	R	TTG GGA TCC CAG ACA TCA GCC GTC GGA

8.1.5 Site directed mutagenesis primers

Gene product	Direction	Primer sequence
UBE2QL1 C88A	F	CGGCGGCGCCATCGCCATGGAGCTGCTC
	R	GAGCAGCTCCATGGCGATGGCGCCGCCG
UBE2QL1 C88S	F	GGCGGCGCCATCAGCATGGAGCTGC
	R	GCAGCTCCATGCTGATGGCGCCGCC

8.1.6 COBRA primers

Gene	Direction	Primer sequence
UBE2QL1	F	YGTTYGTATATATATATTATATAGTGGTAGTAGTAGT
	OR	CAACACCRAATCCTTATCCACCTAATA
	IR	CTCTCRTCCACCAACTCCACRAAAATA

Note – Y = C or T, R= A or G

8.1.7 Custom designed MLPA probes

UBE2QL1 exon	Probe	Probe sequence	Chr5 position (bp)
Exon 1	LPO	GGGTTCCCTAAGGGTTGGATCACCTTCAGATTGTCT GTGGCAGGACATGAAGGAGACCAACA	6449124 - 6449179
	RPO	CCGAGTTCATCCTGCTCAACCTCACCTTAAAATCAC CAGTCTAGATTGGATCTTGCTGGCAC	
Exon 1+	LPO	GGGTTCCCTAAGGGTTGGATAGAGACGCCACGCTC ATGAGTGGCAAGGCTCTGAAATTCATCA	6453375 - 6453440
	RPO	GCATGAGTAAAAGCTGTTGGAAATGGCAGTCGGTA ACTTTCTAGATTGGATCTTGCTGGCAC	
Exon 1-	LPO	GGGTTCCCTAAGGGTTGGATCGAGAGGACGGTCTG TCTGTCTCTACAGCAAACCTGCATGCAGTGAGTGC	6444047 - 6444112
	RPO	TCTTGAGCAGTGGCTACAAGCTCTGTCTGGAGCAC CCTAGTTTCTAGATTGGATCTTGCTGGCAC	
Exon 2	LPO	GGGTTCCCTAAGGGTTGGAACCTCCGTCCCAGTGAC GTTCTAACCTGGTTTTTCTTCTC	6491287 - 6491352
	RPO	ATCTCACGCAGGGACGGATCTGTAGAAAAGCTGTA TCTAGATTGGATCTTGCTGGCAC	
Exon 2+	LPO	GGGTTCCCTAAGGGTTGGACAGGGGCTTGCACCTT CCAAACTGAAATTCTGCAGTG	6497546 - 6497611

	RPO	CATGTCTACTGCTGAGGGCTGTAGTGACAAGACTC TAGATTGGATCTTGCTGGCAC	
Exon 2-	LPO	GGGTTCCCTAAGGGTTGGACTTGGAAGTCCACTAC TTCGATGGTTGGTAATTATGCGCCTGCCAGTACAT	6490089 – 6490172
	RPO	AAAGCTCAGCCAGTTCTTTCCAGGCATTTCTGCAA ACGAGTACCCTCTAGATTGGATCTTGCTGGCAC	

8.1.8 LOH microsatellite marker primers

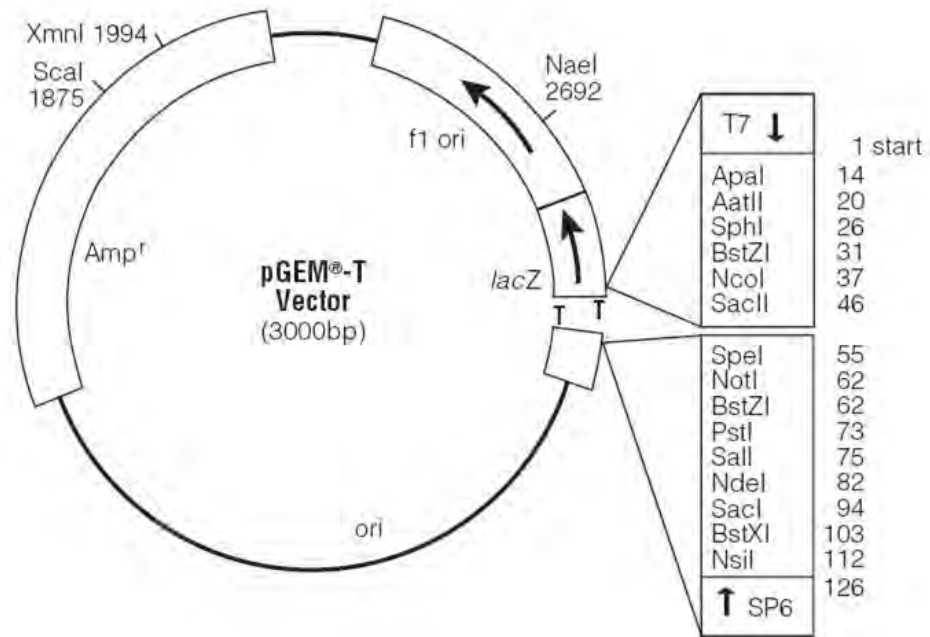
Microsatellite Marker	Chr 5 position (bp)	Chr band	Direction	Primer sequence
D5S2505	5869996- 5870453	P15.32	F	TGTTGGAAGACTTCTCAGCC
			R	CACACATGCTGTGTCTCTCA
D5S2054	5944886- 5945198	P15.32	F	TGAGATTTTCAGCCCACC
			R	AGCCACTTCCCGATGTT

8.1.9 RT-PCR primers

Gene	Direction	Primer sequence
UBE2QL1	F	CACCAGGTGGACAAGGACTC
	R	GTAGCTTCAGCTTCCTTGCG
GAPDH	F	GACCCCTTCATGACCTCAACTACA
	R	CTAAGCAGTTGGTGGTGCAGGA

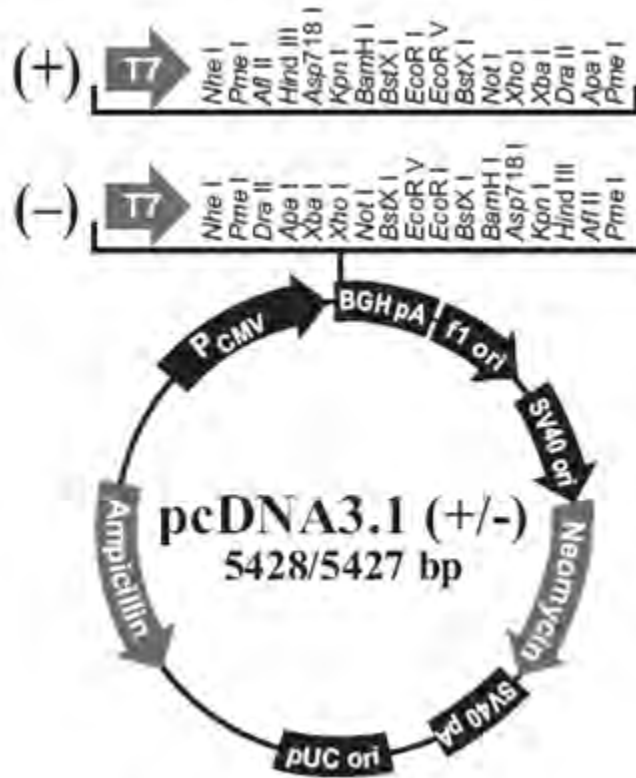
8.2 Plasmid Maps

8.2.1 PGEM-T



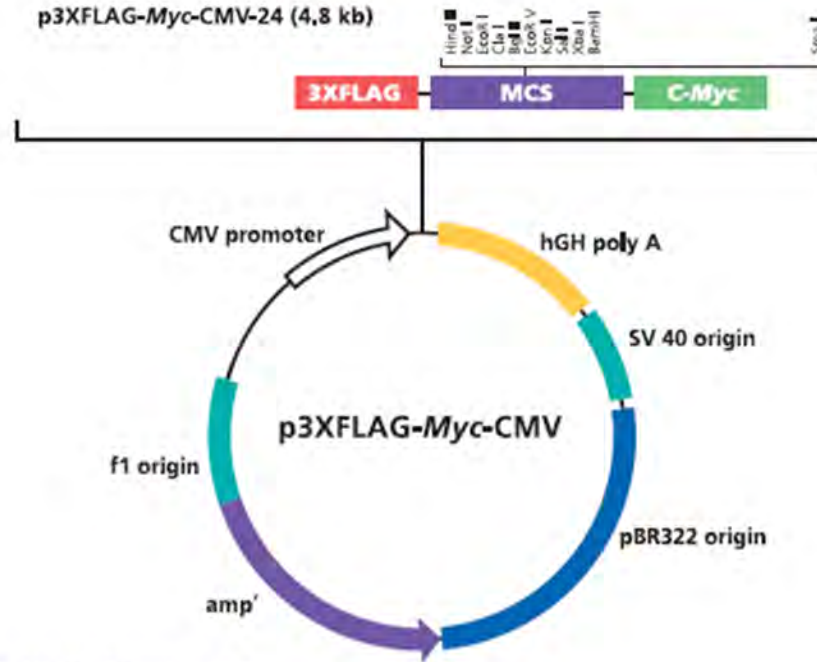
[www.promega.com/products/pcr/pcr-cloning/pgem_t-easy-vector-systems/]

8.2.2 PCDNA 3.1-



[\[//tools.invitrogen.com/content/sfs/manuals/pcdna3_1_man.pdf\]](http://tools.invitrogen.com/content/sfs/manuals/pcdna3_1_man.pdf)

8.2.4 p3xFLAG-MYC-CMV-24



Multiple Cloning Site

(p3XFLAG-Myc-CMV-23 and p3XFLAG-Myc-CMV-24)

3XFLAG Peptide Sequence															
Met	Asp	Tyr	Lys	Asp	His	Asp	Gly	Asp	Tyr	Lys	Asp	His	Asp	Ile	
ATG	GAC	TAC	AAA	GAC	CAT	GAC	GGT	GAT	TAT	AAA	GAT	CAT	GAC	ATC	
TAC	CTG	ATG	TTT	CTG	GTA	CTG	CCA	CTA	ATA	TTT	CTA	GTA	CTG	TAG	

3XFLAG Peptide Sequence								NotI		EcoRI		ClaI			
Asp	Tyr	Lys	Asp	Asp	Asp	Asp	Lys	AA	CTT	GCG	GCC	GCG	AA	TCA	TCC
GAC	TAC	AAA	GAC	GAT	GAC	GAC	AAA	CTT	GCG	GCC	GCG	AA	TCA	TCC	
CTG	ATC	TTT	CTG	CTA	CAG	CTG	TTC	GAA	CGC	CGG	CGC	TTA	AGT	AAC	

C-Myc Sequence															
Leu	Ile	Asp	Glu	Glu	Asp	Leu	STOP								
CTC	ATC	TCA	GAA	GAG	GAT	CTG	TGA	CCC	GGG						
GAG	TAG	AGT	CTT	CTC	CTA	GAC	ACT	GGG	CCC						

[//www.sigmaaldrich.com/catalog/product/sigma/e9283?lang=en®ion=GB]

8.3 *UBE2QL1* nucleotide and amino acid sequence

1 ATGAAGGAGCTGCAGGACATCGCGCGCCTTAGCGACCGCTTCATCTCCGTGGAGCTGGTGGACGAGAGC
1 -M--K--E--L--Q--D--I--A--R--L--S--D--R--F--I--S--V--E--L--V--D--E--S--
70 CTGTTTCGACTGGAACGTGAAGCTGCACCAGGTGGACAAGGACTCGGTGCTGTGGCAGGACATGAAGGAG
24 -L--F--D--W--N--V--K--L--H--Q--V--D--K--D--S--V--L--W--Q--D--M--K--E--
140 ACCAACACCGAGTTCATCCTGCTCAACCTCACCTTCCCCGACAACCTTCCCCTTCTCGCCGCCCTTCATG
47 -T--N--T--E--F--I--L--L--N--L--T--F--P--D--N--F--P--F--S--P--P--F--M--
210 CGGGTGCTCAGCCCGCGCCTGGAGAACGGCTACGTGCTGGACGGCGGCCATCTGCATGGAGCTGCTC
70 -R--V--L--S--P--R--L--E--N--G--Y--V--L--D--G--G--A--I--C--M--E--L--L--
280 ACGCCGCGCGGCTGGTCCAGCGCCTACACCGTGGAGGCCGTCATGCGCCAGTTCGCAGCCAGCCTGGTC
93 -T--P--R--G--W--S--S--A--Y--T--V--E--A--V--M--R--Q--F--A--A--S--L--V--
350 AAGGGCCAGGGACGGATCTGTAGAAAAGCTGGCAAATCAAAAAAGTCCTTCAGTCGCAAGGAAGCTGAA
116 -K--G--Q--G--R--I--C--R--K--A--G--K--S--K--K--S--F--S--R--K--E--A--E--
420 GCTACCTTTAAGAGTTTGGTGAAGACGCATGAAAAATATGGTTGGGTCACCCCGCCCGTGTCCGACGGC
139 -A--T--F--K--S--L--V--K--T--H--E--K--Y--G--W--V--T--P--P--V--S--D--G--
490 TGA
162 -*-

[www.ensembl.org]

8.4 UBE2QL1 Orthologue sequence variation

Species	Ensemble identifier & gene name	% sequence alignment to human UBE2QL1
Bushbaby (<i>Otolemur Garnettii</i>)	ENSOGAG00000032403UBE2QL1	100
Elephant (<i>Loxodonta africana</i>)	ENSLAFG00000027273UBE2QL1	100
Gorilla (<i>Gorilla gorilla</i>)	ENSGGOG00000024242UBE2QL1	100
Microbat (<i>Myotis Lucifugus</i>)	ENSMLUG00000029107UBE2QL1	100
Pig (<i>Sus scrofa</i>)	ENSSSCG00000017105UBE2QL1	100
Chicken (<i>Gallus gallus</i>)	ENSGALG00000013065UBE2QL1	99
Chimpanzee (<i>Pan troglodytes</i>)	ENSPTRG00000033811UBE2QL1	99
Dog (<i>Canis lupus familiaris</i>)	ENSCAFG00000030271UBE2QL1	99
Mouse (<i>Mus musculus</i>)	ENSMUSG00000052981Ube2ql1	99
Opossum (<i>Monodelphis domestica</i>)	ENSMODG00000028962UBE2QL	99
Orangutan (<i>Pongo abelii</i>)	ENSPPYG00000015331UBE2QL1	99
Rat (<i>Rattus norvegicus</i>)	ENSRNOG00000034075Ube2ql1	99
Turkey (<i>Meleagris gallopavo</i>)	ENSMGAG00000006402UBE2QL	99
Anole lizard (<i>Anolis carolinensis</i>)	ENSACAG00000000772UBE2QL1	98
Guinea Pig (<i>Cavia porcellus</i>)	ENSCPOG00000021028UBE2QL1	96
Xenopus (<i>Xenopus tropicalis</i>)	ENSXETG00000001734ube2ql1	95
Chinese softshell turtle (<i>Pelodiscus sinensis</i>)	ENSPSIG00000015214UBE2QL1	94
Zebrafish (<i>Danio rerio</i>)	ENSDARG00000079276UBE2QL1	92
Fugu (<i>Takifugu rubripes</i>)	ENSTRUG00000011783UBE2QL1	91

Medaka (<i>Oryzias latipes</i>)	ENSORLG00000014317UBE2QL1	91
Tilapia (<i>Oreochromis niloticus</i>)	ENSONIG00000007760UBE2QL1	91
Platyfish (<i>Xiphophorus maculatus</i>)	ENSXMAG00000013614UBE2QL	90
Stickleback (<i>Gasterosteus aculeatus</i>)	ENSGACG00000008986UBE2QL1	90
Tetraodon (<i>Tetraodon nigroviridis</i>)	ENSTNIG00000009260UBE2QL1	90
Cod (<i>Gadus morhua</i>)	ENSGMOG00000013361UBE2QL	88
Marmoset (<i>Callithrix jacchus</i>)	ENSCJAG00000008686LOC100392145	88
Panda (<i>Ailuropoda melanoleuca</i>)	ENSAMEG00000006771UBE2QL1	86
Pika (<i>Ochotona princeps</i>)	ENSOPRG00000019027UBE2QL1	83
Wallaby (<i>Macropus eugenii</i>)	ENSMEUG00000003995UBE2QL1	83
Armadillo (<i>Dasypus novemcinctus</i>)	ENSDNOG00000024031	82
Platypus (<i>Ornithorhynchus anatinus</i>)	ENSOANG00000001753UBE2QL1	77
Tasmanian devil (<i>Sarcophilus harrisii</i>)	ENSSHAG00000009846UBE2QL1	73
Coelacanth (<i>Latimeria chalumnae</i>)	ENSLACG00000001694UBE2QL1	71
Zebra Finch (<i>Taeniopygia guttata</i>)	ENSTGUG00000007820UBE2QL1	71
Fruitfly (<i>Drosophila melanogaster</i>)	FBgn0031896CG4502	66
Kangaroo rat (<i>Dipodomys ordii</i>)	ENSDORG00000011538Ube2ql1	57
Rabbit (<i>Oryctolagus cuniculus</i>)	ENSOCUG00000028162UBE2QL1	51
Armadillo (<i>Dasypus novemcinctus</i>)	ENSDNOG00000024355UBE2QL1	47
Sea Squirt (<i>Ciona savignyi</i>)	ENSCSAVG00000002205	43
Sea Squirt (<i>Ciona intestinalis</i>)	ENSCING00000005637	14

8.5 *UBE2QL1* known single nucleotide polymorphisms (SNPs)

Position in cDNA	Position in protein	Type of mutation	Source identified in	Frequency	Variation ID
c.G114C	p.S38S	synonymous	NHLBI Exome Sequencing Project	0.022%	TMP_ESP_5_6449120
c.C300T	p.A100A	synonymous	dbSNP	NA	rs11959306
c.G441A	p.T147T	synonymous	dbSNP + 1000 Genomes	0.002%	rs114648003

Chapter Nine: References

- Akhoondi, S. et al., 2007. FBXW7/hCDC4 is a general tumor suppressor in human cancer. *Cancer Research*, 67(19), pp.9006–9012.
- Albertson, D.G. et al., 2003. Chromosome aberrations in solid tumors. *Nature Genetics*, 34(4), pp.369–376.
- Alpi, A.F. et al., 2008. Mechanistic insight into site-restricted monoubiquitination of FANCD2 by Ube2t, FANCL, and FANCI. *Molecular Cell*, 32(6), pp.767–777.
- Anandappa, G., Hollingdale, A. & Eisen, Tg, 2010. Everolimus - a new approach in the treatment of renal cell carcinoma. *Cancer management and research*, 2, pp.61–70.
- Ananth, S. et al., 1999. Transforming growth factor beta1 is a target for the von Hippel-Lindau tumor suppressor and a critical growth factor for clear cell renal carcinoma. *Cancer Research*, 59(9), pp.2210–2216.
- Andersen, S.D. et al., 2012. Functional characterization of MLH1 missense variants identified in lynch syndrome patients. *Human mutation*, 33(12), pp.1647–1655.
- Antequera, F. & Bird, A, 1999. CpG islands as genomic footprints of promoters that are associated with replication origins. *Current Biology: CB*, 9(17), pp.R661–667.
- Ardley, H.C. & Robinson, P.A., 2005. E3 ubiquitin ligases. *Essays in Biochemistry*, 41, pp.15–30.
- Argani, P. & Ladanyi, M., 2005. Translocation carcinomas of the kidney. *Clinics in Laboratory Medicine*, 25(2), pp.363–378.
- Awakura, Y. et al., 2008. Methylation-associated silencing of SFRP1 in renal cell carcinoma. *Oncology Reports*, 20(5), pp.1257–1263.
- Baba, Masaya et al., 2006. Folliculin encoded by the BHD gene interacts with a binding protein, FNIP1, and AMPK, and is involved in AMPK and mTOR signaling. *Proceedings of the National Academy of Sciences of the United States of America*, 103(42), pp.15552–15557.
- Bai, C. et al., 1996. SKP1 connects cell cycle regulators to the ubiquitin proteolysis machinery through a novel motif, the F-box. *Cell*, 86(2), pp.263–274.
- Baldewijns, M.M. et al., 2010. VHL and HIF signalling in renal cell carcinogenesis. *The Journal of Pathology*, 221(2), pp.125–138.
- Balmain, A., Gray, J. & Ponder, B., 2003. The genetics and genomics of cancer. *Nature Genetics*, 33 Suppl, pp.238–244.
- Bandyopadhyay, R. et al., 2002. Parental origin and timing of de novo Robertsonian translocation formation. *American Journal of Human Genetics*, 71(6), pp.1456–1462.
- Barrett, M.T. et al., 2004. Comparative genomic hybridization using oligonucleotide microarrays and total genomic DNA. *Proceedings of the National Academy of Sciences of the United States of America*, 101(51), pp.17765–17770.
- Bauman, J.G. et al., 1980. A new method for fluorescence microscopical localization of specific DNA sequences by in situ hybridization of fluorochromelabelled RNA. *Experimental Cell Research*, 128(2), pp.485–490.

- Bellizzi, A.M. & Frankel, W.L., 2009. Colorectal cancer due to deficiency in DNA mismatch repair function: a review. *Advances in anatomic pathology*, 16(6), pp.405–417.
- Benedict, W.F. et al., 1983. Patient with 13 chromosome deletion: evidence that the retinoblastoma gene is a recessive cancer gene. *Science (New York, N.Y.)*, 219(4587), pp.973–975.
- Berger, A.H., Knudson, Alfred G & Pandolfi, P.P., 2011. A continuum model for tumour suppression. *Nature*, 476(7359), pp.163–169.
- Berger, A.H. & Pandolfi, P.P., 2011. Haplo-insufficiency: a driving force in cancer. *The Journal of Pathology*, 223(2), pp.137–146.
- Bernard, O. et al., 1990. Two distinct mechanisms for the SCL gene activation in the t(1;14) translocation of T-cell leukemias. *Genes, Chromosomes & Cancer*, 1(3), pp.194–208.
- Bernassola, F. et al., 2008. The HECT family of E3 ubiquitin ligases: multiple players in cancer development. *Cancer cell*, 14(1), pp.10–21.
- Bird, A.P., 1980. DNA methylation and the frequency of CpG in animal DNA. *Nucleic Acids Research*, 8(7), pp.1499–1504.
- Bodmer, D et al., 1998. An alternative route for multistep tumorigenesis in a novel case of hereditary renal cell cancer and a t(2;3)(q35;q21) chromosome translocation. *American journal of human genetics*, 62(6), pp.1475–1483.
- Bodmer, Daniëlle et al., 2003. Disruption of a novel gene, DIRC3, and expression of DIRC3-HSPBAP1 fusion transcripts in a case of familial renal cell cancer and t(2;3)(q35;q21). *Genes, chromosomes & cancer*, 38(2), pp.107–116.
- Bodmer, Daniëlle et al., 2002. Understanding familial and non-familial renal cell cancer. *Human Molecular Genetics*, 11(20), pp.2489–2498.
- Bonne, A. et al., 2007. Mapping of constitutional translocation breakpoints in renal cell cancer patients: identification of KCNIP4 as a candidate gene. *Cancer Genetics and Cytogenetics*, 179(1), pp.11–18.
- Bos, J.L., 1988. The ras gene family and human carcinogenesis. *Mutation Research*, 195(3), pp.255–271.
- Brenner, W. et al., 2002. Loss of tumor suppressor protein PTEN during renal carcinogenesis. *International journal of cancer. Journal international du cancer*, 99(1), pp.53–57.
- Bretones, G. et al., 2011. SKP2 oncogene is a direct MYC target gene and MYC down-regulates p27(KIP1) through SKP2 in human leukemia cells. *The Journal of biological chemistry*, 286(11), pp.9815–9825.
- Bunin, G.R. et al., 1989. Frequency of 13q abnormalities among 203 patients with retinoblastoma. *Journal of the National Cancer Institute*, 81(5), pp.370–374.
- Cáceres, W. & Cruz-Chacón, A., 2011. Renal cell carcinoma: molecularly targeted therapy. *Puerto Rico Health Sciences Journal*, 30(2), pp.73–77.
- Cairns, J., 1975. Mutation selection and the natural history of cancer. *Nature*, 255(5505), pp.197–200.
- Cairns, P et al., 1995. Frequency of homozygous deletion at p16/CDKN2 in primary human tumours. *Nature genetics*, 11(2), pp.210–212.

- Cairns, Paul, 2010. Renal cell carcinoma. *Cancer biomarkers: section A of Disease markers*, 9(1-6), pp.461–473.
- Capon, D.J. et al., 1983. Complete nucleotide sequences of the T24 human bladder carcinoma oncogene and its normal homologue. *Nature*, 302(5903), pp.33–37.
- Chapman, J.R., Taylor, M.R.G. & Boulton, S.J., 2012. Playing the end game: DNA double-strand break repair pathway choice. *Molecular cell*, 47(4), pp.497–510.
- Chen, J. et al., 2008. Deficiency of FLCN in mouse kidney led to development of polycystic kidneys and renal neoplasia. *PloS one*, 3(10), p.e3581.
- Chen, J. et al., 2003. The t(1;3) breakpoint-spanning genes LSAMP and NORE1 are involved in clear cell renal cell carcinomas. *Cancer Cell*, 4(5), pp.405–413.
- Cheung, H.-H. et al., 2009. DNA methylation of cancer genome. *Birth Defects Research. Part C, Embryo Today: Reviews*, 87(4), pp.335–350.
- Choo, Y.S. & Zhang, Z., 2009. Detection of protein ubiquitination. *Journal of visualized experiments: JoVE*, (30). Available at: <http://www.ncbi.nlm.nih.gov/pubmed/19692941> [Accessed August 14, 2012].
- Clark, S.J. & Melki, J., 2002. DNA methylation and gene silencing in cancer: which is the guilty party? *Oncogene*, 21(35), pp.5380–5387.
- Clifford, S C et al., 1998. Inactivation of the von Hippel-Lindau (VHL) tumour suppressor gene and allelic losses at chromosome arm 3p in primary renal cell carcinoma: evidence for a VHL-independent pathway in clear cell renal tumourigenesis. *Genes, chromosomes & cancer*, 22(3), pp.200–209.
- Cockman, M.E. et al., 2000. Hypoxia inducible factor-alpha binding and ubiquitylation by the von Hippel-Lindau tumor suppressor protein. *The Journal of Biological Chemistry*, 275(33), pp.25733–25741.
- Coffey, A.J. et al., 2011. The GENCODE exome: sequencing the complete human exome. *European Journal of Human Genetics: EJHG*, 19(7), pp.827–831.
- Cohen, A.J. et al., 1979. Hereditary renal-cell carcinoma associated with a chromosomal translocation. *The New England Journal of Medicine*, 301(11), pp.592–595.
- Conaway, J.W., Kamura, T. & Conaway, R.C., 1998. The Elongin BC complex and the von Hippel-Lindau tumor suppressor protein. *Biochimica Et Biophysica Acta*, 1377(2), pp.M49–54.
- Contractor, H. et al., 1997. Mutation of the p53 tumour suppressor gene occurs preferentially in the chromophobe type of renal cell tumour. *The Journal of pathology*, 181(2), pp.136–139.
- Cornelisse, C.J. & Devilee, P., 1997. Facts in cancer genetics. *Patient Education and Counseling*, 32(1-2), pp.9–17.
- Costa, V.L. et al., 2007. Quantitative promoter methylation analysis of multiple cancer-related genes in renal cell tumors. *BMC Cancer*, 7, p.133.
- Cremer, T. et al., 1988. Detection of chromosome aberrations in metaphase and interphase tumor cells by in situ hybridization using chromosome-specific library probes. *Human Genetics*, 80(3), pp.235–246.
- Croce, C.M., 2008. Oncogenes and cancer. *The New England Journal of Medicine*, 358(5), pp.502–511.

- Di Croce, L. et al., 2002. Methyltransferase recruitment and DNA hypermethylation of target promoters by an oncogenic transcription factor. *Science (New York, N.Y.)*, 295(5557), pp.1079–1082.
- Crossey, P.A. et al., 1994. Identification of intragenic mutations in the von Hippel-Lindau disease tumour suppressor gene and correlation with disease phenotype. *Human Molecular Genetics*, 3(8), pp.1303–1308.
- Dahl, E. et al., 2007. Frequent loss of SFRP1 expression in multiple human solid tumours: association with aberrant promoter methylation in renal cell carcinoma. *Oncogene*, 26(38), pp.5680–5691.
- Dalgliesh, G.L. et al., 2010. Systematic sequencing of renal carcinoma reveals inactivation of histone modifying genes. *Nature*, 463(7279), pp.360–363.
- Darai-Ramqvist, E. et al., 2006. Array-CGH and multipoint FISH to decode complex chromosomal rearrangements. *BMC Genomics*, 7, p.330.
- Darvish, H. et al., 2011. Exceptional human core promoter nucleotide compositions. *Gene*, 475(2), pp.79–86.
- Dawson, N.A. et al., 2004. A phase II trial of gefitinib (Iressa, ZD1839) in stage IV and recurrent renal cell carcinoma. *Clinical Cancer Research: An Official Journal of the American Association for Cancer Research*, 10(23), pp.7812–7819.
- Deshaies, R.J. & Joazeiro, C.A.P., 2009. RING domain E3 ubiquitin ligases. *Annual review of biochemistry*, 78, pp.399–434.
- Deshmukh, M. et al., 2011. Tubulocystic carcinoma of kidney associated with papillary renal cell carcinoma. *Indian Journal of Pathology & Microbiology*, 54(1), pp.127–130.
- Dibb, N.J., Dilworth, S.M. & Mol, C.D., 2004. Switching on kinases: oncogenic activation of BRAF and the PDGFR family. *Nature Reviews. Cancer*, 4(9), pp.718–727.
- Dikic, I., Wakatsuki, S. & Walters, K.J., 2009. Ubiquitin-binding domains - from structures to functions. *Nature Reviews. Molecular Cell Biology*, 10(10), pp.659–671.
- Dinkel, H. et al., 2012. ELM--the database of eukaryotic linear motifs. *Nucleic acids research*, 40(Database issue), pp.D242–251.
- Donnellan, R. & Chetty, R., 1999. Cyclin E in human cancers. *FASEB journal: official publication of the Federation of American Societies for Experimental Biology*, 13(8), pp.773–780.
- Dryja, T.P. et al., 1984. Homozygosity of chromosome 13 in retinoblastoma. *The New England Journal of Medicine*, 310(9), pp.550–553.
- Edelmann, L. et al., 1999. A common breakpoint on 11q23 in carriers of the constitutional t(11;22) translocation. *American Journal of Human Genetics*, 65(6), pp.1608–1616.
- Escudier, B. et al., 2007. Bevacizumab plus interferon alfa-2a for treatment of metastatic renal cell carcinoma: a randomised, double-blind phase III trial. *Lancet*, 370(9605), pp.2103–2111.
- Esteller, M. et al., 2001. DNA methylation patterns in hereditary human cancers mimic sporadic tumorigenesis. *Human Molecular Genetics*, 10(26), pp.3001–3007.

- Evers, B., Helleday, T. & Jonkers, J., 2010. Targeting homologous recombination repair defects in cancer. *Trends in pharmacological sciences*, 31(8), pp.372–380.
- Fearon, E.R. & Vogelstein, B., 1990. A genetic model for colorectal tumorigenesis. *Cell*, 61(5), pp.759–767.
- Feinberg, A.P., Ohlsson, R. & Henikoff, S., 2006. The epigenetic progenitor origin of human cancer. *Nature Reviews. Genetics*, 7(1), pp.21–33.
- Fernandez-Sanchez, M.E. et al., 2010. The human COP9 signalosome protects ubiquitin-conjugating enzyme 3 (UBC3/Cdc34) from beta-transducin repeat-containing protein (betaTrCP)-mediated degradation. *The Journal of biological chemistry*, 285(23), pp.17390–17397.
- Fiegler, H. et al., 2003. DNA microarrays for comparative genomic hybridization based on DOP-PCR amplification of BAC and PAC clones. *Genes, Chromosomes & Cancer*, 36(4), pp.361–374.
- Fisher, E. & Scambler, P., 1994. Human haploinsufficiency--one for sorrow, two for joy. *Nature Genetics*, 7(1), pp.5–7.
- Foster, R.E. et al., 2007. Characterization of a 3;6 translocation associated with renal cell carcinoma. *Genes, Chromosomes & Cancer*, 46(4), pp.311–317.
- Frigola, J. et al., 2006. Epigenetic remodeling in colorectal cancer results in coordinate gene suppression across an entire chromosome band. *Nature Genetics*, 38(5), pp.540–549.
- Gad, S et al., 2007. Mutations in BHD and TP53 genes, but not in HNF1beta gene, in a large series of sporadic chromophobe renal cell carcinoma. *British journal of cancer*, 96(2), pp.336–340.
- Gazdoui, S. et al., 2007. Human Cdc34 employs distinct sites to coordinate attachment of ubiquitin to a substrate and assembly of polyubiquitin chains. *Molecular and cellular biology*, 27(20), pp.7041–7052.
- Gemmill, R M et al., 1998. The hereditary renal cell carcinoma 3;8 translocation fuses FHIT to a patched-related gene, TRC8. *Proceedings of the National Academy of Sciences of the United States of America*, 95(16), pp.9572–9577.
- Gemmill, Robert M et al., 2005. Growth suppression induced by the TRC8 hereditary kidney cancer gene is dependent upon JAB1/CSN5. *Oncogene*, 24(21), pp.3503–3511.
- Gemmill, Robert M et al., 2002. The TRC8 hereditary kidney cancer gene suppresses growth and functions with VHL in a common pathway. *Oncogene*, 21(22), pp.3507–3516.
- Gerullis, H. et al., 2010. mTOR-inhibition in metastatic renal cell carcinoma. Focus on temsirolimus: a review. *Minerva urologica e nefrologica = The Italian journal of urology and nephrology*, 62(4), pp.411–423.
- Gnarra, J.R. et al., 1994. Mutations of the VHL tumour suppressor gene in renal carcinoma. *Nature Genetics*, 7(1), pp.85–90.
- Golub, T.R. et al., 1994. Fusion of PDGF receptor beta to a novel ets-like gene, tel, in chronic myelomonocytic leukemia with t(5;12) chromosomal translocation. *Cell*, 77(2), pp.307–316.

- Golub, T.R. et al., 1995. Fusion of the TEL gene on 12p13 to the AML1 gene on 21q22 in acute lymphoblastic leukemia. *Proceedings of the National Academy of Sciences of the United States of America*, 92(11), pp.4917–4921.
- Gonen, H. et al., 1999. Identification of the ubiquitin carrier proteins, E2s, involved in signal-induced conjugation and subsequent degradation of IkappaBalpha. *The Journal of Biological Chemistry*, 274(21), pp.14823–14830.
- Gonzalez Garcia, J.R. & Meza-Espinoza, J.P., 2006. Use of the International System for Human Cytogenetic Nomenclature (ISCN). *Blood*, 108(12), pp.3952–3953; author reply 3953.
- Greaves, M. & Maley, C.C., 2012. Clonal evolution in cancer. *Nature*, 481(7381), pp.306–313.
- Greger, V. et al., 1989. Epigenetic changes may contribute to the formation and spontaneous regression of retinoblastoma. *Human Genetics*, 83(2), pp.155–158.
- Gribble, S M et al., 2007. Ultra-high resolution array painting facilitates breakpoint sequencing. *Journal of Medical Genetics*, 44(1), pp.51–58.
- Gribble, Susan M et al., 2009. Array painting: a protocol for the rapid analysis of aberrant chromosomes using DNA microarrays. *Nature Protocols*, 4(12), pp.1722–1736.
- Gudmundsson, J. et al., 1995. Different tumor types from BRCA2 carriers show wild-type chromosome deletions on 13q12-q13. *Cancer Research*, 55(21), pp.4830–4832.
- Guo, G. et al., 2011. Frequent mutations of genes encoding ubiquitin-mediated proteolysis pathway components in clear cell renal cell carcinoma. *Nature Genetics*, 44(1), pp.17–19.
- Hadian, K. et al., 2011. NF-κB essential modulator (NEMO) interaction with linear and lys-63 ubiquitin chains contributes to NF-κB activation. *The Journal of Biological Chemistry*, 286(29), pp.26107–26117.
- Hamerton, J.L. et al., 1975. A cytogenetic survey of 14,069 newborn infants. I. Incidence of chromosome abnormalities. *Clinical Genetics*, 8(4), pp.223–243.
- Han, L. & Zhao, Z., 2009. CpG islands or CpG clusters: how to identify functional GC-rich regions in a genome? *BMC Bioinformatics*, 10, p.65.
- Harris, H. et al., 1969. Suppression of malignancy by cell fusion. *Nature*, 223(5204), pp.363–368.
- Hasumi, Y. et al., 2009. Homozygous loss of BHD causes early embryonic lethality and kidney tumor development with activation of mTORC1 and mTORC2. *Proceedings of the National Academy of Sciences of the United States of America*, 106(44), pp.18722–18727.
- Heng, H.H. & Tsui, L.C., 1998. High resolution free chromatin/DNA fiber fluorescent in situ hybridization. *Journal of Chromatography. A*, 806(1), pp.219–229.
- Herman, J.G. et al., 1994. Silencing of the VHL tumor-suppressor gene by DNA methylation in renal carcinoma. *Proceedings of the National Academy of Sciences of the United States of America*, 91(21), pp.9700–9704.
- Herman, J.G. & Baylin, S B, 2003. Gene silencing in cancer in association with promoter hypermethylation. *The New England Journal of Medicine*, 349(21), pp.2042–2054.

- Herrmann, J., Lerman, L.O. & Lerman, A., 2007. Ubiquitin and Ubiquitin-Like Proteins in Protein Regulation. *Circulation Research*, 100(9), pp.1276–1291.
- Hirata, H. et al., 2011. Wnt antagonist DKK1 acts as a tumor suppressor gene that induces apoptosis and inhibits proliferation in human renal cell carcinoma. *International Journal of Cancer. Journal International Du Cancer*, 128(8), pp.1793–1803.
- Hirata, H. et al., 2009. Wnt antagonist gene DKK2 is epigenetically silenced and inhibits renal cancer progression through apoptotic and cell cycle pathways. *Clinical Cancer Research: An Official Journal of the American Association for Cancer Research*, 15(18), pp.5678–5687.
- Hoeijmakers, J.H.J., 2009. DNA damage, aging, and cancer. *The New England journal of medicine*, 361(15), pp.1475–1485.
- Hofer, F. et al., 1994. Activated Ras interacts with the Ral guanine nucleotide dissociation stimulator. *Proceedings of the National Academy of Sciences of the United States of America*, 91(23), pp.11089–11093.
- Horsthemke, B., 1992. Genetics and cytogenetics of retinoblastoma. *Cancer Genetics and Cytogenetics*, 63(1), pp.1–7.
- Huang, T.H., Perry, M.R. & Laux, D.E., 1999. Methylation profiling of CpG islands in human breast cancer cells. *Human Molecular Genetics*, 8(3), pp.459–470.
- Hudes, G.R. et al., 2009. Clinical trial experience with temsirolimus in patients with advanced renal cell carcinoma. *Seminars in Oncology*, 36 Suppl 3, pp.S26–36.
- Iwatsuki, M. et al., 2010. Loss of FBXW7, a cell cycle regulating gene, in colorectal cancer: clinical significance. *International journal of cancer. Journal international du cancer*, 126(8), pp.1828–1837.
- Jin, B. & Robertson, K.D., 2013. DNA methyltransferases, DNA damage repair, and cancer. *Advances in experimental medicine and biology*, 754, pp.3–29.
- Jin, J. et al., 2007. Dual E1 activation systems for ubiquitin differentially regulate E2 enzyme charging. *Nature*, 447(7148), pp.1135–1138.
- Jin, J. et al., 2004. Systematic analysis and nomenclature of mammalian F-box proteins. *Genes & Development*, 18(21), pp.2573–2580.
- Jin, J. & Harper, J Wade, 2002. RING finger specificity in SCF-driven protein destruction. *Developmental cell*, 2(6), pp.685–687.
- Jin, L. et al., 2008. Mechanism of ubiquitin-chain formation by the human anaphase-promoting complex. *Cell*, 133(4), pp.653–665.
- Jing, F. et al., 2007. Hypermethylation of tumor suppressor genes BRCA1, p16 and 14-3-3sigma in serum of sporadic breast cancer patients. *Onkologie*, 30(1-2), pp.14–19.
- Jones, P.A. & Baylin, Stephen B, 2002. The fundamental role of epigenetic events in cancer. *Nature Reviews. Genetics*, 3(6), pp.415–428.
- Joos, S. et al., 1992. Variable breakpoints in Burkitt lymphoma cells with chromosomal t(8;14) translocation separate c-myc and the IgH locus up to several hundred kb. *Human Molecular Genetics*, 1(8), pp.625–632.
- Kanayama, H et al., 2001. Association of a novel constitutional translocation t(1q;3q) with familial renal cell carcinoma. *Journal of Medical Genetics*, 38(3), pp.165–170.

- Kasperek, T.R. & Humphrey, T.C., 2011. DNA double-strand break repair pathways, chromosomal rearrangements and cancer. *Seminars in cell & developmental biology*, 22(8), pp.886–897.
- Van Kessel, A G et al., 1999. Renal cell cancer: chromosome 3 translocations as risk factors. *Journal of the National Cancer Institute*, 91(13), pp.1159–1160.
- Killary, A.M. et al., 1992. Definition of a tumor suppressor locus within human chromosome 3p21-p22. *Proceedings of the National Academy of Sciences of the United States of America*, 89(22), pp.10877–10881.
- Kim, C.J. et al., 2007. Somatic mutations of the beta-TrCP gene in gastric cancer. *APMIS: acta pathologica, microbiologica, et immunologica Scandinavica*, 115(2), pp.127–133.
- Kim, H.T. et al., 2007. Certain pairs of ubiquitin-conjugating enzymes (E2s) and ubiquitin-protein ligases (E3s) synthesize nondegradable forked ubiquitin chains containing all possible isopeptide linkages. *The Journal of Biological Chemistry*, 282(24), pp.17375–17386.
- Kirkin, V. & Dikic, I., 2007. Role of ubiquitin- and Ubl-binding proteins in cell signaling. *Current Opinion in Cell Biology*, 19(2), pp.199–205.
- Kirkin, V. & Dikic, I., 2011. Ubiquitin networks in cancer. *Current Opinion in Genetics & Development*, 21, pp.21–28.
- Kirkpatrick, D.S. et al., 2006. Quantitative analysis of in vitro ubiquitinated cyclin B1 reveals complex chain topology. *Nature Cell Biology*, 8(7), pp.700–710.
- Kitagawa, K., Kotake, Y. & Kitagawa, M., 2009. Ubiquitin-mediated control of oncogene and tumor suppressor gene products. *Cancer Science*, 100(8), pp.1374–1381.
- Kleiger, G. et al., 2009. Rapid E2-E3 assembly and disassembly enable processive ubiquitylation of cullin-RING ubiquitin ligase substrates. *Cell*, 139(5), pp.957–968.
- Knudson, A G, Jr, 1971. Mutation and cancer: statistical study of retinoblastoma. *Proceedings of the National Academy of Sciences of the United States of America*, 68(4), pp.820–823.
- Koff, A. et al., 1992. Formation and activation of a cyclin E-cdk2 complex during the G1 phase of the human cell cycle. *Science (New York, N.Y.)*, 257(5077), pp.1689–1694.
- Koolen, M.I. et al., 1998. A familial case of renal cell carcinoma and a t(2;3) chromosome translocation. *Kidney International*, 53(2), pp.273–275.
- Kovacs, G et al., 1991. Cytogenetics of papillary renal cell tumors. *Genes, chromosomes & cancer*, 3(4), pp.249–255.
- Kovacs, G et al., 1997. The Heidelberg classification of renal cell tumours. *The Journal of Pathology*, 183(2), pp.131–133.
- Kovacs, G, Brusa, P. & De Riese, W., 1989. Tissue-specific expression of a constitutional 3;6 translocation: development of multiple bilateral renal-cell carcinomas. *International Journal of Cancer. Journal International Du Cancer*, 43(3), pp.422–427.
- Kovacs, G & Hoene, E., 1988. Loss of der(3) in renal carcinoma cells of a patient with constitutional t(3;12). *Human Genetics*, 78(2), pp.148–150.

- Kraft, C. et al., 2005. The WD40 propeller domain of Cdh1 functions as a destruction box receptor for APC/C substrates. *Molecular Cell*, 18(5), pp.543–553.
- Kuiper, R.P. et al., 2009. The tumor suppressor gene FBXW7 is disrupted by a constitutional t(3;4)(q21;q31) in a patient with renal cell cancer. *Cancer Genetics and Cytogenetics*, 195(2), pp.105–111.
- Kvasha, S. et al., 2008. Hypermethylation of the 5' CpG island of the FHIT gene in clear cell renal carcinomas. *Cancer letters*, 265(2), pp.250–257.
- Kwak, E.L. et al., 2005. Infrequent mutations of Archipelago (hAGO, hCDC4, Fbw7) in primary ovarian cancer. *Gynecologic oncology*, 98(1), pp.124–128.
- Lafarga, M. et al., 2002. Clastosome: a subtype of nuclear body enriched in 19S and 20S proteasomes, ubiquitin, and protein substrates of proteasome. *Molecular biology of the cell*, 13(8), pp.2771–2782.
- Latif, F et al., 1993. Identification of the von Hippel-Lindau disease tumor suppressor gene. *Science (New York, N.Y.)*, 260(5112), pp.1317–1320.
- Laureys, G. et al., 1995. Constitutional translocation t(1;17)(p36.31-p36.13;q11.2-q12.1) in a neuroblastoma patient. Establishment of somatic cell hybrids and identification of PND/A12M2 on chromosome 1 and NF1/SCYA7 on chromosome 17 as breakpoint flanking single copy markers. *Oncogene*, 10(6), pp.1087–1093.
- Li, W. & Ye, Y., 2008. Polyubiquitin chains: functions, structures, and mechanisms. *Cellular and Molecular Life Sciences: CMLS*, 65(15), pp.2397–2406.
- Li, Z. et al., 2002. Ubiquitination of a novel deubiquitinating enzyme requires direct binding to von Hippel-Lindau tumor suppressor protein. *The Journal of Biological Chemistry*, 277(7), pp.4656–4662.
- Liang, Y. et al., 2010. Stem-like cancer cells are inducible by increasing genomic instability in cancer cells. *The Journal of Biological Chemistry*, 285(7), pp.4931–4940.
- Lieber, M.R. et al., 2010. Nonhomologous DNA end joining (NHEJ) and chromosomal translocations in humans. *Sub-cellular biochemistry*, 50, pp.279–296.
- Lin, H.-K. et al., 2010. Skp2 targeting suppresses tumorigenesis by Arf-p53-independent cellular senescence. *Nature*, 464(7287), pp.374–379.
- Lindblom, A. et al., 1994. Predisposition for breast cancer in carriers of constitutional translocation 11q;22q. *American Journal of Human Genetics*, 54(5), pp.871–876.
- Liu, J. et al., 2004. Targeted degradation of beta-catenin by chimeric F-box fusion proteins. *Biochemical and Biophysical Research Communications*, 313(4), pp.1023–1029.
- Loginov, V.I. et al., 2009. [Methylation of promoter region of RASSF1A gene and frequencies of allelic imbalances in chromosome 3 critical regions are correlated with progression of clear cell renal cell carcinoma]. *Molekuliarnaia biologii*, 43(3), pp.429–438.
- Lopez-Beltran, A. et al., 2006. 2004 WHO classification of the renal tumors of the adults. *European Urology*, 49(5), pp.798–805.

- Lopez-Beltran, A. et al., 2009. 2009 update on the classification of renal epithelial tumors in adults. *International Journal of Urology: Official Journal of the Japanese Urological Association*, 16(5), pp.432–443.
- Lusher, M.E. et al., 2002. Biallelic epigenetic inactivation of the RASSF1A tumor suppressor gene in medulloblastoma development. *Cancer Research*, 62(20), pp.5906–5911.
- Maher, E R et al., 1990. Clinical features and natural history of von Hippel-Lindau disease. *The Quarterly Journal of Medicine*, 77(283), pp.1151–1163.
- Maher, Eamonn R, 2011. Genetics of familial renal cancers. *Nephron. Experimental Nephrology*, 118(1), pp.e21–26.
- Malkin, D. et al., 1990. Germ line p53 mutations in a familial syndrome of breast cancer, sarcomas, and other neoplasms. *Science (New York, N.Y.)*, 250(4985), pp.1233–1238.
- Mao, J.-H. et al., 2008. FBXW7 targets mTOR for degradation and cooperates with PTEN in tumor suppression. *Science (New York, N.Y.)*, 321(5895), pp.1499–1502.
- Margottin-Goguet, F. et al., 2003. Prophase destruction of Emil by the SCF(betaTrCP/Slimb) ubiquitin ligase activates the anaphase promoting complex to allow progression beyond prometaphase. *Developmental cell*, 4(6), pp.813–826.
- Marti, T.M., Kunz, C. & Fleck, O., 2002. DNA mismatch repair and mutation avoidance pathways. *Journal of cellular physiology*, 191(1), pp.28–41.
- Martinez, A. et al., 2000. Role of chromosome 3p12-p21 tumour suppressor genes in clear cell renal cell carcinoma: analysis of VHL dependent and VHL independent pathways of tumorigenesis. *Molecular pathology: MP*, 53(3), pp.137–144.
- Mathias, N., Steussy, C.N. & Goebel, M.G., 1998. An essential domain within Cdc34p is required for binding to a complex containing Cdc4p and Cdc53p in *Saccharomyces cerevisiae*. *The Journal of Biological Chemistry*, 273(7), pp.4040–4045.
- Maxwell, P.H. et al., 1999. The tumour suppressor protein VHL targets hypoxia-inducible factors for oxygen-dependent proteolysis. *Nature*, 399(6733), pp.271–275.
- Maynard, M.A. & Ohh, M., 2007. The role of hypoxia-inducible factors in cancer. *Cellular and Molecular Life Sciences: CMLS*, 64(16), pp.2170–2180.
- Meléndez, B. et al., 2003. Molecular study of a new family with hereditary renal cell carcinoma and a translocation t(3;8)(p13;q24.1). *Human Genetics*, 112(2), pp.178–185.
- Milne, A.N. et al., 2010. Loss of CDC4/FBXW7 in gastric carcinoma. *Cellular oncology: the official journal of the International Society for Cellular Oncology*, 32(5-6), pp.347–359.
- Mitelman, F., Johansson, B. & Mertens, F., 2007. The impact of translocations and gene fusions on cancer causation. *Nature Reviews. Cancer*, 7(4), pp.233–245.
- Miyaki, M. et al., 2009. Somatic mutations of the CDC4 (FBXW7) gene in hereditary colorectal tumors. *Oncology*, 76(6), pp.430–434.

- Möröy, T. & Geisen, C., 2004. Cyclin E. *The international journal of biochemistry & cell biology*, 36(8), pp.1424–1439.
- Morris, Mark R & Maher, Eamonn R, 2010. Epigenetics of renal cell carcinoma: the path towards new diagnostics and therapeutics. *Genome Medicine*, 2(9), p.59.
- Morrissey, C. et al., 2001. Epigenetic inactivation of the RASSF1A 3p21.3 tumor suppressor gene in both clear cell and papillary renal cell carcinoma. *Cancer Research*, 61(19), pp.7277–7281.
- Motzer, R.J. et al., 2007. Sunitinib versus interferon alfa in metastatic renal-cell carcinoma. *The New England Journal of Medicine*, 356(2), pp.115–124.
- Mullighan, C.G. et al., 2007. Genome-wide analysis of genetic alterations in acute lymphoblastic leukaemia. *Nature*, 446(7137), pp.758–764.
- Na, X. et al., 2003. Identification of the RNA polymerase II subunit hsRPB7 as a novel target of the von Hippel-Lindau protein. *The EMBO Journal*, 22(16), pp.4249–4259.
- Nagy, A. et al., 2004. Lack of mutation of the folliculin gene in sporadic chromophobe renal cell carcinoma and renal oncocytoma. *International journal of cancer. Journal international du cancer*, 109(3), pp.472–475.
- Nakayama, K.I. & Nakayama, K., 2006. Ubiquitin ligases: cell-cycle control and cancer. *Nature Reviews. Cancer*, 6(5), pp.369–381.
- Nambiar, M., Kari, V. & Raghavan, S.C., 2008. Chromosomal translocations in cancer. *Biochimica Et Biophysica Acta*, 1786(2), pp.139–152.
- Nash, P. et al., 2001. Multisite phosphorylation of a CDK inhibitor sets a threshold for the onset of DNA replication. *Nature*, 414(6863), pp.514–521.
- Ohh, M et al., 2000. Ubiquitination of hypoxia-inducible factor requires direct binding to the beta-domain of the von Hippel-Lindau protein. *Nature Cell Biology*, 2(7), pp.423–427.
- Ohh, Michael, 2006. Ubiquitin pathway in VHL cancer syndrome. *Neoplasia (New York, N.Y.)*, 8(8), pp.623–629.
- Okamoto, Y. et al., 2003a. UbcH10 is the cancer-related E2 ubiquitin-conjugating enzyme. *Cancer Research*, 63(14), pp.4167–4173.
- Okamoto, Y. et al., 2003b. UbcH10 is the cancer-related E2 ubiquitin-conjugating enzyme. *Cancer research*, 63(14), pp.4167–4173.
- Okuda, H. et al., 1999. Direct interaction of the beta-domain of VHL tumor suppressor protein with the regulatory domain of atypical PKC isoforms. *Biochemical and Biophysical Research Communications*, 263(2), pp.491–497.
- Oosterwijk, E. et al., 2011. Basic research in kidney cancer. *European Urology*, 60(4), pp.622–633.
- Ougolkov, A. et al., 2004. Associations among beta-TrCP, an E3 ubiquitin ligase receptor, beta-catenin, and NF-kappaB in colorectal cancer. *Journal of the National Cancer Institute*, 96(15), pp.1161–1170.
- Page, S L et al., 1996. Breakpoint diversity illustrates distinct mechanisms for Robertsonian translocation formation. *Human Molecular Genetics*, 5(9), pp.1279–1288.

- Paige, A.J.W., 2003. Redefining tumour suppressor genes: exceptions to the two-hit hypothesis. *Cellular and Molecular Life Sciences: CMLS*, 60(10), pp.2147–2163.
- Peruzzi, B. & Bottaro, D.P., 2006. Beta-catenin signaling: linking renal cell carcinoma and polycystic kidney disease. *Cell Cycle (Georgetown, Tex.)*, 5(24), pp.2839–2841.
- Peters, I. et al., 2007. RASSF1A promoter methylation and expression analysis in normal and neoplastic kidney indicates a role in early tumorigenesis. *Molecular cancer*, 6, p.49.
- Petroski, M.D. & Deshaies, R.J., 2005. Mechanism of lysine 48-linked ubiquitin-chain synthesis by the cullin-RING ubiquitin-ligase complex SCF-Cdc34. *Cell*, 123(6), pp.1107–1120.
- Pickart, C.M. & Fushman, D., 2004. Polyubiquitin chains: polymeric protein signals. *Current Opinion in Chemical Biology*, 8(6), pp.610–616.
- Pierce, A.J. et al., 2001. Double-strand breaks and tumorigenesis. *Trends in Cell Biology*, 11(11), pp.S52–59.
- Pierce, N.W. et al., 2009. Detection of sequential polyubiquitylation on a millisecond timescale. *Nature*, 462(7273), pp.615–619.
- Pinto Marín, A. et al., 2012. mTOR pathway inhibition in renal cell carcinoma. *Urologic oncology*, 30(4), pp.356–361.
- Plimack, E.R., Kantarjian, H.M. & Issa, J.-P., 2007. Decitabine and its role in the treatment of hematopoietic malignancies. *Leukemia & Lymphoma*, 48(8), pp.1472–1481.
- Podolski, J. et al., 2001. Characterization of a familial RCC-associated t(2;3)(q33;q21) chromosome translocation. *Journal of Human Genetics*, 46(12), pp.685–693.
- Poland, K.S. et al., 2007. A constitutional balanced t(3;8)(p14;q24.1) translocation results in disruption of the TRC8 gene and predisposition to clear cell renal cell carcinoma. *Genes, Chromosomes & Cancer*, 46(9), pp.805–812.
- Popov, N. et al., 2010. Ubiquitylation of the amino terminus of Myc by SCF(β -TrCP) antagonizes SCF(Fbw7)-mediated turnover. *Nature Cell Biology*, 12(10), pp.973–981.
- Prendergast, G.C. & Ziff, E.B., 1991. Methylation-sensitive sequence-specific DNA binding by the c-Myc basic region. *Science (New York, N.Y.)*, 251(4990), pp.186–189.
- Presta, L.G. et al., 1997. Humanization of an anti-vascular endothelial growth factor monoclonal antibody for the therapy of solid tumors and other disorders. *Cancer Research*, 57(20), pp.4593–4599.
- Puntervoll, P. et al., 2003. ELM server: A new resource for investigating short functional sites in modular eukaryotic proteins. *Nucleic acids research*, 31(13), pp.3625–3630.
- Randolph, T.R., 2005. Chronic myelocytic leukemia--Part I: History, clinical presentation, and molecular biology. *Clinical Laboratory Science: Journal of the American Society for Medical Technology*, 18(1), pp.38–48.
- Ratain, M.J. et al., 2006. Phase II placebo-controlled randomized discontinuation trial of sorafenib in patients with metastatic renal cell carcinoma. *Journal of Clinical*

- Oncology: Official Journal of the American Society of Clinical Oncology*, 24(16), pp.2505–2512.
- Read, M.A. et al., 2000. Nedd8 modification of cul-1 activates SCF(beta(TrCP))-dependent ubiquitination of IkappaBalpha. *Molecular and cellular biology*, 20(7), pp.2326–2333.
- Richly, H. et al., 2005. A series of ubiquitin binding factors connects CDC48/p97 to substrate multiubiquitylation and proteasomal targeting. *Cell*, 120(1), pp.73–84.
- Ricketts, Christopher et al., 2008. Germline SDHB mutations and familial renal cell carcinoma. *Journal of the National Cancer Institute*, 100(17), pp.1260–1262.
- Rini, B.I. et al., 2009. Phase II study of axitinib in sorafenib-refractory metastatic renal cell carcinoma. *Journal of Clinical Oncology: Official Journal of the American Society of Clinical Oncology*, 27(27), pp.4462–4468.
- Rodrigo-Brenni, M.C. & Morgan, David O, 2007. Sequential E2s drive polyubiquitin chain assembly on APC targets. *Cell*, 130(1), pp.127–139.
- Roos, F.C. et al., 2011a. Deregulation of E2-EPF ubiquitin carrier protein in papillary renal cell carcinoma. *The American Journal of Pathology*, 178(2), pp.853–860.
- Roos, F.C. et al., 2011b. Deregulation of E2-EPF ubiquitin carrier protein in papillary renal cell carcinoma. *The American journal of pathology*, 178(2), pp.853–860.
- Sadowski, M. et al., 2007. Cdc34 C-terminal tail phosphorylation regulates Skp1/cullin/F-box (SCF)-mediated ubiquitination and cell cycle progression. *The Biochemical journal*, 405(3), pp.569–581.
- Saini, S., Majid, S. & Dahiya, R., 2011. The complex roles of Wnt antagonists in RCC. *Nature Reviews. Urology*, 8(12), pp.690–699.
- Sanchez, Y. et al., 1994. A tumor suppressor locus within 3p14-p12 mediates rapid cell death of renal cell carcinoma in vivo. *Proceedings of the National Academy of Sciences of the United States of America*, 91(8), pp.3383–3387.
- Sandberg, A.A., 1985. Application of cytogenetics in neoplastic diseases. *Critical Reviews in Clinical Laboratory Sciences*, 22(3), pp.219–274.
- Santarosa, M. & Ashworth, A., 2004. Haploinsufficiency for tumour suppressor genes: when you don't need to go all the way. *Biochimica Et Biophysica Acta*, 1654(2), pp.105–122.
- Santini, V., 2009. Azacitidine: activity and efficacy as an epigenetic treatment of myelodysplastic syndromes. *Expert Review of Hematology*, 2(2), pp.121–127.
- Sarikas, A. et al., 2008. The cullin7 E3 ubiquitin ligase: a novel player in growth control. *Cell Cycle (Georgetown, Tex.)*, 7(20), pp.3154–3161.
- Schappert-Kimmijser, J., Hemmes, G.D. & Nijland, R., 1966. The heredity of retinoblastoma. *Ophthalmologica. Journal International D'ophtalmologie. International Journal of Ophthalmology. Zeitschrift Für Augenheilkunde*, 151(2), pp.197–213.
- Schmidt, L. et al., 1997. Germline and somatic mutations in the tyrosine kinase domain of the MET proto-oncogene in papillary renal carcinomas. *Nature genetics*, 16(1), pp.68–73.
- Schmidt, L. et al., 1999. Novel mutations of the MET proto-oncogene in papillary renal carcinomas. *Oncogene*, 18(14), pp.2343–2350.

- Schröck, E. et al., 1996. Multicolor spectral karyotyping of human chromosomes. *Science (New York, N.Y.)*, 273(5274), pp.494–497.
- Schulman, B.A. & Harper, J Wade, 2009. Ubiquitin-like protein activation by E1 enzymes: the apex for downstream signalling pathways. *Nature Reviews. Molecular Cell Biology*, 10(5), pp.319–331.
- Schwob, E. et al., 1994. The B-type cyclin kinase inhibitor p40SIC1 controls the G1 to S transition in *S. cerevisiae*. *Cell*, 79(2), pp.233–244.
- Le Scouarnec, S. & Gribble, S M, 2012. Characterising chromosome rearrangements: recent technical advances in molecular cytogenetics. *Heredity*, 108(1), pp.75–85.
- Seghatoleslam, A. et al., 2012. Expression of UBE2Q2, a putative member of the ubiquitin-conjugating enzyme family in pediatric acute lymphoblastic leukemia. *Archives of Iranian medicine*, 15(6), pp.352–355.
- Semenza, G.L., 2001. HIF-1 and mechanisms of hypoxia sensing. *Current Opinion in Cell Biology*, 13(2), pp.167–171.
- Shaffer, L G & Lupski, J R, 2000. Molecular mechanisms for constitutional chromosomal rearrangements in humans. *Annual Review of Genetics*, 34, pp.297–329.
- Da Silva, N.F. et al., 2003. Analysis of the Birt-Hogg-Dubé (BHD) tumour suppressor gene in sporadic renal cell carcinoma and colorectal cancer. *Journal of Medical Genetics*, 40(11), pp.820–824.
- Simon, J.A. & Lange, C.A., 2008. Roles of the EZH2 histone methyltransferase in cancer epigenetics. *Mutation Research*, 647(1-2), pp.21–29.
- Smith, S.A. et al., 1992. Allele losses in the region 17q12-21 in familial breast and ovarian cancer involve the wild-type chromosome. *Nature Genetics*, 2(2), pp.128–131.
- Song, Jee Hoon et al., 2008. FBXW7 mutation in adult T-cell and B-cell acute lymphocytic leukemias. *Leukemia research*, 32(11), pp.1751–1755.
- Sonpavde, G., Hutson, T.E. & Sternberg, C.N., 2008. Pazopanib, a potent orally administered small-molecule multitargeted tyrosine kinase inhibitor for renal cell carcinoma. *Expert Opinion on Investigational Drugs*, 17(2), pp.253–261.
- Spector, D L, 2001. Nuclear domains. *Journal of cell science*, 114(Pt 16), pp.2891–2893.
- Spector, David L & Lamond, A.I., 2011. Nuclear speckles. *Cold Spring Harbor perspectives in biology*, 3(2). Available at: <http://www.ncbi.nlm.nih.gov/pubmed/20926517> [Accessed June 13, 2012].
- Speicher, M.R. et al., 1994. Specific loss of chromosomes 1, 2, 6, 10, 13, 17, and 21 in chromophobe renal cell carcinomas revealed by comparative genomic hybridization. *The American journal of pathology*, 145(2), pp.356–364.
- Spratt, D.E. et al., 2012. Selective recruitment of an E2~ubiquitin complex by an E3 ubiquitin ligase. *The Journal of biological chemistry*, 287(21), pp.17374–17385.
- Stankiewicz, P. & Lupski, James R, 2002. Genome architecture, rearrangements and genomic disorders. *Trends in Genetics: TIG*, 18(2), pp.74–82.
- Strefford, J.C., An, Q. & Harrison, C.J., 2009. Modeling the molecular consequences of unbalanced translocations in cancer: lessons from acute lymphoblastic leukemia. *Cell Cycle (Georgetown, Tex.)*, 8(14), pp.2175–2184.

- Sükösd, F. et al., 2003. Deletion of chromosome 3p14.2-p25 involving the VHL and FHIT genes in conventional renal cell carcinoma. *Cancer research*, 63(2), pp.455–457.
- Sun, M. et al., 2010. Treatment of metastatic renal cell carcinoma. *Nature Reviews. Urology*, 7(6), pp.327–338.
- Sun, Y., 2006. E3 ubiquitin ligases as cancer targets and biomarkers. *Neoplasia (New York, N.Y.)*, 8(8), pp.645–654.
- Sun, Y., 2003. Targeting E3 ubiquitin ligases for cancer therapy. *Cancer biology & therapy*, 2(6), pp.623–629.
- Sung, P., Prakash, S. & Prakash, L., 1990. Mutation of cysteine-88 in the *Saccharomyces cerevisiae* RAD6 protein abolishes its ubiquitin-conjugating activity and its various biological functions. *Proceedings of the National Academy of Sciences of the United States of America*, 87(7), pp.2695–2699.
- Suzuki, M.M. & Bird, Adrian, 2008. DNA methylation landscapes: provocative insights from epigenomics. *Nature Reviews. Genetics*, 9(6), pp.465–476.
- Szyf, M., 2006. Targeting DNA methylation in cancer. *Bulletin Du Cancer*, 93(9), pp.961–972.
- Tan, Y., Sangfelt, O. & Spruck, C., 2008. The Fbxw7/hCdc4 tumor suppressor in human cancer. *Cancer letters*, 271(1), pp.1–12.
- Tedesco, D. et al., 2007. The ubiquitin-conjugating enzyme E2-EPF is overexpressed in primary breast cancer and modulates sensitivity to topoisomerase II inhibition. *Neoplasia (New York, N.Y.)*, 9(7), pp.601–613.
- Thoenes, W. et al., 1990. Cytomorphological typing of renal cell carcinoma--a new approach. *European Urology*, 18 Suppl 2, pp.6–9.
- Toro, J.R. et al., 2008. BHD mutations, clinical and molecular genetic investigations of Birt-Hogg-Dubé syndrome: a new series of 50 families and a review of published reports. *Journal of medical genetics*, 45(6), pp.321–331.
- Uchida, S. et al., 2011. SCF β (TrCP) mediates stress-activated MAPK-induced Cdc25B degradation. *Journal of cell science*, 124(Pt 16), pp.2816–2825.
- Varela, I. et al., 2011. Exome sequencing identifies frequent mutation of the SWI/SNF complex gene PBRM1 in renal carcinoma. *Nature*, 469(7331), pp.539–542.
- Varley, J.M., Evans, D.G. & Birch, J.M., 1997. Li-Fraumeni syndrome--a molecular and clinical review. *British Journal of Cancer*, 76(1), pp.1–14.
- Veikkola, T. & Alitalo, K., 1999. VEGFs, receptors and angiogenesis. *Seminars in Cancer Biology*, 9(3), pp.211–220.
- Venkatachalam, S. et al., 1998. Retention of wild-type p53 in tumors from p53 heterozygous mice: reduction of p53 dosage can promote cancer formation. *The EMBO Journal*, 17(16), pp.4657–4667.
- Vignoli, G.C. & Martorana, G., 1997. Molecular genetics of renal cell carcinoma. *Archivio italiano di urologia, andrologia: organo ufficiale [di] Società italiana di ecografia urologica e nefrologica / Associazione ricerche in urologia*, 69(4), pp.265–269.

- Vincan, E., 2004. Frizzled/WNT signalling: the insidious promoter of tumour growth and progression. *Frontiers in Bioscience: A Journal and Virtual Library*, 9, pp.1023–1034.
- Vlaykova, T. et al., 2011. Microsatellite instability and promoter hypermethylation of MLH1 and MSH2 in patients with sporadic colorectal cancer. *Journal of B.U.ON.: Official Journal of the Balkan Union of Oncology*, 16(2), pp.265–273.
- Wada, H., Yeh, E.T. & Kamitani, T., 2000. A dominant-negative UBC12 mutant sequesters NEDD8 and inhibits NEDD8 conjugation in vivo. *The Journal of biological chemistry*, 275(22), pp.17008–17015.
- Wang, G. et al., 2012. Novel roles of Skp2 E3 ligase in cellular senescence, cancer progression, and metastasis. *Chinese journal of cancer*, 31(4), pp.169–177.
- Wang, Yong & Leung, F.C.C., 2004. An evaluation of new criteria for CpG islands in the human genome as gene markers. *Bioinformatics (Oxford, England)*, 20(7), pp.1170–1177.
- Watanabe, Nobumoto et al., 2004. M-phase kinases induce phospho-dependent ubiquitination of somatic Wee1 by SCFbeta-TrCP. *Proceedings of the National Academy of Sciences of the United States of America*, 101(13), pp.4419–4424.
- Welchman, R.L., Gordon, C. & Mayer, R.J., 2005. Ubiquitin and ubiquitin-like proteins as multifunctional signals. *Nature Reviews. Molecular Cell Biology*, 6(8), pp.599–609.
- Welcker, M. & Clurman, B.E., 2008. FBW7 ubiquitin ligase: a tumour suppressor at the crossroads of cell division, growth and differentiation. *Nature reviews. Cancer*, 8(2), pp.83–93.
- Van Wijk, S.J.L. & Timmers, H.T.M., 2010a. The family of ubiquitin-conjugating enzymes (E2s): deciding between life and death of proteins. *The FASEB Journal: Official Publication of the Federation of American Societies for Experimental Biology*, 24(4), pp.981–993.
- Van Wijk, S.J.L. & Timmers, H.T.M., 2010b. The family of ubiquitin-conjugating enzymes (E2s): deciding between life and death of proteins. *FASEB journal: official publication of the Federation of American Societies for Experimental Biology*, 24(4), pp.981–993.
- Wilhelm, M. et al., 2002. Array-based comparative genomic hybridization for the differential diagnosis of renal cell cancer. *Cancer research*, 62(4), pp.957–960.
- Wilhelm, S.M. et al., 2004. BAY 43-9006 exhibits broad spectrum oral antitumor activity and targets the RAF/MEK/ERK pathway and receptor tyrosine kinases involved in tumor progression and angiogenesis. *Cancer Research*, 64(19), pp.7099–7109.
- Windheim, M., Peggie, M. & Cohen, P., 2008. Two different classes of E2 ubiquitin-conjugating enzymes are required for the mono-ubiquitination of proteins and elongation by polyubiquitin chains with a specific topology. *The Biochemical Journal*, 409(3), pp.723–729.
- Winston, J.T. et al., 1999. The SCFbeta-TRCP-ubiquitin ligase complex associates specifically with phosphorylated destruction motifs in IkappaBalpha and beta-catenin and stimulates IkappaBalpha ubiquitination in vitro. *Genes & development*, 13(3), pp.270–283.

- Woodward, E R et al., 2000. Familial clear cell renal cell carcinoma (FCRC): clinical features and mutation analysis of the VHL, MET, and CUL2 candidate genes. *Journal of medical genetics*, 37(5), pp.348–353.
- Woodward, Emma R et al., 2008. Familial non-VHL clear cell (conventional) renal cell carcinoma: clinical features, segregation analysis, and mutation analysis of FLCN. *Clinical Cancer Research: An Official Journal of the American Association for Cancer Research*, 14(18), pp.5925–5930.
- Woodward, Emma R et al., 2010. Population-based survey of cancer risks in chromosome 3 translocation carriers. *Genes, Chromosomes & Cancer*, 49(1), pp.52–58.
- Xu, X. et al., 2008. The CUL7 E3 ubiquitin ligase targets insulin receptor substrate 1 for ubiquitin-dependent degradation. *Molecular Cell*, 30(4), pp.403–414.
- Yamada, N.A. et al., 2011. Visualization of fine-scale genomic structure by oligonucleotide-based high-resolution FISH. *Cytogenetic and Genome Research*, 132(4), pp.248–254.
- Yang, G. et al., 2010. Mucinous tubular and spindle cell carcinoma of the kidney. *The Journal of Urology*, 183(2), pp.738–739.
- Ye, Yihong & Rape, M., 2009. Building ubiquitin chains: E2 enzymes at work. *Nature Reviews. Molecular Cell Biology*, 10(11), pp.755–764.
- Yip, C.K. et al., 2010. Structure of the human mTOR complex I and its implications for rapamycin inhibition. *Molecular cell*, 38(5), pp.768–774.
- Yoo, C.B. & Jones, P.A., 2006. Epigenetic therapy of cancer: past, present and future. *Nature Reviews. Drug Discovery*, 5(1), pp.37–50.
- Youngs, S. et al., 2004. A study of reciprocal translocations and inversions detected by light microscopy with special reference to origin, segregation, and recurrent abnormalities. *American Journal of Medical Genetics. Part A*, 126A(1), pp.46–60.
- Yu, H. et al., 2010. The ubiquitin carboxyl hydrolase BAP1 forms a ternary complex with YY1 and HCF-1 and is a critical regulator of gene expression. *Molecular and Cellular Biology*, 30(21), pp.5071–5085.
- Zhang, W. & Koepp, D.M., 2006. Fbw7 isoform interaction contributes to cyclin E proteolysis. *Molecular cancer research: MCR*, 4(12), pp.935–943.
- Zheng, N. et al., 2000. Structure of a c-Cbl-UbcH7 complex: RING domain function in ubiquitin-protein ligases. *Cell*, 102(4), pp.533–539.
- Zhuang, Z. et al., 1998. Trisomy 7-harboring non-random duplication of the mutant MET allele in hereditary papillary renal carcinomas. *Nature genetics*, 20(1), pp.66–69.

Chapter Ten: Peer Reviewed Publications

1. Astuti, D, Morris, MR, Cooper, WN, Staals, RHJ, **Wake, NC**, Fewes, GA, Gill, H, Gentle, D, Shuib, S, Ricketts, CJ, Cole, T, van Essen, AJ, van Lingen, RA, Neri, G, Opitz, JM, Rump, P, Stolte-Dijkstra, I, Müller, F, Pruijn, GJM, Latif, F & Maher, ER 2012, 'Germline mutations in DIS3L2 cause the Perlman syndrome of overgrowth and Wilms tumor susceptibility', *Nature genetics*, vol. 44, no. 3, pp. 277–284.
2. Ricketts, CJ, Morris, MR, Gentle, D, Brown, M, **Wake, N**, Woodward, ER, Clarke, N, Latif, F & Maher, ER 2012, 'Genome-wide CpG island methylation analysis implicates novel genes in the pathogenesis of renal cell carcinoma', *Epigenetics: official journal of the DNA Methylation Society*, vol. 7, no. 3, pp. 278–290.
3. **Wake, NC**, Ricketts, CJ, Morris, MR, Prigmore, E, Gribble, SM, Skytte, AB, Brown, M, Clarke, N, Banks, RE, Hodgson, S, Turnell, AS, Maher, ER, Woodward, ER 2012, 'UBE2QL1 is a novel candidate renal tumour suppressor gene', *Human Molecular Genetics*, (in review).